Correlation effects on the nuclear matrix element of neutrinoless double β-decay

Facoltà di Scienze Matematiche, Fisiche e Naturali

Corso di Laurea Magistrale in Fisica

Candidate

Enrico Speranza
ID number 1421150

Thesis Advisor

Prof. Omar Benhar Noccioli

Contents

Introduction

According to the standard model of particle physics, neutrinos are massless. If this were the case, neutrinos of different flavors would be degenerate, and one could always find a basis in which the Hamiltonian and the lepton flavors are both diagonal. However, the observation of neutrino oscillations has unambiguously established that neutrinos have non vanishing masses, although many orders of magnitude smaller that those of charged leptons.

Neutrino oscillation experiments are sensitive to differences between squared neutrino masses, but do not provide any information on either the absolute neutrino mass scale or the neutrino mass hierarchy.

The experimental searches of neutrinoless double β-decay (for a recent review, see, e.g., Ref. [1]), on the other hand, may tell us whether neutrinos are Majorana or Dirac particles and shed light on the absolute mass scale.

In a double β-decay reaction, a very long-lived nucleus with mass number A and atomic number Z disintegrates spontaneously into a nucleus with the same mass number and atomic number decreased by two units, with emission of two electrons and zero or two anti-neutrinos. According to the standard model this process is mediated by the weak interaction and it is always associated with the occurrence of anti-neutrinos in the final state. On the other hand, if the neutrino is a Majorana particle, implying that the same field describes particle and antiparticle, we can observe a final state without neutrinos, as the two neutrino fields are contracted to give rise to a propagator.

The calculation of the nuclear transition matrix element entering the expression of the decay rate involves severe difficulties, as it requires an accurate description of nuclear dynamics. Nucleon-nucleon interactions, besides being non spherically symmetric and spin and isospin dependent, are in fact known to exhibit a strongly repulsive core, which makes standard perturbation theory inapplicable.

Calculations of transition matrix elements for complex nuclei, such as those employed in neutrinoless double β-decay experiments, are carried out within the framework of the nuclear shell model, based on the assumption that the nucleon-nucleon interactions can be described in terms of a mean field. However, this approach, while being very successful in explaining a wealth of nuclear data, fails to take into account nucleon-nucleon correlations, that are expected to play a significant role in a reaction involving two nucleons.

Recently, a number of high precision electron-nucleus scattering experiments aimed at assessing the validity and limits of the shell model picture, made possible by the availability of continuous electron beam facilities, have shown that correlation effects are important, and lead to a sizable deviation from the shell model predictions.

In this Thesis we discuss the inclusion of correlation effects on the nuclear transition matrix element of the neutrinoless double β-decay, and report the numerical results of a preliminary study of this process in ^{48}Ca.

In Chapter 1, we summarize the main elements of the physics of massive neutrinos and briefly discuss neutrino oscillations in vacuum.

In Chapter 2, we outline the theoretical formalism to be employed in the description of β-decays and derive the expression of the decay rate of both two-neutrino and neutrinoless double β-decay, pointing out the differences between the two processes.

The aim of Chapter 3 is to present the main features of nuclear structure and dynamics, based on nucleon-nucleon interaction. We focus on the difficulties associated with the nuclear many-body problem. In the last two Sections we discuss the shell model and the inclusion of correlation effects through two different procedures based on correlated basis function theory: using either correlated two-nucleon states or using the theory of spectroscopic factors.

In Chapter 4, we derive the analytic expression of the nuclear matrix elements. In the first Section we analyze the pure shell model, while in the second Section we show how central and spin-dependent correlations modify the Fermi and Gamow-Teller nature of the transition matrix elements.

Finally, in Chapter 5, we present the numerical results in the case of pure shell model and with inclusion of correlation effects.

Throughout this Thesis we always use a system of units in which $\hbar = c = 1$ where $\hbar$ is Planck's constant and c is the speed of light.

Chapter 1

Physics of massive neutrinos

In the Standard Model of elemenatry particles, neutrino is considered a massles lepton. Moreover neutrino does not carry any electrical charge, it is observable only via weak interactions with definite left-handed chirality and it is paired with a charged lepton (e, μ, τ) in weak isodublets.

However, neutrino oscillations and beta decays experiments have unambiguosly demonstrated that neutrino is a massive particle with a mass much smaller than the electron one. From a theoretical point of view, the nature of the mass the neutrino has not yet been estabilished phenomenologically; neutrino can be a Dirac particle (i.e. different from its antiparticle) or a Majorana particle (i.e. identical from its antiparticle).

1.1 Dirac neutrinos

A Dirac neutrino mass can be generated with the same Higgs mechanism that gives masses to quarks and charged leptons in the Standard Model. We need only to introduce the sterile right-handed neutrinos that do not undergo weak interactions. After the electroweak symmetry breaking we obtain the following Dirac mass Lagrangian:

$$\mathcal{L}_D = -m_D \overline{\nu}\nu = -m_D(\overline{\nu_L}\nu_R + \overline{\nu_R}\nu_L) = -\frac{yv}{\sqrt{2}}(\overline{\nu_L}\nu_R + \overline{\nu_R}\nu_L)\,, \qquad (1.1)$$

where ν_L and ν_R are the left-handed and right-handed neutrino field respectively defined as

$$\nu_L \equiv P_L\nu \equiv \frac{1-\gamma_5}{2}\nu\,, \qquad \nu_R \equiv P_R\nu \equiv \frac{1+\gamma_5}{2}\nu\,, \qquad (1.2)$$

y is a Yukawa coupling constant and v is the vacuum expectation value of the Higgs field. Note that, in this mechanism, the neutrino mass is proportional to v, as the masses of charged leptons and quarks. However we know that the mass of the neutrino is much smaller than those of charged leptons and quarks and there is no explanation of the very small value of y that is needed.

1.2 Majorana neutrinos

In 1937, E. Majorana [2] ~~discovered~~ that a four-component spinor ~~is~~ necessary for the description of a neutral massive fermion as in ~~the Dirac~~ theory. ~~It is sufficient a two-component spinor if we put the so-called Majorana condition~~

$$\psi_L = \psi^C, \tag{1.3}$$

where ψ is the fermion field and ψ^C is the charged conjugated field defined as

$$\psi^C = \mathcal{C}\,\overline{\psi}^T, \tag{1.4}$$

in which $\mathcal{C}$ is the charge conjugation operator[1]. Eq. (1.3) implies the equality of particle and antiparticle.

Applying the operator P_L defined in (1.2) to Eq. (1.3), we obtain:

$$\psi_L = \psi_R^C. \tag{1.5}$$

This equation shows that ψ_L and ψ_R are not independent and therefore we can write the fermion field ~~only with~~ the two independent components of ψ_L (or equivalently ψ_R), e.g.

$$\psi = \psi_L + \psi_L^C. \tag{1.6}$$

We can construct a mass Lagrangian for a Majorana fermion in the following way:

$$\mathcal{L}_M = -m_M(\overline{\nu_L^C}\nu_L + \overline{\nu_L}\nu_L^C), \tag{1.7}$$

where we have introduced an overall factor $1/2$ in order to obtain the correct equations of motion. Note that the Majorana mass term in Eq. (1.7), contrary to the Dirac mass term in Eq. (1.1), is not invariant under the global $U(1)$ gauge transformation $\nu_L \to e^{i\phi}\nu_L$. This implies that, for the Majorana case, the conservation of the total lepton unmber can be violated.

1.3 One-generation Dirac-Majorana mass term

In this section we want to construct the neutrino mass Lagrangian considering, for simplicity, only one generation. In the most genral case, in which there exist both the left-handed neutrino field ν_L and the right-handed neutrino field ν_R, the neutrino mass term can be written as

$$\mathcal{L}_{\text{mass}} = \mathcal{L}_D + \mathcal{L}_M^L + \mathcal{L}_M^R, \tag{1.8}$$

where

$$\mathcal{L}_D = -m_D\overline{\nu_R}\nu_L + \text{h.c.} \tag{1.9}$$

---

[1] The charge conjugation operator satisfies the following relations:

$$\mathcal{C}\,\gamma^{\mu\,T}\,\mathcal{C}^{-1} = -\gamma^\mu, \quad \mathcal{C}^\dagger = \mathcal{C}^{-1}, \quad \mathcal{C}^T = -\mathcal{C}.$$

is the Dirac mass term and

$$\mathcal{L}_M^L = -\frac{1}{2} m_L \overline{\nu_L^C} \nu_L + \text{h.c.} = \frac{1}{2} m_L \nu_L^T \mathcal{C}^\dagger \nu_L + \text{h.c.},\tag{1.10}$$

$$\mathcal{L}_M^R = -\frac{1}{2} m_R \overline{\nu_R^C} \nu_R + \text{h.c.} = \frac{1}{2} m_L \nu_R^T \mathcal{C}^\dagger \nu_R + \text{h.c.}\tag{1.11}$$

are the Majorana mass terms for the left-handed and right-handed fields respectively. If we define the column matrix of left-handed chiral fields

$$N_L = \begin{pmatrix} \nu_L \\ \nu_R^C \end{pmatrix} = \begin{pmatrix} \nu_L \\ \mathcal{C}\overline{\nu_R}^T \end{pmatrix},\tag{1.12}$$

eq. (1.8) can be rewritten in the following way:

$$\mathcal{L}_{\text{mass}} = \frac{1}{2} N_L^T \, \mathcal{C}^\dagger \, M \, N_L + \text{h.c.},\tag{1.13}$$

where

$$M = \begin{pmatrix} m_L & m_D \\ m_D & m_R \end{pmatrix}\tag{1.14}$$

is the mass matrix.

From (1.13) it is clear that the chiral fields ν_L and ν_R do not have a definite mass, because of the off-diagonal term m_D. In order to find the massive neutrinos fields, we have to diagonalize the mass matrix in (1.14). The matrix M is a symmetric complex matrix and it can be diagonalized with a unitary transformation of the chiral fields ($U^\dagger = U^{-1}$), i.e.

$$N_L = U \, n_L,\tag{1.15}$$

where

$$n_L = \begin{pmatrix} \nu_{1L} \\ \nu_{2L} \end{pmatrix}\tag{1.16}$$

is the column matrix of left-handed massive neutrino fields. The unitary matrix U must be such that

$$U^T \, M \, U = \begin{pmatrix} m_1 & 0 \\ 0 & m_2 \end{pmatrix},\tag{1.17}$$

with m_1, m_2 real and positive.

Using the transformation (1.15), the mass term in (1.13) can be rewritten as

$$\mathcal{L}_{\text{mass}} = \frac{1}{2} \sum_{k=1}^{2} m_k \nu_{kL}^T \mathcal{C}^\dagger \nu_{kL} + \text{h.c.} = -\frac{1}{2} \sum_{k=1}^{2} m_k \overline{\nu_k} \nu_k,\tag{1.18}$$

where we have defined the Majorana massive neutrino field

$$\nu_k = \nu_{kL} + \nu_{kL}^C = \nu_{kL} + \mathcal{C}\overline{\nu_{kL}}^T.\tag{1.19}$$

Hence, a Dirac-Majorana mass term implies that massive ~~neutrino~~ are Majorana particles.

In order to determine the values of the masses m_k, let us consider the simplest case in which M is a real matrix. The unitary matrix U can be written as

$$U = \mathcal{O} \rho, \tag{1.20}$$

where

$$\mathcal{O} = \begin{pmatrix} \cos\theta & \sin\theta \\ -\sin\theta & \cos\theta \end{pmatrix} \tag{1.21}$$

is an orthogonal 2×2 matrix and

$$\rho = \begin{pmatrix} \rho_1 & 0 \\ 0 & \rho_2 \end{pmatrix} \tag{1.22}$$

is a diagonal matrix of phases with $\rho_k^2 = 1$. The matrix $\mathcal{O}$ is such that

$$\mathcal{O}^T M \mathcal{O} = \begin{pmatrix} m'_1 & 0 \\ 0 & m'_2 \end{pmatrix}, \tag{1.23}$$

where m'_1 and m'_2 are the eigenvalues of the mass matrix given by

$$m'_{2,1} = \frac{1}{2} \left[m_L + m_R \pm \sqrt{(m_L - m_R)^2 + 4m_D^2} \right]. \tag{1.24}$$

The mixing angle θ in (1.21) is such that

$$\tan 2\theta = \frac{2m_D}{m_R - m_L}. \tag{1.25}$$

Note that the role of the matrix ρ is to change the sign of m'_1 when it is negative, in fact, from Eq. (1.17), we have:

$$U^T M U = \rho^T R^T M R \rho = \begin{pmatrix} \rho_1^2 m'_1 & 0 \\ 0 & \rho_2^2 m'_2 \end{pmatrix}. \tag{1.26}$$

Hence, the two real and positive masses are given by

$$m_k = \rho_k^2 m'_k, \tag{1.27}$$

with $\rho_2^2 = 1$ (from Eq. (1.24) follows that m'_2 is always positive), $\rho_1^2 = 1$ if $m'_1 > 0$ and $\rho_1^2 = -1$ if $m'_1 < 0$.

1.4 The seesaw mechanism

Let us consider the neutrino mass Lagrangian (1.13) in the framework of the Standard Model:

- m_D is allowed because it is generated with the Higgs mechanism;

- m_L must vanish, in fact the mass term $\overline{\nu_L^C} \nu_L$ is not invariant under $SU(2)_L$ because ν_L has third component I_3 of the weak isospin equal to $1/2$, therefore $\overline{\nu_L^C} \nu_L$ has $I_3 = 1$;

- ν_R is a weak isospin singlet. As a consequence, and in constrast with m_D or m_L, the mass parameter m_R is ~~therefore~~ not connected to a Higgs vacuum expectation value, and could be arbitrarily high.

Hence

$$m_L \simeq 0, \qquad m_D \ll m_R \,. \tag{1.28}$$

From Eqs. (1.24), (1.27), (1.25) ~~and taking in~~ mind that, since m_1' is negative, $\rho_1^2 = -1$, we get

$$m_1 \simeq \frac{m_D^2}{m_R} \,, \tag{1.29}$$

$$m_2 \simeq m_R \,, \tag{1.30}$$

$$\tan 2\theta = 2\frac{m_D}{m_R} \ll 1 \,. \tag{1.31}$$

This is the so-called seesaw mechanism: the heavier ν_2 ~~is~~, the lighter ν_1 is the smallness of the mixing angle implies that ν_1 is composed mainly of active ν_L and ν_2 is composed mainly of sterile ν_R:

$$\nu_{1L} \simeq -i\nu_L \,, \qquad \nu_{2L} \simeq \nu_R^C \,. \tag{1.32}$$

The seesaw mechanism is very important because it gives an explanation of the smallness of the neutrino mass with respect to the masses of the charged leptons and quarks.

1.5   Three-generation Dirac-Majorana mixing

The aim of this section is to extend the theory of the neutrino mixing discussed above, to the case of three generations of left-handed neutrinos. The three known active left-handed neutrino fields are ν_{eL}, $\nu_{\mu L}$, $\nu_{\tau L}$; in addition we can consider N_s sterile right-handed neutrino fields ν_{sR}, with $s = s_1, \ldots, s_{N_s}$. We will now consider, for semplicity, only three sterile right-handed neutrino fields ν_{s1}, ν_{s2}, ν_{s3}.

The most general mass term is always the Dirac-Majorana mass term

$$\mathcal{L}_{\text{mass}} = \mathcal{L}_D + \mathcal{L}_M^{\text{left}} + \mathcal{L}_M^{\text{right}} \,, \tag{1.33}$$

with the Dirac mass term

$$\mathcal{L}_D = - \sum_{s=s_1,s_2,s_3} \sum_{\alpha=e,\mu,\tau} \overline{\nu_{sR}} \, M_{s\alpha}^D \, \nu_{\alpha L} + \text{h.c.} \tag{1.34}$$

and the ~~majorana~~ mass terms

$$\mathcal{L}_M^{\text{left}} = \frac{1}{2} \sum_{\alpha,\beta=e,\mu,\tau} \nu_{\alpha L}^T \, \mathcal{C}^\dagger \, M_{\alpha\beta}^L \, \nu_{\beta L} + \text{h.c.} \,, \tag{1.35}$$

$$\mathcal{L}_M^{\text{right}} = \frac{1}{2} \sum_{s,s'=s_1,s_2,s_3} \nu_{sR}^T \mathcal{C}^\dagger \, M_{ss'}^R \, \nu_{s'R} + \text{h.c.} \,. \tag{1.36}$$

All the three mass matrices M^L, M^R and M^D are complex; the Majorana mass matrices M^L and M^R are also symmetric.

Eq. (1.33) can be rewritten as

$$\mathcal{L}_{\text{mass}} = \frac{1}{2} N_L^T \, \mathcal{C}^\dagger \, M N_L + \text{h.c.}\,, \tag{1.37}$$

where we have defined

$$N_L = \begin{pmatrix} \nu_L \\ \nu_R^C \end{pmatrix}, \tag{1.38}$$

with

$$\nu_L = \begin{pmatrix} \nu_{eL} \\ \nu_{\mu L} \\ \nu_{\tau L} \end{pmatrix}, \qquad \nu_R^C = \begin{pmatrix} \nu_{s1R}^C \\ \nu_{s2R}^C \\ \nu_{s3R}^C \end{pmatrix}; \tag{1.39}$$

and the Dirac-Majorana mass matrix is given by

$$M = \begin{pmatrix} M^L & (M^D)^T \\ M^D & M^R \end{pmatrix}. \tag{1.40}$$

In order to find the mass eigenstates, we have to diagonalize M in (1.40). This can be done defining the left-handed flavor fields as unitary linear combinations of the left-handed components of the 6 fields with definite mass:

$$N_L = V \, n_L\,, \qquad \text{with} \quad n_L = \begin{pmatrix} \nu_{1L} \\ \vdots \\ \nu_{6L} \end{pmatrix}. \tag{1.41}$$

The unitary matrix V is chosen such that

$$V^T M V = \begin{pmatrix} m_1 & 0 & \dots & 0 \\ 0 & m_2 & \dots & 0 \\ \vdots & \vdots & \ddots & \vdots \\ 0 & 0 & \dots & m_6 \end{pmatrix}, \tag{1.42}$$

with m_k $(k = 1, \dots, 6)$ real and positive. In this way the Dirac-Majorana mass term in Eq. (1.33) becomes:

$$\mathcal{L}_{\text{mass}} = -\frac{1}{2} \sum_{k=1}^{6} m_k \overline{\nu_{kL}^C} \nu_{kL} + \text{h.c.} = -\frac{1}{2} \sum_{k=1}^{6} m_k \overline{\nu_k} \nu_k\,, \tag{1.43}$$

where

$$\nu = \begin{pmatrix} \nu_1 \\ \vdots \\ \nu_6 \end{pmatrix} \tag{1.44}$$

are Majorana neutrino fields:

$$\nu_k = \nu_{kL} + \nu_{kL}^C = \nu_{kL} + \mathcal{C}\overline{\nu_{kL}}^T\,, \qquad \text{with} \quad \nu_k^C = \nu_k\,. \tag{1.45}$$

The mixing of active and sterile neutrinos is explicitly given by

$$\nu_{\alpha L} = \sum_{k=1}^{6} V_{\alpha k} \nu_{kL} \qquad (\alpha = e, \mu, \tau), \qquad (1.46)$$

$$\nu_{sR}^{C} = \sum_{k=1}^{6} V_{sk} \nu_{kL} \qquad (s = s_1, s_2, s_3), \qquad (1.47)$$

which implies the possibility of oscillations between active and sterile states.

Now we want to generalize the seesaw mechanism discussed in the previous section to the case of three generations. Therefore we consider the case in wich, in Eq. (1.40), $M^L = 0$ and the eigenvalues of M^R are much larger than all the eigenvalues of M^D. In this way, the mixing matrix V can be written as

$$V = W U, \qquad (1.48)$$

where the matrices W and U are unitary; specifically W is such that the mass matrix can be diagonalized by blocks, up to corrections of the order $(M^R)^{-1} M^D$ [3]:

$$W^T M W \simeq \begin{pmatrix} M_{\text{light}} & 0 \\ 0 & M_{\text{heavy}} \end{pmatrix}. \qquad (1.49)$$

The 3×3 mass matrices M_{light} and M_{heavy} are given by

$$M_{\text{light}} \simeq -(M^D)^T (M^R)^{-1} M^D, \quad M_{\text{heavy}} \simeq M^R. \qquad (1.50)$$

The heavy masses are given by the eigenvalues of M^R, whereas the light masses are given by the eigenvalues of M_{light}. Eq. (1.50) realizes the seesaw mechanism in the case of three generations. Since the off-diagonal terms of W are of order of $(M^R)^{-1} M^D$, M_{light} and M_{heavy} are decoupled in low energies processes. Hence, in the Standard Model, we consider M_{light}:

$$U^\dagger M_{\text{light}} U = \begin{pmatrix} m_1 & 0 & 0 \\ 0 & m_2 & 0 \\ 0 & 0 & m_3 \end{pmatrix}, \qquad (1.51)$$

wich implies the mixing

$$\nu_{\alpha L} = \sum_{k=1}^{3} U_{\alpha k} \nu_{kL} \qquad (\alpha = e, \mu, \tau). \qquad (1.52)$$

The 3×3 unitary mixing matrix U, also known as PMNS matrix, has 9 independent real parameters: 3 mixing angles and 6 phases. This matrix is equal to the CKM mixing matrix of quarks apart from the fact that, in our case, we must consider the Majorana nature of the neutrinos. Regarding the CKM, five of the six phases are not physical because they can be eliminated by a suitable transformation of the quark fields, which leave the Lagrangian invariant. Similar arguments can be applied to the mixing of three Dirac neutrinos. Since in the Majorana case the mass term is not invariant under a phase transformation, the left-handed massive

neutrino fields cannot rephased in order to eliminate two phases. This implies that the 3×3 mixing matrix of Majorana neutrinos U depends on three mixing physical CP-violating phases. Hence we can write:

$$U = U^D D^M \,, \tag{1.53}$$

where U^D contains the so-called Dirac phase, and D^M contains the so-called Majorana phases.

A convenient parameterization for U^D is:

$$U^D = \begin{pmatrix} c_{12}c_{13} & s_{12}c_{13} & s_{13}e^{-i\delta_{13}} \\ -s_{12}c_{23} - c_{12}s_{23}s_{13}e^{i\delta_{13}} & c_{12}c_{23} - s_{12}s_{23}s_{13}e^{i\delta_{13}} & s_{23}c_{13} \\ s_{12}s_{23} - c_{12}c_{23}s_{13}e^{i\delta_{13}} & -c_{12}s_{23} - s_{12}c_{23}s_{13}e^{i\delta_{13}} & c_{23}c_{13} \end{pmatrix} \,. \tag{1.54}$$

where $c_{ab} \equiv \cos\theta_{ab}$ and $s_{ab} \equiv \sin\theta_{ab}$. θ_{12}, θ_{13}, θ_{23} are the three mixing angles ($0 \le \theta_{ab} \le \pi/2$) and δ_{13} is the Dirac CP-violating phase ($0 \le \delta_{13} < 2\pi$).

The diagonal unitary matrix D^M can be written as

$$D^M = \begin{pmatrix} 1 & 0 & 0 \\ 0 & e^{i\lambda_{21}} & 0 \\ 0 & 0 & e^{i\lambda_{31}} \end{pmatrix} \,, \tag{1.55}$$

where λ_{21} and λ_{31} are the two physical Majorana CP-violating phases.

1.6 Neutrino oscillation in vacuum

Neutrino oscillation is a phenomenon in which a neutrino created with a specific flavor state, becomes a neutrino with a different flavor state. In order to find the transition probability of this kind of process, let us consider the following weak interaction process:

$$A \to B + \alpha^+ + \nu_\alpha \,, \tag{1.56}$$

the neutrino created together with the charged lepton α^+ is described by the flavor states

$$|\nu_\alpha\rangle = \sum_k U^*_{\alpha k} |\nu_k\rangle \qquad (\alpha = e, \mu, \tau) \,; \tag{1.57}$$

inverting Eq. (1.57) we get the mass states

$$|\nu_k\rangle = \sum_\alpha U_{\alpha k} |\nu_\alpha\rangle \,. \tag{1.58}$$

The time evolution of the flavor state is given by

$$|\nu_\alpha(t)\rangle = \sum_k U^*_{\alpha k} e^{-iE_k t} |\nu_k\rangle \tag{1.59}$$

and, substituting Eq. (1.58) into Eq. (1.59), we obtain

$$|\nu_\alpha(t)\rangle = \sum_{\beta=e,\mu,\tau} \left(\sum_k U^*_{\alpha k} e^{-iE_k t} U_{\beta k} \right) |\nu_\beta\rangle \,. \tag{1.60}$$

Since the mixing matrix U is not diagonal, after a time t, a pure flavor state becomes a superposition of different flavor states. Hence, the amplitude of transitions between two different flavor states $\nu_\alpha \to \nu_\beta$ as a function of time is given by

$$A_{\nu_\alpha \to \nu_\beta}(t) \equiv \langle \nu_\beta | \nu_\alpha(t) \rangle = \sum_k U_{\alpha k}^* U_{\beta k} e^{-iE_k t} \,. \tag{1.61}$$

The tranistion probability is then

$$P_{\nu_\alpha \to \nu_\beta}(t) = \left| A_{\nu_\alpha \to \nu_\beta}(t) \right|^2 = \sum_{k,j} U_{\alpha k}^* U_{\beta k} U_{\alpha j} U_{\beta j}^* e^{-i(E_k - E_j)t} \,. \tag{1.62}$$

Since in oscillation experiments neutrinos are ultrarelativistic particles, the dispersion relation can be approximated by

$$E_k \simeq E + \frac{m_k^2}{2E} \,, \tag{1.63}$$

where E is the neutrino energy neglecting the mass contribution. Hence, in Eq. (1.62), we have

$$E_k - E_j \simeq \frac{\Delta m_{kj}^2}{2E} \,, \tag{1.64}$$

in which Δm_{kj}^2 is the squared-mass difference

$$\Delta m_{kj}^2 \equiv m_k^2 - m_j^2 \,. \tag{1.65}$$

In neutrino oscillation experiments the propagation time t is not measured, only the distance L between the source and the detector is known. Since ultrarelativistic neutrinos propagate almost at the speed of light, we can approximate $t \simeq L$. Therefore the transition probability in Eq. (1.62) can be written as

$$P_{\nu_\alpha \to \nu_\beta}(L, E) = \sum_{k,j} U_{\alpha k}^* U_{\beta k} U_{\alpha j} U_{\beta j}^* \exp\left(-i \frac{\Delta m_{kj}^2 L}{2E} \right) \,. \tag{1.66}$$

This equation shows that the phases of neutrino oscillations

$$\Phi_{kj} = -i \frac{\Delta m_{kj}^2 L}{2E} \tag{1.67}$$

are determined by the two quantities depending on the experiment L, E and by the squared-mass differences Δm_{kj} which are physical constants. Instead, the amplitude of oscillations are determined by the elements of the mixing matrix U, which are constants of nature.

Let us now conisder the case of two-neutrino mixing[2]. We have two flavor neutrino states ν_α and ν_β which are linear combinations of the two massive neutrinos ν_1 and ν_2. The mixing matrix U can be parameterized in the following way:

$$U = \begin{pmatrix} \cos\theta & \sin\theta \\ -\sin\theta & \cos\theta \end{pmatrix} \,. \tag{1.68}$$

---

[2]This approximation is very useful because the oscillation formulas are very simpler and many experiments are not sensitive to the influence of three-neutrino mixing.

From Eq. (1.66), we can derive the tranistion probability

$$P_{\nu_\alpha \to \nu_\beta}(L, E) = \sin^2 2\theta \, \sin^2 \left(\frac{\Delta m^2 L}{4E} \right) , \qquad (1.69)$$

where

$$\Delta m^2 \equiv \Delta m_{21}^2 \equiv m_2^2 - m_1^2 . \qquad (1.70)$$

The transition probability in Eq. (1.69) can be measured if

$$\frac{\Delta m^2 L}{4E} \gtrsim 0.1 \div 1 ; \qquad (1.71)$$

Since the value of Δm^2 is fixed, different experiments can be designed in order to be sensitive to different values of Δm^2, by choosing appropriate values of the ratio L/E.

- **Short-BaseLine experiments (SBL)**, with $L/E \lesssim 1\,\mathrm{eV}^{-2}$ and the associated sensitivity $\Delta m^2 \gtrsim 0.1\,\mathrm{eV}^2$;

- **Long-BaseLine experiments (LBL) and atmospheric neutrinos experiments**, with $L/E \lesssim 10^4\,\mathrm{eV}^{-2}$ and the associated sensitivity $\Delta m^2 \gtrsim 10^{-4}\,\mathrm{eV}^2$;

- **Very Long-BaseLine experiments (VLBL) and solar neutrinos experiments**, with $L/E \lesssim 3 \times 10^5\,\mathrm{eV}^{-2}$ and the associated sensitivity $\Delta m^2 \gtrsim 3 \times 10^{-5}\,\mathrm{eV}^2$.

Atmospheric and solar experiments have measured two different mass splittings, currently their values are:

$$\Delta m_{\mathrm{atm}}^2 = m_2^2 - m_1^2 = (2.35^{+0.12}_{-0.09}) \times 10^{-3}\,\mathrm{eV}^2 , \qquad (1.72)$$

$$|\Delta m_{\mathrm{sol}}^2| = |m_3^2 - (m_1^2 + m_2^2)/2| = (7.58^{+0.22}_{-0.26}) \times 10^{-5}\,\mathrm{eV}^2 , \qquad (1.73)$$

respectively. The best-fit values and 1σ ranges quoted were obtained from s recent global 3-neutrino fit [4]. Note that $\Delta m_{\mathrm{atm}}^2 \gg |\Delta m_{\mathrm{sol}}^2|$. These data are compatible with two different mass orderings: the *normal* and *inverted* orderings (see Fig. 1.1). In the first case $|\Delta m_{\mathrm{sol}}^2|$ corresponds to the gap between the two lightest mass eigenstates, while in the second case $|\Delta m_{\mathrm{sol}}^2|$ corresponds to the gap between the two heaviest mass eigenvalues. Therefore, to complete our knowledge on neutrino masses, we need two pieces of information: the neutrino mass ordering and the absolute value of the lightest neutrino mass. The latter can be obtained from neutrinoless double beta decay searches, to be discussed in the following Chapters.
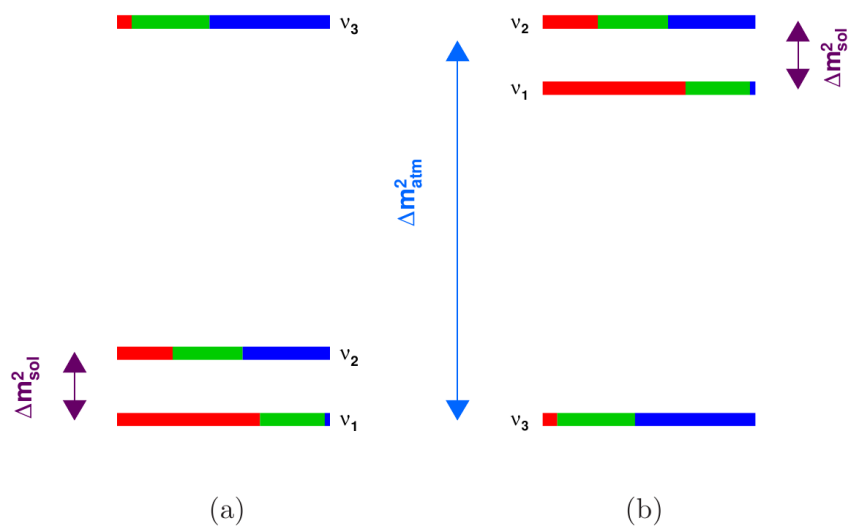
Figure 1.1. Knowledge on neutrino masses and mixings from neutrino oscillation experiments. Panels (a) and (b) show the normal and inverted mass orderings, respectively. Neutrino masses increase from bottom to top. The electron, muon and tau flavor content of each neutrino mass eigenstate is shown via the red, green and blue fractions, respectively.

Chapter 2

Beta decays

The aim of this Chapter is to describe the main features of beta decays. For pedagogical purposes we will first focus the single beta decay based on the Fermi theory and extend the analysis to both two-neutrino and neutrinoless double beta decay, pointing out the differences between the two processes.

In our discussion we will use the interaction Lagrangian first proposed by Fermi:

$$
\begin{aligned}
\mathcal{L}_F(x) &= \frac{G}{2}\left[\overline{N}(x)\tau^+\gamma^\mu(g_V - g_A\gamma_5)N(x)\right]\left[\overline{e}(x)\gamma_\mu(1-\gamma_5)\nu(x)\right] + \text{h.c.} \\
&= \frac{G}{2}J^\mu(x)j_\mu(x) + \text{h.c.} .
\end{aligned}
\tag{2.1}
$$

In the above equation, $G = G_F\cos\theta_C = 1.15 \times 10^{-5}\,\text{GeV}^{-2}$, G_F being the Fermi weak coupling constant, θ_C the Cabibbo angle, $g_V = 1$ and $g_A = 1.25$. The nucleon field is defined as an isospin doublet

$$
N = \begin{pmatrix} p \\ n \end{pmatrix},
\tag{2.2}
$$

where p and n are the proton and neutron field, respectively, while τ^+ is the isospin raising operator; e and ν are the electron and neutrino fields, respectively. The Fermi Lagrangian violates charge conjugation and, due to its $V - A$ nature, parity.

2.1 Single beta decay

Single β^- (β^+) decay is a process in which a parent nucleus $\mathcal{N}$ with mass number A and atomic number Z decays into a daughter nucleus $\mathcal{N}'$ with same mass number but atomic number increased (decreased) by one unit and emits an electron (positron) and an antineutrino (neutrino), i.e.

$$
\mathcal{N}(A, Z) \rightarrow \mathcal{N}'(A, Z+1) + e^- + \overline{\nu}_e \qquad (\beta^-),
\tag{2.3}
$$

$$
\mathcal{N}(A, Z) \rightarrow \mathcal{N}'(A, Z-1) + e^+ + \nu_e \qquad (\beta^+).
\tag{2.4}
$$

In the following, let us consider the β^- decay (an analogous calculation holds for the β^+ decay). The Fermi Lagrangian in Eq. (2.1), being an effective interaction term, can be used in the limit of low momentum transfer. Using relativistic perturbation

theory at first order, the expression for the S matrix element for the β^- decay is given by

$$S_\beta = i \int d^4x \, \langle e, \overline{\nu}_e, \mathcal{N}' | \mathcal{L}_F(x) | \mathcal{N} \rangle = (2\pi)^4 \delta^{(4)}(P_f - P_i) \mathcal{M}_{if} \,, \qquad (2.5)$$

where P_i and P_f denote the total four-momentum of initial and final states, respectively and $\mathcal{M}_{if}$ the Feynman amplitude. The differential decay rate of the process is given by

$$d\Gamma_\beta = \frac{1}{2s_\mathcal{N}+1} \sum_{s_\mathcal{N},s_{\mathcal{N}'}} \sum_{s_e,s_\nu} |S_\beta|^2 F(Z,E_e) \frac{d^3p_e}{(2\pi)^3} \frac{d^3p_\nu}{(2\pi)^3} \,, \qquad (2.6)$$

where $s_\mathcal{N}$ and $s_{\mathcal{N}'}$ are the spins of the initial and final nucleus, respectively, while $P_e = (E_e, \mathbf{p}_e)$, s_e, $P_\nu = (E_\nu, \mathbf{p}_\nu)$ and s_ν denote the four-momenta and spins of the electron and the antineutrino, respectively. The function $F(Z, E_e)$, called Fermi factor, results from the effect of the Coulomb field of the daughter nucleus on the emitted electron [1]. The amplitude $\mathcal{M}_{if}$ can be written in the form:

$$\mathcal{M}_{if} = \frac{G}{\sqrt{2}} \langle \Psi_{\mathcal{N}'} | \sum_{n=1}^{A} J_n^\mu | \Psi_\mathcal{N} \rangle \langle e, \overline{\nu} | j_\mu | 0 \rangle =$$

$$= \frac{G}{\sqrt{2}} \langle \Psi_{\mathcal{N}'} | \sum_{n=1}^{A} J_n^\mu | \Psi_\mathcal{N} \rangle \frac{1}{2\sqrt{E_e E_\nu}} \overline{u}_e \gamma_\mu (1 - \gamma_5) v_\nu \,, \qquad (2.8)$$

where, in the non relativistic limit,

$$\langle \Psi_{\mathcal{N}'} | \sum_{n=1}^{A} J_n^\mu | \Psi_\mathcal{N} \rangle = \langle \Psi_{\mathcal{N}'} | \sum_{n=1}^{A} \left(g_V \delta^{\mu 0} + g_A \delta^{\mu i} \sigma_n^i \right) \tau_n^+ | \Psi_\mathcal{N} \rangle \,, \qquad (2.9)$$

$\Psi_\mathcal{N}$ and $\Psi_{\mathcal{N}'}$ being the wave functions characterizing the states of the initial and final nucleus, respectively, and σ^i ($i = 1, 2, 3$) are the spin Pauli matrices.

Using the above results we can finally obtain the halflife for neutron beta decay in the form:

$$\frac{\ln 2}{T_{1/2}^\beta} = \int d\Gamma_\beta = \frac{1}{(2\pi)^2} \int F(Z, E_e) |\mathbf{p}_e| E_e E_\nu^2$$

$$\times \left[g_V^2 \left(1 + \frac{\mathbf{p}_e \cdot \mathbf{p}_\nu}{E_e E_\nu} \right) |M_\beta^F|^2 + g_A^2 \left(1 - \frac{1}{3} \frac{\mathbf{p}_e \cdot \mathbf{p}_\nu}{E_e E_\nu} \right) |M_\beta^{GT}|^2 \right] dE_e d\Omega_e d\Omega_\nu \quad (2.10)$$

where $E_\nu = E_0 - E_e$, E_0 being the total energy released in the decay process. In Eq. (2.10), $|M_\beta^F|^2$ and $|M_\beta^{GT}|^2$ are the square moduli of the single β decay Fermi and

---

[1]The Fermi factor is approximately given by

$$F(Z, E_e) = \left(\pm \frac{2\pi Z e^2}{v} \right) \frac{1}{1 - e^{\mp 2\pi Z e^2/v}} \quad \text{for } \beta^\mp \qquad (2.7)$$

where $v = |\mathbf{p}_e|/E_e$ is the velocity of the electron. Note that the Fermi factor enhances the probability of β^- emission and decreases that of β^+ especially at low energies.

Gamow-Teller nuclear matrix elements, respectively, defined as

$$|M_\beta^F|^2 = |\langle \Psi_{\mathcal{N}'}| \sum_{n=1}^{A} \tau_n^+ |\Psi_\mathcal{N}\rangle|^2 \,, \tag{2.11}$$

$$|M_\beta^{GT}|^2 = |\langle \Psi_{\mathcal{N}'}| \sum_{n=1}^{A} \tau_n^+ \boldsymbol{\sigma}_n |\Psi_\mathcal{N}\rangle|^2 \,. \tag{2.12}$$

2.2 Double beta decay

Double beta decay is a rare nuclear transition in which a parent nucleus with Z protons decays into a daughter nucleus with $Z + 2$ protons and the same mass number A. The decay can occur only if the initial nucleus is less bound than the final nucleus, and both more bound than the intermediate one. Such a condition, in nature, is satisfied for many even-even nuclei, but it is not for all the odd-odd ones because of the nuclear paring force (see Section 3.1). The decay can usually proceed from the ground state of the initial nucleus with spin and parity always 0^+, to the ground state of the final nucleus with 0^+, although, in some cases, decays into excited states with 0^+ or 2^+ are energetically possible.

Double beta decays are second order processes in the weak interaction and can occur in two modes: the two-neutrino double beta decay ($2\beta_{2\nu}$) and the neutrinoless double beta decay ($2\beta_{0\nu}$). The $2\beta_{2\nu}$ decay, first proposed by M. Goeppert-Mayer in 1935 [5], is a process of the type

$$\mathcal{N}(A, Z) \to \mathcal{N}'(A, Z + 2) + e_1^- + e_2^- + \overline{\nu}_{e1} + \overline{\nu}_{e2} \qquad (2\beta_{2\nu}^-) \,, \tag{2.13}$$
$$\mathcal{N}(A, Z) \to \mathcal{N}'(A, Z - 2) + e_1^+ + e_2^+ + \nu_{e1} + \nu_{e2} \qquad (2\beta_{2\nu}^+) \,, \tag{2.14}$$

and it consists of the simultaneous beta decay of two neutrons in a nucleus.

The $2\beta_{0\nu}$ decay, first proposed by W. H. Furry in 1939 [6], is a process of the type

$$\mathcal{N}(A, Z) \to \mathcal{N}'(A, Z + 2) + e_1^- + e_2^- \qquad (2\beta_{0\nu}^-) \,, \tag{2.15}$$
$$\mathcal{N}(A, Z) \to \mathcal{N}'(A, Z - 2) + e_1^+ + e_2^+ \qquad (2\beta_{0\nu}^+) \,. \tag{2.16}$$

$2\beta_{0\nu}$ decays are possible if neutrinos are massive Majorana particles and, for this reason, are forbidden in the Standard Model.

The Q-value of 2β decays (the recoil energy of the final nucleus is negligible) is given by

$$Q_{2\beta} = M_\mathcal{N} - M_{\mathcal{N}'} - 2m_e \,, \tag{2.17}$$

where $M_\mathcal{N}$ and $M_{\mathcal{N}'}$ are the masses of the initial and final nuclei, respectively, and m_e is the electron mass. Since the $2\beta_{2\nu}$ decays have a four-body leptonic final state, the sum of the kinetic energies of the two decay electrons have a continuous spectrum from zero to the Q-value, while in the $2\beta_{0\nu}$ decays the sum of the kinetic energies of the two decay electrons is equal to the Q-value.

Other details regarding the properties of $2\beta_{2\nu}$ and $2\beta_{0\nu}$ will be provided in the following Subsections.

2.2.1 Two-neutrino double beta decay

The $2\beta_{2\nu}$ is a second order process in the weak interaction, therefore in the case of $2\beta_{2\nu}$ (2.13) the transition matrix element reads (the Feynman diagram is depicted in Fig. 2.1):

$$S_{2\nu} = - \int d^4x\, d^4y\, \langle e_1, e_2, \overline{\nu}_{e1}, \overline{\nu}_{e2}, \mathcal{N}' | T\left\{ \mathcal{L}_F(x)\mathcal{L}_F(y) \right\} | \mathcal{N} \rangle . \qquad (2.18)$$

The amplitude consists of a lepton part

$$L_{\rho\sigma} = \langle e_1, e_2, \overline{\nu}_{e1}, \overline{\nu}_{e2} | j_\rho(x) j_\sigma(y) | 0 \rangle = \langle e_1, \overline{\nu}_{e1} | j_\rho(x) | 0 \rangle \langle e_2, \overline{\nu}_{e2} | j_\sigma(y) | 0 \rangle \qquad (2.19)$$

and an hadronic part

$$H^{\rho\sigma} = \langle \Psi_{\mathcal{N}'} | J_A^\rho(x) J_A^\sigma(y) | \Psi_{\mathcal{N}} \rangle , \qquad (2.20)$$

with

$$J_A^\rho = \sum_{n=1}^{A} J_n^\rho . \qquad (2.21)$$

The calculation of $L_{\rho\sigma}$ is straightforward (see the previous Section), and gives the result

$$L_{\rho\sigma} = \frac{1}{4} \frac{1}{\sqrt{E_{e_1} E_{\nu_1}}} \frac{1}{\sqrt{E_{e_1} E_{\nu_1}}} \overline{u}_{e_1} \gamma_\mu \left(1 - \gamma_5\right) v_{\nu_1} \overline{u}_{e_2} \gamma_\mu \left(1 - \gamma_5\right) v_{\nu_2} e^{i(P_{e_1} + P_{\nu_1})x} e^{i(P_{e_2} + P_{\nu_2})y} . \qquad (2.22)$$

In the calculation of the hadronic contribution we have to take into account the fact that beta decay processes involve a neutron belonging to the unobserved intermediate state. Hence we write

$$H^{\rho\sigma} = \sum_m \langle \Psi_{\mathcal{N}'} | J_A^\rho(x) | \Psi_m \rangle \langle \Psi_m | J_A^\sigma(y) | \Psi_{\mathcal{N}} \rangle \qquad (2.23)$$

where Ψ_m is a complete set of states of the intermediate $(A, Z+1)$ nucleus. The time dependence of $H^{\rho\sigma}$ can be factorized according to

$$H^{\rho\sigma} = \sum_m e^{i(E_{\mathcal{N}'} - E_m)x_0} e^{i(E_m - E_{\mathcal{N}})y_0} \langle \Psi_{\mathcal{N}'} | J^\rho(\mathbf{x})_A | \Psi_m \rangle \langle \Psi_m | J^\sigma(\mathbf{y})_A | \Psi_{\mathcal{N}} \rangle \qquad (2.24)$$

and combined with the time dependence of $L_{\rho\sigma}$. Carrying out the x_0 and y_0 integrations, taking into account the time ordering operator and exchange term, we find

$$\int dx_0 dy_0\, T \left\{ \sum_m \langle \Psi_{\mathcal{N}'} | J_A^\rho(x) | \Psi_m \rangle \langle \Psi_m | J_A^\sigma(y) | \Psi_{\mathcal{N}} \rangle\, e^{i(E_{e_1} + E_{\nu_1})x_0} e^{i(E_{e_2} + E_{\nu_2})y_0} \right\} =$$

$$= (2\pi)\, \delta\left(E_{\mathcal{N}'} + E_{e_1} + E_{\nu_1} + E_{e_2} + E_{\nu_2} - E_{\mathcal{N}} \right)$$

$$\times \sum_m \left[\frac{\langle \Psi_{\mathcal{N}'} | J_A^\rho(\mathbf{x}) | \Psi_m \rangle \langle \Psi_m | J_A^\sigma(\mathbf{y}) | \Psi_{\mathcal{N}} \rangle}{E_m + E_{e_2} + E_{\nu_2} - E_{\mathcal{N}}} + \frac{\langle \Psi_{\mathcal{N}'} | J_A^\rho(\mathbf{y}) | \Psi_m \rangle \langle \Psi_m | J_A^\sigma(\mathbf{x}) | \Psi_{\mathcal{N}} \rangle}{E_m + E_{e_1} + E_{\nu_1} - E_{\mathcal{N}}} \right] . \qquad (2.25)$$

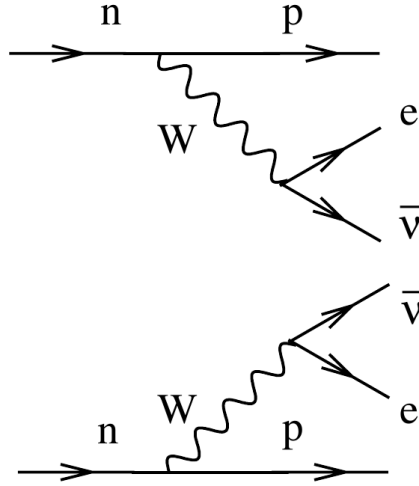In numerical calculations, one often uses the approximation

Figure 2.1. Feynman diagram for two-neutrino double beta decay.

$$E_{e_1} + E_{\nu_1} \approx E_{e_2} + E_{\nu_2} \approx \frac{M_{\mathcal{N}} - M_{\mathcal{N}'}}{2} \,, \tag{2.26}$$

where $M_{\mathcal{N}}$ and $M_{\mathcal{N}'}$ are the masses of initial and final nucleus, respectively.

Carrying out the phase-space integration, yielding the factor $G_{2\nu}^{\mathcal{N}}$, we finally find the expression for the halflife

$$[T_{1/2}^{2\nu}]^{-1} = G_{2\nu}^{\mathcal{N}} \, |\mathcal{M}_{2\nu}^{\mathcal{N}}|^2 \,, \tag{2.27}$$

where

$$\mathcal{M}_{2\nu}^{\mathcal{N}} = M_{2\nu}^{GT} - \left(\frac{g_V}{g_A}\right)^2 M_{2\nu}^F \,. \tag{2.28}$$

In Eq. (2.28), $M_{2\nu}^F$ and $M_{2\nu}^{GT}$ are the the $2\beta_{2\nu}$ decay Fermi and Gamow-Teller nuclear matrix elements, respectively, defined as

$$M_{2\nu}^F = \sum_m \frac{\langle \Psi_{\mathcal{N}'}| \sum_{j=1}^A \tau_j^+ |\Psi_m\rangle\langle\Psi_m| \sum_{k=1}^A \tau_k^+ |\Psi_{\mathcal{N}}\rangle}{E_m - \frac{M_{\mathcal{N}}+M_{\mathcal{N}'}}{2}} \,, \tag{2.29}$$

$$M_{2\nu}^{GT} = \sum_m \frac{\langle \Psi_{\mathcal{N}'}| \sum_{j=1}^A \boldsymbol{\sigma}_j\tau_j^+ |\Psi_m\rangle \cdot \langle\Psi_m| \sum_{k=1}^A \boldsymbol{\sigma}_k\tau_k^+ |\Psi_{\mathcal{N}}\rangle}{E_m - \frac{M_{\mathcal{N}}+M_{\mathcal{N}'}}{2}} \,. \tag{2.30}$$

2.2.2 Neutrinoless double beta decay

In neutrinoless double beta decay the conservation of the total lepton number is violated by two units. Since in the Standard Model the total lepton number is conserved, $2\beta_{0\nu}$ decay is forbidden in the Standard Model. In order to understand what is missing in the Standard Model, let us consider the $2\beta_{0\nu}^-$ decay in (2.15) illustrated in Fig. 2.2. Since no antineutrino is emitted, the two antineutrino lines should be joined to form a virtual neutrino propagator. In the Standard Model this is not possible for two reasons:
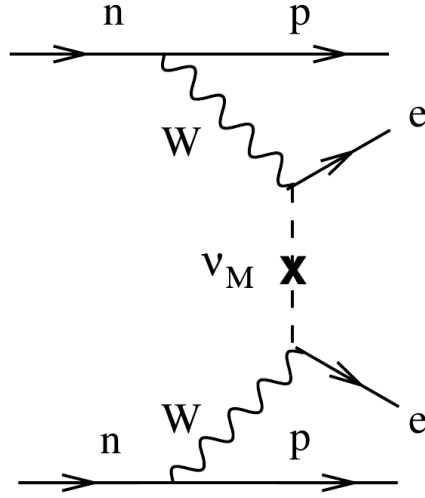
Figure 2.2. Feynman diagram for neutrinoless double beta decay.

- An antineutrino $\bar{\nu}_e$ emitted in the upper leptonic vertex cannot be absorbed in the lower leptonic vertex, which can absorb only a neutrino ν_e.

- The helicity of the neutral lepton emitted in the upper leptonic vertex is positive and the lower leptonic vertex can absorb only a neutral lepton with negative helicity.

Therefore, there are two necessary conditions for the occurrence of $2\beta_{0\nu}$ decay:

- The electron neutrino must be a Majorana particle, i.e. $\bar{\nu}_e = \nu_e$. In this case the total lepton number is not conserved.

- The electron neutrino must be a massive particle, i.e. $m_{\nu_e} \neq 0$. In this case, the upper leptonic vertex can emit a neutrino with negative helicity with relative amplitude m_{ν_e}/E_{ν_e}, which is absorbed by the lower leptonic vertex with relative amplitude equal to unity.

Massive Majorana neutrinos are described by the field

$$\nu_e(x) = \int \frac{d^3p}{(2\pi)^3 2E} \sum_r \left[a_r(\mathbf{p}) u_r(\mathbf{p}) e^{-ipx} + a_r^\dagger(\mathbf{p}) v_r(\mathbf{p}) e^{ipx} \right]. \tag{2.31}$$

The corresponding second order S matrix element for $2\beta_{0\nu}^-$ is

$$S_{0\nu} = - \int d^4x d^4y \, \langle e_1, e_2, \mathcal{N}' | \, T \left\{ \mathcal{L}_F(x) \mathcal{L}_F(y) \right\} | \mathcal{N} \rangle. \tag{2.32}$$

Note from Figs. 2.1 and 2.2 that the hadronic contribution to the amplitude is the same as in the case of $2\beta_{2\nu}$. The leptonic contribution is given by

$$\begin{aligned} L_{\rho\sigma} &= \langle e_1, e_2 | \, T \left\{ j_\rho(x) j_\sigma(y) \right\} | 0 \rangle = \\ &= \langle e_1, e_2 | \, T \left\{ \bar{e}(x) \gamma_\rho \left(1 - \gamma_5 \right) \nu_e(x) \bar{e}(y) \gamma_\sigma \left(1 - \gamma_5 \right) \nu_e(y) \right\} | 0 \rangle. \end{aligned} \tag{2.33}$$

Let us now consider neutrino mixing, i.e. the electron neutrino state is a superposition of mass eigenstates

$$\nu_{eL}(x) = \sum_{k=1}^{3} U_{ek}\nu_{kL}\,, \tag{2.34}$$

hence the weak interaction vertex is described by $\overline{e_L}\gamma_\rho U_{ek}\nu_{kL}$. Moreover, we have to consider that neutrinos are Majorana particles, i.e.

$$\nu_k^T = -\overline{\nu_k}\,\mathcal{C}\,, \tag{2.35}$$

$\mathcal{C}$ being the charge conjugation matrix. Using the above two properties, the propagator describing the internal neutrino line in Fig. 2.2 is given by

$$\begin{aligned}
G(x-y) &= \langle 0|\, T\left\{\nu_{eL}(x)\nu_{eL}^T(y)\right\}|0\rangle \\
&= \frac{1-\gamma_5}{2}\sum_{k=1}^{3}U_{ek}^2\langle 0|\, T\left\{\nu_k(x)\nu_k^T(y)\right\}|0\rangle\left(\frac{1-\gamma_5}{2}\right)^T \\
&= -\frac{1-\gamma_5}{2}\sum_{k=1}^{3}U_{ek}^2\langle 0|\, T\left\{\nu_k(x)\overline{\nu_k}(y)\right\}|0\rangle\,\mathcal{C}\,\frac{1-(\gamma_5)^T}{2} \\
&= -i\sum_{k=1}^{3}U_{ek}^2\int\frac{d^4q}{(2\pi)^4}\frac{m_k}{q^2-m_k^2}e^{-iq(x-y)}\frac{1-\gamma_5}{2}\,\mathcal{C}\,, \tag{2.36}
\end{aligned}$$

where we used $(1-\gamma_5)\slashed{q}(1-\gamma_5) = 0$. The squared neutrino mass in the dominator is negligible in comparison with the average neutrino energy and momentum. Hence, the neutrino propagator can be approximated by[2]

$$G(x-y) = -i\,\langle m_\nu\rangle\int\frac{d^4q}{(2\pi)^4}\frac{e^{-iq(x-y)}}{q^2-m_k^2}\frac{1-\gamma_5}{2}\,\mathcal{C}\,, \tag{2.37}$$

where $\langle m_\nu\rangle$ is the so called *effective Majorana mass* defined as

$$\langle m_\nu\rangle = \sum_{k=}^{3}U_{ek}^2 m_k\,. \tag{2.38}$$

Eq. (2.37) shows that the lepton contribution to the amplitude is proportional to $\langle m_\nu\rangle$. In addition, we can perform the q_0 integration in Eq. (2.37), obtaining

$$G(x-y) = -i\,\langle m_\nu\rangle\int\frac{d^3q}{(2\pi)^3}\frac{e^{-i[\omega_q(x_0-y_0)-\mathbf{q}\cdot(\mathbf{x}-\mathbf{y})]}}{2\omega_q}\frac{1-\gamma_5}{2}\,\mathcal{C}\,, \tag{2.39}$$

where $\omega_q = \sqrt{|\mathbf{q}|^2+m_k^2}$. As already stated, the hadronic contribution to the amplitude is the same as in the case of $2\beta_{2\nu}$, however, in the neutrinoless case its time dependence is combined with a different time dependence arising from the

---

[2]We do not consider here the possibility of mixing of the electron neutrino with heavy massive neutrinos.

leptonic contribution. Carrying out the time integration we find (compare to the right hand side of Eq. (2.25))

$$(2\pi)\,\delta\left(E_{\mathcal{N}'} + E_{e_1} + E_{e_2} - E_{\mathcal{N}}\right)$$

$$\times \sum_m \left[\frac{\langle \Psi_{\mathcal{N}'}|\,J_A^\rho(\mathbf{x})\,|\Psi_m\rangle\langle \Psi_m|\,J_A^\sigma(\mathbf{y})\,|\Psi_{\mathcal{N}}\rangle}{\omega_q + E_m + E_{e_2} - E_{\mathcal{N}}} + \frac{\langle \Psi_{\mathcal{N}'}|\,J_A^\rho(\mathbf{y})\,|\Psi_m\rangle\langle \Psi_m|\,J_A^\sigma(\mathbf{x})\,|\Psi_{\mathcal{N}}\rangle}{\omega_q + E_m + E_{e_1} - E_{\mathcal{N}}} \right]. \tag{2.40}$$

We can now use the closure approximation for intermediate nuclear states. Within this approximation, energies of intermediate states $E_m + E_e - E_{\mathcal{N}}$ are replaced by an average value $\langle E \rangle \approx 5 \div 10\,\text{MeV}$, and the sum over intermediate states is taken by closure, i.e. $\sum_m |\Psi_m\rangle\langle \Psi_m| = 1$. This simplifies the numerical calculation drastically. Finally, collecting the nuclear and leptonic parts together and carrying out the integrations we obtain the expression of the halflife

$$[T_{1/2}^{0\nu}]^{-1} = G_{0\nu}^{\mathcal{N}}\,|\mathcal{M}_{0\nu}^{\mathcal{N}}|^2\,\frac{|\langle m_\nu \rangle|^2}{m_e^2}\,, \tag{2.41}$$

In the above equation, m_e is the electron mass, $G_{0\nu}^{\mathcal{N}}$ is the phase space factor given by [7]

$$G_{0\nu}^{\mathcal{N}} = \frac{a_{0\nu}}{m_e^2 \ln 2} \int d\Omega_{0\nu}\, F(Z, E_{e1}) F(Z, E_{e2}) \tag{2.42}$$

with

$$a_{0\nu} = \frac{(G g_A)^4 m_e^9}{64\pi^2} \tag{2.43}$$

$$d\Omega_{0\nu} = m_e^{-5}|\mathbf{p}_{e1}||\mathbf{p}_{e2}|E_{e1}E_{e2}\delta\left(E_{e1} + E_{e2} + E_{\mathcal{N}'} - E_{\mathcal{N}}\right)\,dE_{e1}dE_{e2}d(\hat{\mathbf{p}}_{e1} \cdot \hat{\mathbf{p}}_{e2})\,, \tag{2.44}$$

and $\mathcal{M}_{0\nu}^{\mathcal{N}}$ is the $2\beta_{0\nu}$ decay nuclear transition matrix element

$$\mathcal{M}_{0\nu}^{\mathcal{N}} = M_{0\nu}^{GT} - \left(\frac{g_V}{g_A}\right)^2 M_{0\nu}^F\,, \tag{2.45}$$

in which $M_{0\nu}^F$ and $M_{0\nu}^{GT}$ are the $2\beta_{0\nu}$ decay Fermi and Gamow-Teller nuclear matrix elements obtained using the closure approximation, respectively, defined as

$$M_{0\nu}^F = \langle \Psi_{\mathcal{N}'}| \sum_{j,k=1}^A \tau_j^+ \tau_k^+ H(r)\,|\Psi_{\mathcal{N}}\rangle\,, \tag{2.46}$$

$$M_{0\nu}^{GT} = \langle \Psi_{\mathcal{N}'}| \sum_{j,k=1}^A (\boldsymbol{\sigma}_j \cdot \boldsymbol{\sigma}_k)\,\tau_j^+ \tau_k^+ H(r)\,|\Psi_{\mathcal{N}}\rangle\,. \tag{2.47}$$

The function $H(r)$ in Eqs. (2.46) and (2.47) is the so called *neutrino potential* given by

$$H(r) = \frac{2R_A}{\pi r} \int_0^{+\infty} dq\, \frac{q \sin(qr)}{\omega_q(\omega_q + \langle E \rangle)}\,, \tag{2.48}$$

in which R_A is the nuclear radius. The neutrino potential is what remains after performing the integration over the virtual neutrino momentum $\mathbf{q}$ in Eq. (2.39).

Since the neutrino mass is very small, we have $\omega_q \sim |\mathbf{q}|$ and the neutrino potential can be approximated by

$$H(r) = \frac{2R_A}{\pi r} \int_0^{+\infty} dq \, \frac{\sin(qr)}{q + \langle E \rangle} \, . \tag{2.49}$$

2.3   Summary of experimental results

Studying $2\beta_{0\nu}$ decay may give access to the absolute scale of neutrino mass, since, as discussed in details in the previous Sections, the halflife of a nucleus is given by Eq. (2.41). Hence, by studying $2\beta_{0\nu}$ decay rate, we can obtain information on the effective Majorana mass and, therefore, on the masses of light neutrinos.

$2\beta_{2\nu}$ decay the longest ever observed among radioactive decay processes, typical lifetimes are of the order of $10^{18} \div 10^{21}$ years. The observed values of $\mathcal{M}_{2\nu}$ are used to investigate the nuclear structure and the nuclear interactions associated with the $2\beta_{0\nu}$ decay. For a list of $2\beta_{2\nu}$ halflives measured in several isotopes, see Table 2.1 [8].

Isotope	$T_{1/2}^{2\nu}$ (years)	Experiments
^{48}Ca	$(4.4^{+0.6}_{-0.5}) \times 10^{19}$	Irvine TPC [9], TGV [10], NEMO3 [11]
^{76}Ge	$(1.5 \pm 0.1) \times 10^{21}$	PNL-USC-ITEP-YPI [12], IGEX [13], H-M [14]
^{82}Se	$(0.92 \pm 0.07) \times 10^{20}$	NEMO3 [15], Irvine TPC [16], NEMO2 [17]
^{96}Zr	$(2.3 \pm 0.2) \times 10^{19}$	NEMO2 [18], NEMO3 [19]
^{100}Mo	$(7.1 \pm 0.4) \times 10^{18}$	NEMO3 [15], NEMO2 [20], Irvine TPC [21]
^{116}Cd	$(2.8 \pm 0.2) \times 10^{19}$	NEMO3 [11], ELEGANT [22], Solotvina [23], NEMO2 [24]
^{130}Te	$(6.8^{+1.2}_{-1.1}) \times 10^{20}$	CUORICINO [25], NEMO3 [26]
^{136}Xe	$(2.11 \pm 0.21) \times 10^{21}$	EXO-200 [27]
^{150}Nd	$(8.2 \pm 0.9) \times 10^{18}$	Irvine TPC [21], NEMO3 [28]

Table 2.1. Current best direct measurements of the halflife of $2\beta_{2\nu}$ processes. The values reported are taken from the averaging procedure described in [8].

$2\beta_{0\nu}$ double beta decay searches have been carried out over more than half a century and several double beta emitting isotopes have been investigated. The currents best limits on the halflife of $2\beta_{0\nu}$ are listed In Table (2.2).

From the expression of the effective Majorana mass of Eq. (2.38), it is clear that $2\beta_{0\nu}$ is directly connected to neutrino oscillations phenomenolgy and it provides direct information on the absolute neutrino mass scale, as cosmology and β decay experiments do. The relationship between the effective Majorana mass and the lightest neutrino mass is affected by the uncertinities in the measured oscillation parameters, the unknown neutrino mass ordering and the unknown phases of neutrino mixing matrix (see Fig. 2.3).

Isotope	$T^{0\nu}_{1/2}$ (years)	Experiment
^{48}Ca	$> 5.8 \times 10^{22}$	ELEGANT [29]
^{76}Ge	$> 1.9 \times 10^{25}$	Heidelberg-Moscow [30]
^{82}Se	$> 3.6 \times 10^{23}$	NEMO3 [31]
^{96}Zr	$> 9.2 \times 10^{21}$	NEMO3 [19]
^{100}Mo	$> 1.1 \times 10^{24}$	NEMO3 [31]
^{116}Cd	$> 1.7 \times 10^{23}$	Solotvina [23]
^{130}Te	$> 2.8 \times 10^{24}$	CUORICINO [32]
^{136}Xe	$> 4.5 \times 10^{23}$	DAMA [33]
^{150}Nd	$> 1.8 \times 10^{22}$	NEMO3 [28]

Table 2.2. Current best limits on the halflife of $2\beta_{0\nu}$ processes for the most interesting isotopes. All values are at 90% C.L.
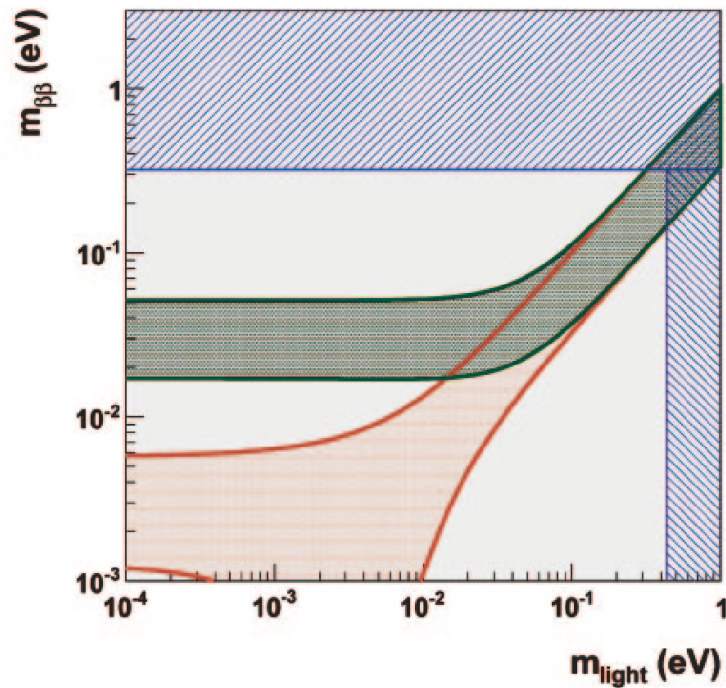
Figure 2.3. The effective neutrino Majorana mass $m_{\beta\beta}$ as a function as a function of the lightest neutrino mass, m_{light}. The light gray, red (dark gray, green) band corresponds to the normal (inverted) ordering, respectively, in which case m_{light} is equal to m_1 (m_3) (see Section 1.6). The excluded region comes from cosmological bounds, the horizontally excluded one from $2\beta_{0\nu}$ constraints.

Chapter 3

Nuclear structure and dynamics

3.1 The nuclear charge density and the semiempirical-mass formula

Let us consider an atomic nucleus with atomic number Z and mass number A. The nuclear charge density $\rho_{ch}(r)$ can be parametrized in the form

$$\rho_{ch}(r) = \rho_0 \, \frac{1}{1 + e^{(r - R_A)/D}} \, , \tag{3.1}$$

where $R_A = r_0 A^{1/3}$ is the nuclear radius, with $r_0 = 1.20\,\text{fm}$ and $D = 0.54\,\text{fm}$. The nuclear charge density is nearly constant within the nuclear volume, its value is roughly the same for all stable nuclei within a distance $R_T \sim 2.5\,\text{fm}$ independent of A, called surface thickness; over R_T, $\rho_{ch}(r)$ drops from $\sim 90\,\%$ to $\sim 10\,\%$ of the maximum (see Fig. 3.1).

The measured mass of a nucleus is given by

$$M(Z, A) = Z m_p + (A - Z) m_n - B(Z, A) \, , \tag{3.2}$$

where m_p and m_n are the rest mass of the proton and the neutron respectively and $B(Z, A)$ is the (positive) nuclear binding energy. The semiempirical-mass formula states that the A and Z dependence of the binding energy can be parametrized in the following way:

$$B(Z, A) = a_V A - a_S A^{2/3} - a_C \, \frac{Z^2}{A^{1/3}} - a_A \, \frac{(A - 2Z)^2}{4A} + \lambda \, a_P \, \frac{1}{A^{1/2}} \, . \tag{3.3}$$

In the above equation, the first term proportional to A is the *volume term* and describes the bulk energy of nuclear matter; the second term proportional to $A^{2/3}$ is the *surface* term; the third term is the the *Coulomb* term which takes into account the electrostatic repulsion between protons; the fourth term, called *asymmetry term*, is required to describe the experimental observation that stable nuclei tend to have the same number of neutrons and protons. The last term, called *pairing term*, is needed to describe the property that even-even nuclei (i.e. nuclei having even Z and even $A - Z$) tend to be more stable than even-odd or odd-odd nuclei; λ can assume
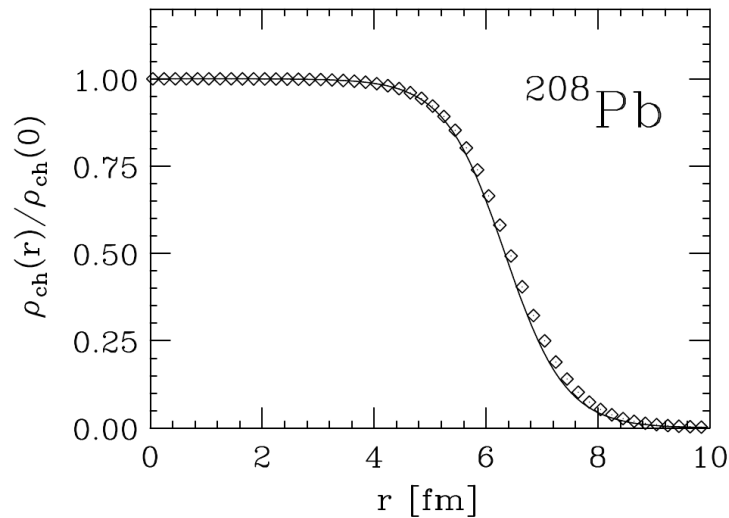
Figure 3.1. Nuclear charge distribution of ^{128}Pb, normalized to $Z/\rho(0)$ ($Z = 82$). The solid line has been obtained using the parametrization of Eq. (3.1), while the diamonds represent the results of a model independent analysis of electron scattering data.

-1, 0 and $+1$ for even-even, even-odd and odd-odd nuclei, respectively. a_V, a_S, a_C, a_A and a_P are constants.

Let us now consider the case of nuclei with the same number of protons and neutrons, i.e. $Z = A/2$. The nuclear density and binding energy of such nuclei have the following proprieties.

- The nuclear densities exhibits a saturation to a value $\rho_0 \sim 0.16 \, \text{fm}^{-3}$, i.e. the density of atomic nuclei, measured by elastic electron-nucleus scattering, is nearly constant and does not depend upon A for large A (see Fig. 3.2).

- The binding energy per nucleon, in the large A limit ($A \geq 20$) and neglecting the Coulomb term, becomes approximately constant because only the volume term survives, i.e.

$$\frac{B(Z, A)}{A} \sim 8.5 \, \text{MeV} \,. \tag{3.4}$$

3.2 The nucleon-nucleon interaction

In our model of the nucleon-nucleon (NN) interaction we will consider nucleons as nonrelativistic pointlike particles. We can infer the main features of the NN interaction from the proprieties of the nuclear charge distribution and binding energy per nucleon discussed in the previous section.

The saturation of the nuclear density discussed above implies that nucleons cannot be packed together too tightly. Hence, at short distances, the NN force must be repulsive. If we describe the NN interaction with a nonrelativistic potential v
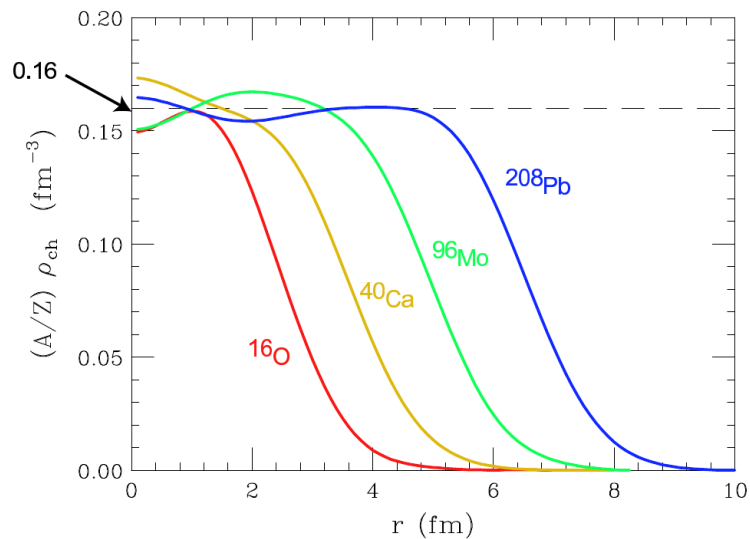
Figure 3.2. Saturation of central nuclear densities measured by elastic electron-nucleus scattering.

depending on the interparticle distance $\mathbf{r}$, we can write

$$v(\mathbf{r}) > 0 \quad \text{for} \quad |\mathbf{r}| < r_C \,, \tag{3.5}$$

where r_C is the radius of the repulsive core.

The fact that the nuclear binding energy per nucleon is roughly the same for all nuclei with $A \geq 20$ (see Eq. (3.4)), tells us that the NN interaction has a finite range r_0, i.e.

$$v(\mathbf{r}) = 0 \quad \text{for} \quad |\mathbf{r}| > r_0 \,. \tag{3.6}$$

Moreover, the energies of the levels with the same parity and angular momentum of the spectra of the so-called *mirror nuclei* are the same up to small electromagnetic corrections[1]. This fact shows that the NN interaction does not distinguish protons and neutrons, i.e. nuclear forces are *charge symmetric*. Charge symmetry is a manifestation of a more general property of the NN interaction, called *isotopic invariance*. Since the mass difference between proton and neutron is very small, they can be considered as two states of the same particle, the nucleon. The Lagrangian density of these two states can be written as

$$\mathcal{L} = \overline{N}(i\gamma^\mu \partial_\mu - m)N \,, \tag{3.7}$$

where

$$N = \begin{pmatrix} p \\ n \end{pmatrix} \,, \tag{3.8}$$

p and n being the four-spinors associated with the proton and the neutron, respectively. We say that the theory is isotopic invariant, as in the case of Eq. (3.7), if the

---

[1]Mirror nuclei are pairs of nuclei having the same A and charges differing by one unit, e.g. $^{15}_{7}\text{N}$ ($A = 15$, $Z = 7$) and $^{15}_{8}\text{O}$ ($A = 15$, $Z = 8$).

Lagrangian density is invariant under the $SU(2)$ global phase transformation

$$U = e^{i\,\boldsymbol{\alpha}\cdot\boldsymbol{\tau}}\,, \tag{3.9}$$

where $\boldsymbol{\alpha} = (\alpha_1, \alpha_2, \alpha_3)$ is a constant vector and $\boldsymbol{\tau} = (\tau_1, \tau_2, \tau_3)$ is the vector of the Pauli matrices. We have just seen that the nucleon can be described as a doublet in isospin space; proton and neutron correspond to isospin projections $T_3 = +1/2$ and $T_3 = -1/2$, respectively. Proton-proton and neutron-neutron pairs always have total isospin $T = 1$ (triplet state), whereas a proton-neutron pair may have either $T = 0$ (singlet state) or $T = 1$. Hence, isospin invariance implies that the NN interaction depends on the total isospin T but not on the projection T_3. For example, the potential $v(\mathbf{r})$ acting between two protons with spins coupled to $S = 0$ is the same as the potential acting between a proton and a neutron with spins and isospins coupled to $S = 0$ and $T = 1$.

The details of the NN interaction can be best understood in the two-nucleon system. There is only one NN bound state, the nucleus of deuterion, or deuteron (^{2}H), consisting of a proton and a neutron coupled to total spin and isospin $S = 1$ and $T = 0$, respectively. This is a clear manifestation of the *spin dependence* of nuclear forces.

Another important feature of the NN interaction can be inferred from the observation that the deuteron exhibits a nonvanishing quadrupole moment, implying that its charge distribution is not spherically symmetric. Hence, the NN interaction is *noncentral.*

3.3   The two-nucleon system

H. Yukawa, in 1935, first proposed the theoretical description of the NN interaction. He made the hypothesis that nucleons interact through the exchange of a particle (it is the same mechanism of the electromagnetic interaction, in which the exchanged particle is the photon). The relation between the mass μ of the particle and the interaction range r_0 is

$$r_0 \sim \frac{1}{\mu}\,. \tag{3.10}$$

Using $r_0 \sim 1\,\mathrm{fm}$, the above relation yields $\mu \sim 200\,\mathrm{MeV}$.

Yukawa's idea has been successfully implemented identifying the exchanged particle with the π meson (or pion), discovered in 1947, whose mass is $m_\pi \sim 140\,\mathrm{MeV}$. The pion is a spin zero pseudoscalar particle (i.e. it has spin parity 0^-) that comes in three charge states, denoted π^+, π^0 and π^-. The mass differences between these three states is very small and hence the pion can be considered as an isospin triplet $T = 1$. The associated isospin projections to π^+, π^0 and π^- are $T_3 = +1$, 0, and -1, respectively.

The pion-nucleon interaction Lagrangian, compatible with the observation that nuclear interactions conserve parity, can be written as

$$\mathcal{L}_I = -ig\overline{N}\gamma_5(\boldsymbol{\pi}\cdot\boldsymbol{\tau})N\,, \tag{3.11}$$
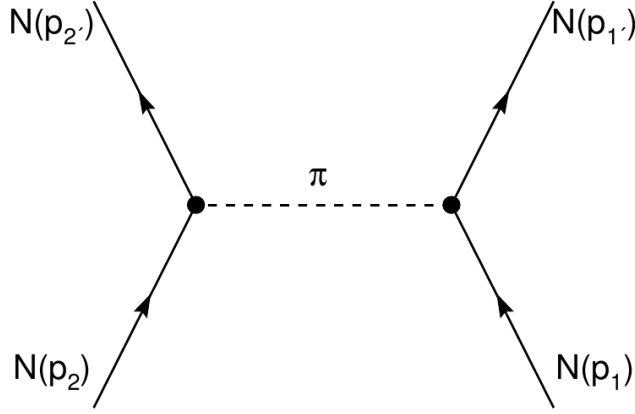
Figure 3.3. Feynman diagram describing the one-pion-exchange process between two nucleons. The corresponding amplitude is given by (3.13).

where g is the coupling constant, $\boldsymbol{\tau}$ is the isospin of the nucleon and $\boldsymbol{\pi} = (\pi_1, \pi_2, \pi_3)$ is the vector whose elements are defined as

$$\pi_1 = \frac{\pi^+ + \pi^-}{\sqrt{2}}, \quad \pi_2 = \frac{i(\pi^+ - \pi^-)}{\sqrt{2}}, \quad \pi_3 = \pi_0. \tag{3.12}$$

The two-nucleon interaction through the exchange of a pion is described by the Feynman's diagram in Fig. 3.3. Using standard Feynman's diagram techniques, the amplitude of this process can be written as

$$\langle f| M |i\rangle = -ig^2 \frac{\overline{u}(p_2', s_2')\gamma_5 u(p_2, s_2)\overline{u}(p_1', s_1')\gamma_5 u(p_1, s_1)}{k^2 - m_\pi^2} \langle \boldsymbol{\tau}_1 \cdot \boldsymbol{\tau}_2\rangle, \tag{3.13}$$

where $k = p_1' - p_1 = p_2 - p_2'$, $k^2 = k_\mu k^\mu = k_0^2 - |\mathbf{k}|^2$, $u(p, s)$ is the Dirac spinor associated with a nucleon of four momentum $p \equiv (E, \mathbf{p})$ $(E = \sqrt{|\mathbf{p}|^2 + m^2})$ and spin projection s and

$$\langle \boldsymbol{\tau}_1 \cdot \boldsymbol{\tau}_2\rangle = \eta_{2'}^\dagger \boldsymbol{\tau} \, \eta_2 \, \eta_{1'}^\dagger \boldsymbol{\tau} \, \eta_1, \tag{3.14}$$

η_i being the two-component Pauli spinor describing the isospin state of particle i. Since the ratio between the momentum and the mass of the nucleons inside the nucleus is small (typically $\lesssim 3\%$), we can take the nonrelativistic limit of Eq. (3.13), leading to define a NN interaction potential that can be written in coordinate space as

$$\begin{aligned}
v_\pi &= \frac{g^2}{4m^2} (\boldsymbol{\tau}_1 \cdot \boldsymbol{\tau}_2)(\boldsymbol{\sigma}_1 \cdot \boldsymbol{\nabla})(\boldsymbol{\sigma}_2 \cdot \boldsymbol{\nabla}) \frac{e^{-m_\pi r}}{r} \\
&= \frac{g^2}{(4\pi)^2} \frac{m_\pi^3}{4m^2} \frac{1}{3} (\boldsymbol{\tau}_1 \cdot \boldsymbol{\tau}_2) \left\{ \left[(\boldsymbol{\sigma}_1 \cdot \boldsymbol{\sigma}_2) + S_{12} \left(1 + \frac{3}{x} + \frac{3}{x^2} \right) \right] \frac{e^{-x}}{x} \right. \\
&\quad \left. - \frac{4\pi}{m_\pi^3} (\boldsymbol{\sigma}_1 \cdot \boldsymbol{\sigma}_2) \, \delta^{(3)}(\mathbf{r}) \right\},
\end{aligned} \tag{3.15}$$

where $x = m_\pi |\mathbf{r}|$ and

$$S_{12} = \frac{3}{r^2}(\boldsymbol{\sigma}_1 \cdot \mathbf{r})(\boldsymbol{\sigma}_2 \cdot \mathbf{r}) - (\boldsymbol{\sigma}_1 \cdot \boldsymbol{\sigma}_2). \tag{3.16}$$
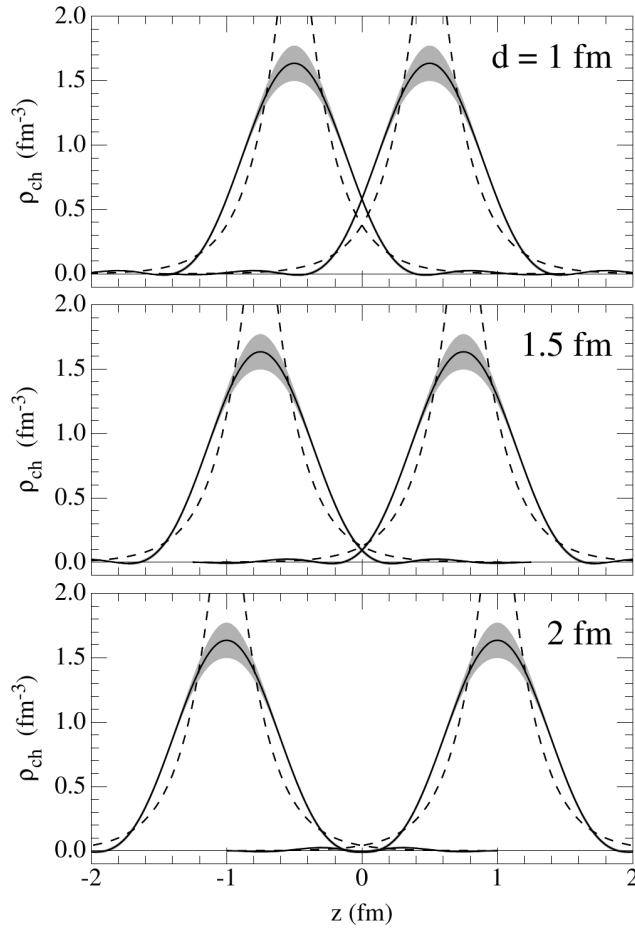
Figure 3.4. Charge densities of two nucleons set at three different values of the relative distance d. Note that in the case with $d = 1$ fm the two nucleons begin to overlap.

is the operator describing the noncentral nature of nuclear forces. The interaction potential in Eq. (3.15) satisfies all the proprieties discussed in the above Section. Note that the repulsive nature of the NN interaction is described by the term proportional to $\delta^{(3)}(\mathbf{r})$.

For $g^2/(4\pi) \sim 14$, v_π provides an accurate description of the long range part ($|\mathbf{r}| > 1.5$ fm) of the NN interaction, as shown by the very good fit of the experimental data in NN scattering processes with high angular momentum. In these processes, due to the strong centrifugal barrier, the probability of finding the two nucleons at small relative distances becomes in fact negligibly small. At medium- and short-range we have to take into account more complicated processes, such as the exchange of two or more pions (possibly interacting among themselves) or havier particles like the ρ and ω mesons ($m_\rho = 770$ MeV and $m_\rho = 782$ MeV). Moreover, if the relative distance between becomes very small ($|\mathbf{r}| \lesssim 0.5 \div 1$ fm), nucleons, being composite and finite in size, are expected to overlap (see Fig. 3.4). In this regime, NN interactions should in principle be described in terms of interactions between nucleon constituents (i.e. quarks and gluons) according to the quantum chromodynamics.

3.4   Phenomenological potentials

Phenomenological potentials describing the *full* NN interaction are generally written as

$$v = \tilde{v}_\pi + v_R \,, \tag{3.17}$$

where $\tilde{v}_\pi$ is the one-pion-exchange potential, defined by Eq. (3.15), stripped of the δ-function contribution, whereas v_R describes the interaction at medium and short range. The spin-isospin dependence and the noncentral nature of the NN interactions can be properly described rewriting Eq. (3.17) in the form

$$v_{ij} = \sum_{ST} [v_{TS}(r_{ij}) + \delta_{S1} v_{tT}(r_{ij}) S_{12}] P_{2S+1} \Pi_{2T+1} \,, \tag{3.18}$$

S and T being the total spin and isospin of the interacting pair, respectively. In the above equation, P_{2S+1} ($S = 0, 1$) are the spin projection operators

$$P_1 = \frac{1}{4}[1 - (\boldsymbol{\sigma}_1 \cdot \boldsymbol{\sigma}_2)] \,, \quad P_3 = \frac{1}{4}[3 + (\boldsymbol{\sigma}_1 \cdot \boldsymbol{\sigma}_2)] \,, \tag{3.19}$$

satisfying

$$P_1 + P_3 = 1 \,, \quad P_{2S+1} \left| S' \right\rangle = \delta_{SS'} \left| S' \right\rangle \,, \quad P_{2S+1}^2 = P_{2S+1} \,, \tag{3.20}$$

and Π_{2T+1} ($T = 0, 1$) are the isospin projection operators that can be written as in Eq. (3.19) replacing $\boldsymbol{\sigma}$ with $\boldsymbol{\tau}$. The functions $v_{TS}(r_{ij})$ and $v_{tT}(r_{ij})$ describe the radial dependence of the interaction in the different spin-isospin channels and reduce to the corresponding components of the one-pion-exchange potential at large r_{ij}. Their shapes are chosen in such a way as to reproduce the available NN data (deuteron binding energy, charge radius and quadrupole moment and the NN scattering data).

An alternative representation of the NN potential, based on the set of six operators

$$O_{ij}^{n=1,\dots,6} = [1, (\boldsymbol{\sigma}_i \cdot \boldsymbol{\sigma}_j), S_{ij}] \otimes [1, (\boldsymbol{\tau}_i \cdot \boldsymbol{\tau}_j)] \,, \tag{3.21}$$

is given by

$$v_{ij} = \sum_{n=1}^{6} v^n(r_{ij}) O_{ij}^n \,. \tag{3.22}$$

Note that the operators defined in Eq. (3.21) form an algebra, as they satisfy the relation

$$O_{ij}^n O_{ij}^m = \sum_l K_{nml} O_{ij}^l \,, \tag{3.23}$$

where the coefficients K_{nml} can be easily obtained from the properties of Pauli matrices. The typical shape of the NN potential of (3.22) in the state of relative angular momentum $l = 0$ and total spin and isospin $S = 0$ and $T = 1$ is shown in Fig. 3.5. The short range repulsive core, to be ascribed to heavy meson exchange or to complicated mechanisms involving nucleon constituents, is followed by an intermediate range attractive region, largely due to two-pion exchange processes. Finally, at large interparticle distance the one-pion-exchange mechanism dominates
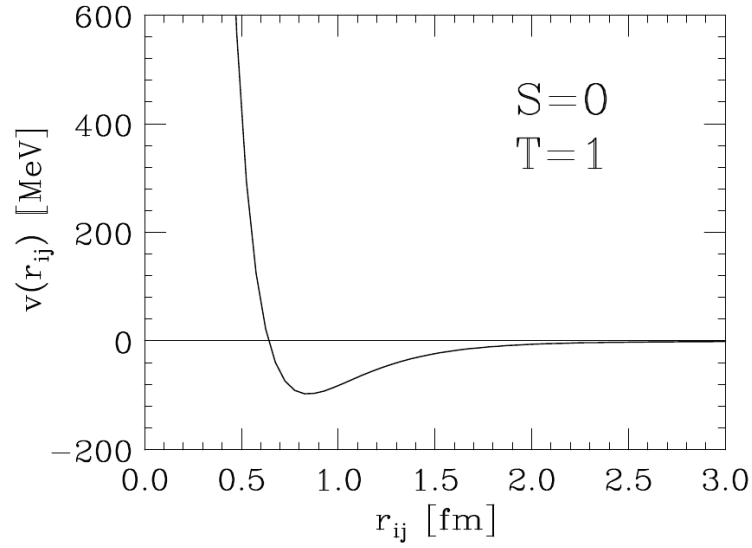
Figure 3.5. Radial dependence of the NN potential describing the interaction between two nucleons in the state of relative angular momentum $l = 0$, and total spin and isospin $S = 0$ and $T = 1$, respectively.

While the static potential of Eq. (3.22) provides a reasonable account of deuteron properties, in order to describe NN scattering in S and P wave, we have to include the two additional momentum dependent operators

$$O_{ij}^{n=7,8} = \mathbf{L} \cdot \mathbf{S} \otimes [1, (\boldsymbol{\tau}_i \cdot \boldsymbol{\tau}_j)] , \tag{3.24}$$

$\mathbf{L}$ being the orbital angular momentum.

The potentials yielding the best available fits of NN scattering data are written in terms of eighteen operators, with

$$O_{ij}^{n=9,\dots,14} = [\mathbf{L}^2, \mathbf{L}(\boldsymbol{\sigma}_i \cdot \boldsymbol{\sigma}_j), (\mathbf{L} \cdot \mathbf{S})^2] \otimes [1, (\boldsymbol{\tau}_i \cdot \boldsymbol{\tau}_j)] , \tag{3.25}$$

$$O_{ij}^{n=15,\dots,18} = [1, (\boldsymbol{\sigma}_i \cdot \boldsymbol{\sigma}_j), S_{ij}] \otimes T_{ij}, (\tau_{zi} + \tau_{zj}) , \tag{3.26}$$

where

$$T_{ij} = \frac{3}{r^2} (\boldsymbol{\tau}_i \cdot \mathbf{r})(\boldsymbol{\tau}_j \cdot \mathbf{r}) - (\boldsymbol{\tau}_i \cdot \boldsymbol{\tau}_j) . \tag{3.27}$$

The operators $O_{ij}^{n=15,\dots,18}$ take care of small charge symmetry breaking effects, due to the different masses and coupling constants of the charged and neutral pions.

3.5 Nonrelativistic many-body theory

Within nonrelativistic many-body theory, a nucleus is seen as a collection of pointlike protons and neutrons whose dynamics are described by the Hamiltonian

$$H = \sum_{i=1}^{A} \frac{\mathbf{p}_i^2}{2m} + \sum_{j>i=1}^{A} v_{ij} + \dots , \tag{3.28}$$

where $\mathbf{p}_i$ is the momentum carried by the i-th nucleon, v_{ij} is the two body potentials describing NN interactions of Eq. (3.22) and the ellipsis refer to the possible existence of interactions involving more than two nucleons.

The Schrödinger equation

$$H\Psi = E\Psi \tag{3.29}$$

associated to the Hamiltonian in Eq. (3.28) has been solved for nuclei with not too large A. The numerical solution is trivial for $A = 2$ only; for $A = 3$ the Schrödinger equation can still be solved using deterministic approaches; while for $A > 3$ stochastic methods have to be employed.

Another important aspect of the Hamiltonian of Eq. (3.28) is that we cannot easily carry out perturbation theory in the basis provided by the eigenstates of the noninteracting system because of the strongly repulsive nature at short distances of the NN interactions.

The simplest approximation we can carry out is the so called mean field approximation. In this scheme the complicated NN potential is replaced by a mean field in Eq. (3.28), i.e.

$$\sum_{j>i=1}^{A} v_{ij} \rightarrow \sum_{i=1}^{A} U_i \,, \tag{3.30}$$

with the potential U chosen in such a way that the single particle Hamiltonian

$$h = \frac{\mathbf{p}^2}{2m} + U \tag{3.31}$$

be diagonalizable. Within this framework the nuclear ground state wave function reduces to a Slater determinant, constructed using the A lowest energy eigenstates of h:

$$\Psi_0 = \frac{1}{\sqrt{A!}} \det\{\phi_i\} \,, \tag{3.32}$$

the ϕ_i's $(i = 1, 2, \ldots, A)$ being solutions of the Schrödinger equation

$$h\phi_i = \epsilon_i \phi_i \,, \tag{3.33}$$

and the corresponding ground state energy is given by

$$E_0 = \sum_{i=1}^{A} \epsilon_i \,. \tag{3.34}$$

In other words, we treat nucleons as independent particles. This procedure is the basis of the Nuclear Shell Model, to be discussed in the next Section.

3.6 The Nuclear Shell Model

The Nuclear Shell Model (NSM) is based on the assumption that nucleons in a nucleus behave as independent particles moving in a mean field. Let us assume that the potential describing the nuclear mean field U_0 be central. the most popular choices of the central potential are the Woods-Saxon and the isotropic three-dimensional harmonic oscillator. The latter is the one that will be used in our work because,

unlike the Woods-Saxon potential, it allows for an exact factorization of the center of mass contributions in the calculation of matrix elements of two-body operators. Hence, we set

$$U_0(r) = \frac{1}{2}m\omega r^2 \,, \tag{3.35}$$

where m is the nucleon mass and ω is a parameter. The Schrödinger equation for the nucleon wave function ϕ is

$$[T + U_0(r)]\,\phi_{k,l,m_l}(\mathbf{r}) = E_{k,l,m_l}\,\phi_{k,l,m_l}(\mathbf{r})\,, \tag{3.36}$$

where T is the kinetic term

$$T = -\frac{1}{2m}\nabla^2 = -\frac{1}{2m}\left(\frac{1}{r}\frac{d^2}{dr^2}r - \frac{\mathbf{l}^2}{r^2}\right)\,, \tag{3.37}$$

k, l and m_l being the principal, orbital angular momentum and orbital angular momentum projection quantum numbers, respectively. Eq. (3.36) can be solved exactly, leading to

$$\phi_{k,l,m_l}(\mathbf{r}) = R_{k,l}(r)Y_{m_l}^l(\hat{r})\,, \tag{3.38}$$

in which

$$R_{k,l}(r) = N_{k,l}r^l e^{-\nu r^2}L_k^{l+\frac{1}{2}}(2\nu r^2) \tag{3.39}$$

is the radial wave function, where $\nu = m\omega/2$,

$$N_{k,l} = \sqrt{\sqrt{\frac{2\nu^3}{\pi}}\frac{2^{k+2l+3}\,k!\,\nu^l}{(2k+2l+1)!!}} \tag{3.40}$$

is a normalization factor, $L_k^{l+\frac{1}{2}}(2\nu r^2)$ is the generalized Laguerre polynomial of degree k defined as

$$L_k^{l+\frac{1}{2}}(2\nu r^2) = \sum_{i=0}^k \frac{(-2\nu r^2)^i}{i!}\binom{k+l+\frac{1}{2}}{k-i} \tag{3.41}$$

and $Y_{m_l}^l(\hat{r})$ is the spherical harmonic[2]. The energy spectrum does not depend on the magnetic quantum number (i.e. $E_{k,l,m_l} = E_{k,l}$) and it is given by

$$E_{k,l} = \left(2k + l + \frac{3}{2}\right)\omega\,. \tag{3.42}$$

---

[2]Recall that the spherical harmonics are eigenfunctions of the $\mathbf{l}^2$ and l_z operators

$$\mathbf{l}^2 Y_{m_l}^l(\hat{r}) = l(l+1)Y_{m_l}^l(\hat{r})$$

and

$$l_z Y_{m_l}^l(\hat{r}) = m_l Y_{m_l}^l(\hat{r})\,,$$

and are orthonormal functions

$$\int Y_{m_l}^l(\hat{r})Y_{m_l'}^{l'}(\hat{r})\,d\Omega = \delta_{ll'}\delta_{m_l m_l'}\,.$$

If we consider the spin **s** of the nucleons, the central potential of the NSM may also contain a spin-orbit term of the form

$$U_{\text{SO}} = -2\lambda \mathbf{l} \cdot \mathbf{s} \,, \tag{3.43}$$

where λ is a constant. The total angular momentum $\mathbf{j} = \mathbf{l} + \mathbf{s}$ is conserved and the wave function takes the form

$$\phi_\alpha(\mathbf{r}) = R_{k,l}(r) \, [Y^l_{m_l}(\hat{r}) \otimes \chi^s_{m_s}]^j_m \,, \tag{3.44}$$

where $\chi^s_{m_s}$ is the spin wave functions, s and m_s being the spin and spin projection quantum numbers, respectively, α stands for the set of all quantum numbers $(k, l, m_l, s, m_s, j, m)$, j and m being the total angular momentum and the total angular momentum projection quantum numbers, respectively. The symbol $\otimes$ denotes the Clebsch-Gordan product, i.e.

$$[Y^l_{m_l}(\hat{r}) \otimes \chi^s_{m_s}]^j_m = \sum_{m_l, m_s} \langle l, m_l, s, m_s | j, m \rangle \, Y^l_{m_l}(\hat{r}) \chi^s_{m_s} \,. \tag{3.45}$$

Taking $s = \frac{1}{2}$ and $j = l \pm \frac{1}{2}$, we obtain the following energy spectrum:

$$E_{k,l,j} = \begin{cases} \left(2k + l + \dfrac{3}{2}\right)\omega - \lambda l & \text{for } j = l + \dfrac{1}{2} \\[2ex] \left(2k + l + \dfrac{3}{2}\right)\omega + \lambda(l+1) & \text{for } j = l - \dfrac{1}{2} \end{cases} \,. \tag{3.46}$$

The addition of the spin-orbit potential to the harmonic oscillator reproduces the main features of the observed nuclear spectra, exhibiting the so called magic numbers[3]. Fig. 3.6 shows the energy levels obtained using the harmonic oscillator plus spin-orbit potential. It clearly appears that this model provides a correct prediction of the magic numbers, reported in round brackets.

In Table 3.1 we summarize the information on the harmonic oscillator plus spin-orbit orbitals employed in the calculation discussed in this Thesis.

Using the eigenfunctions obtained from the solution of the Schrödinger equation, one can compute the nuclear density distribution, $\rho(r)$, from

$$\rho(r) = \sum_\alpha |\phi_\alpha(r)|^2 \,, \tag{3.47}$$

where the sum runs over all occupied orbitals of the ground state. In Fig. 3.7 we have plotted $\rho(r)$ for the nucleus ^{48}Ca. Experimental data obtained from elastic electron-nucleus scattering experiments show that the overall shape is reproduced, but sizable discrepancies occur. However, these differences are not to be ascribed to the limitations of the NSM because, if one replace the harmonic oscillator with the Woods-Saxon potential, the densities obtained turn out to be in very good agreement with experiments.

---

[3]A magic number is a number of nucleons arranged into complete shells within the atomic nucleus. Atomic nuclei consisting of such a magic number of nucleons are more stable. The seven most widely recognized magic numbers are: 2, 8, 20, 28, 50, 82, 126.
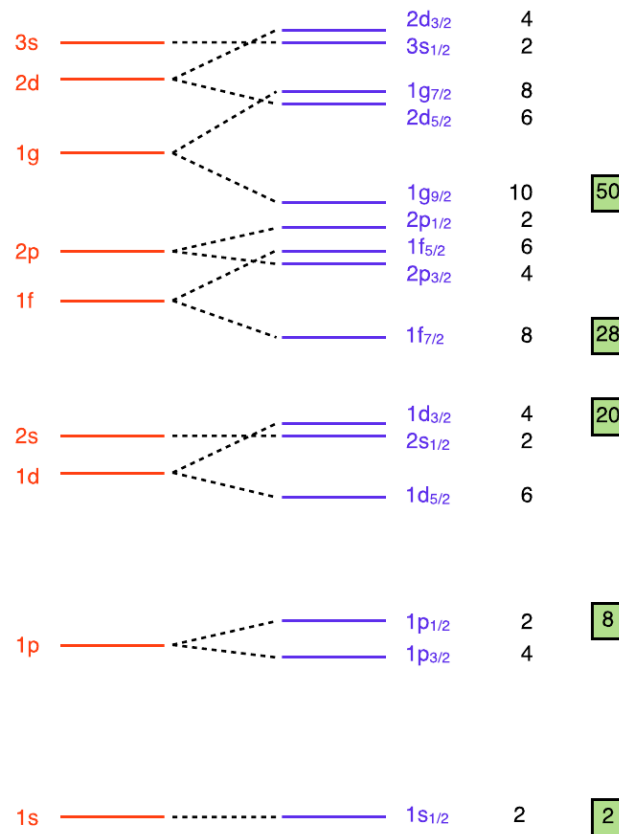
Figure 3.6. Energy spectrum predicted by the nuclear shell model with an isotropic oscillator potential without spin-orbit (left) and with spin-orbit (right) interaction. The number to the right of a level indicates its degeneracy. The boxed integers indicate the magic numbers.

.

$N = 2k + l$	k	l	Orbital	Energy	n_j	$\sum_j n_j$
0	0	0	$1s_{\frac{1}{2}}$	$3/2\omega$	2	2
1	0	1	$1p_{\frac{3}{2}}$	$5/2\omega - \lambda$	4	
1	0	1	$1p_{\frac{1}{2}}$	$5/2\omega + 2\lambda$	2	8
2	0	2	$1d_{\frac{5}{2}}$	$7/2\omega - 2\lambda$	6	
2	1	0	$2s_{\frac{1}{2}}$	$7/2\omega$	2	
2	0	2	$1d_{\frac{3}{2}}$	$7/2\omega + 3\lambda$	4	20
3	0	3	$1f_{\frac{7}{2}}$	$9/2\omega - 3\lambda$	8	28

Table 3.1. Harmonic oscillator plus spin-orbit orbitals employed in the calculations discussed in this Thesis. The number of nucleons in the j-th orbital is denoted by n_j, the number of the last column denote the magic numbers.
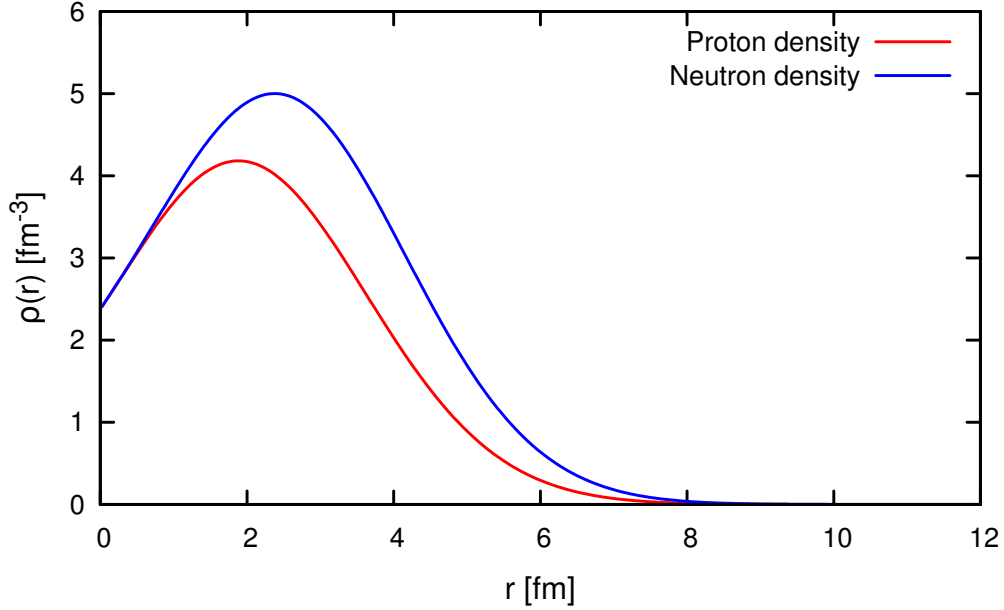
Figure 3.7. Nucleon densities for ^{48}Ca: protons (red line) and neutrons (blue line) calculated with the harmonic oscillator wave function parameter for ^{48}Ca. We set $\nu = 0.126\,\mathrm{fm}^{-1}$
.

3.7   Nucleon-nucleon correlations

The NSM has been successfully applied to explain many nuclear properties. However, single-nucleon knock out experiments, aimed at establishing its validity, also exposed its failure to properly describe the full complexity of nuclear dynamics [34].

Consider, for example, the process

$$e + A \rightarrow e' + p + (A - 1) \; . \tag{3.48}$$

In the impulse approximation regime, in which the space resolution of the probe is less than the average NN separation distance, electron-nucleus scattering reduces to the incoherent sum of elementary scattering processes involving individual nucleons (see Fig. 3.8) and the final state interactions between the knocked out nucleon and the spectator $(A - 1)$-particle system can be neglected. Within this picture, energy conservation requires that

$$\omega = \sqrt{|\mathbf{p}|^2 + m^2} + E_{A-1} - M_A \; , \tag{3.49}$$

where $\omega = E_e - E_{e'}$ is the energy transfer, $\mathbf{p}$ is the momentum of the outgoing proton and $E_{A-1} = \sqrt{|\mathbf{q} - \mathbf{p}|^2 + M_{A-1}^2}$. According to the NSM, if the knocked out nucleon is initially in the single particle state of binding energy B_α, the mass of the recoiling nucleus is given by

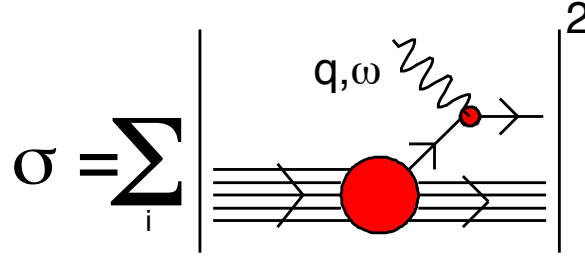$$M_{A-1} = M_A - m + B_\alpha \; . \tag{3.50}$$

Figure 3.8. Schematic representation of the impulse approximation regime, in which the nuclear cross section is replaced by the incoherent sum of cross sections describing scattering of individual nucleons, the recoiling $(A-1)$-nucleon system acting as a spectator.

In the non-relativistic limit, i.e. assuming $E_{A-1} \approx M_{A-1}$, the missing energy $E = \omega - T_p$, where $T_p = \sqrt{|\mathbf{p}|^2 + m^2} - m$, is given by $E = B_\alpha$. As a consequence, the measured missing energy spectra are expected to exhibit spectroscopic lines, corresponding to the occupied shell model states in the ground state of the target nucleus, the strength of which provides a measure of the degeneracy, $d = 2j + 1$.

Experimental data show that, while the peaks corresponding to knock-out from shell model orbits can be clearly identified in the missing energy spectra, the corresponding strengths turn out to be consistently and sizable lower than expected, independent of the nuclear mass number. This discrepancy is mainly due to the effect of dynamical correlations induced by the NN force, whose effect is not taken into account in the independent particle model. Correlations give rise to scattering processes, leading to the virtual excitation of the participating nucleons to states of energy larger than the Fermi energy, thus depleting the NSM states within the Fermi sea. As an example, Fig. 3.9 shows the missing energy spectrum of the reaction

$$e + {}^{16}\text{O} \rightarrow e' + p + {}^{15}\text{N}\,, \tag{3.51}$$

featuring the spectroscopic lines corresponding to the $1p_{1/2}$ and $1p_{3/2}$ states.

Fig. 3.10 shows a compilation of the strengths of the valence NSM orbits of a number of nuclei, ranging from carbon to lead, measured by both electron- and hadron-induced proton knock out. Note that the fractional strengths are normalized in such a way that the NSM prediction is 100. It clearly appears that all observed strengths are largely below this value.

3.7.1 Spectral function and spectroscopic factors

In the plane wave impulse approximation, the cross section of process (3.48) can be written as

$$\frac{d\sigma}{d\omega d\Omega_{e'} d\Omega_p dT_p} = |\mathbf{p}|(m + T_p)\sigma_{ep}P(\mathbf{p} - \mathbf{q}, E)\,, \tag{3.52}$$

where σ_{ep} is the elementary electron-proton cross section and $P(\mathbf{k}, E)$ is the spectral function, which contains all the information on nuclear dynamics. In the NSM, the

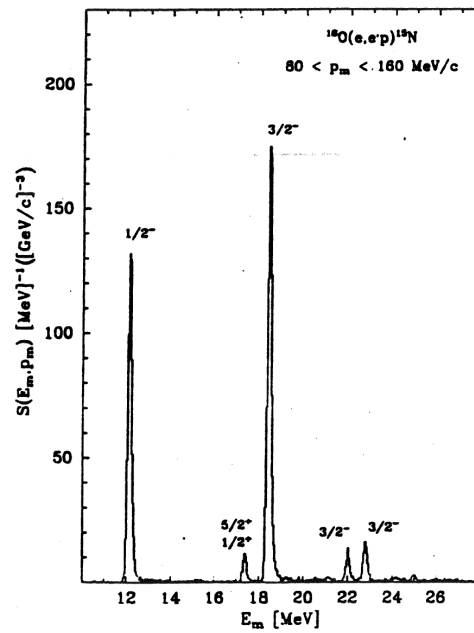**Figure 3.9.** Missing energy spectrum of the reaction $e + {}^{16}O \rightarrow e' + p + {}^{15}N$.
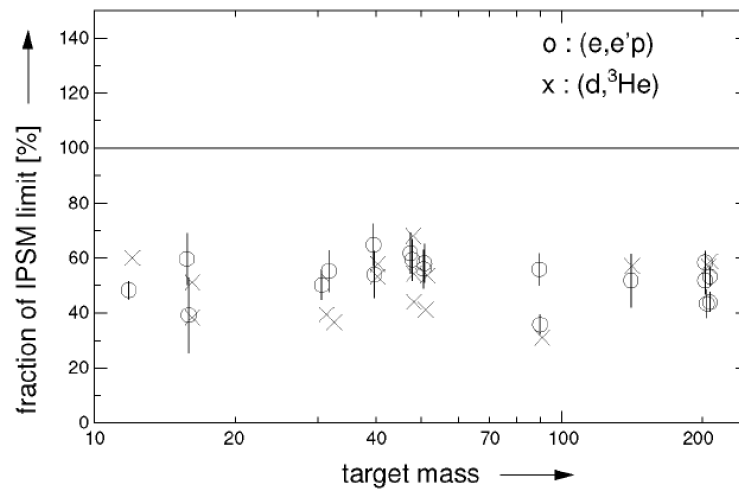

Figure 3.10. Integrated strengths of the valence NSM states, measured in electron- (open circles) and hadron-induced (crosses) proton knock out experiments, as a function of the target mass number (taken from [35]). The solid horizontal line represents the NSM prediction.

spectral function takes the simple form

$$P(\mathbf{k}, E) = \sum_\alpha |\phi_\alpha(\mathbf{k})|^2 \delta(E - B_\alpha) \ , \tag{3.53}$$

showing that $|\mathbf{k}|^2 P(\mathbf{k}, E)$ is the probability distribution of finding a proton of momentum $\mathbf{k}$ and binding energy E in the nuclear ground state.

In the presence of correlations, the NSM states are depleted, i.e.

$$Z_\alpha = \int d^3k \, |\widetilde{\phi}_\alpha(\mathbf{k})|^2 < 1 \ , \tag{3.54}$$

$\widetilde{\phi}_\alpha(\mathbf{k})$ being the new states, and the δ-function acquires a width, providing a measure of the finite lifetime of single particle states. In addition, correlations give rise to final states in which one of the spectator particle is excited to the continuum. These processes contribute a background term to the spectral function, extending to larger values of E. The spectral function of a correlated system is usually written in the form

$$P(\mathbf{k}, E) = P_{MF}(\mathbf{k}, E) + P_B(\mathbf{k}, E) \ , \tag{3.55}$$

where $P_B(\mathbf{k}, E)$ denotes the correlation background, while $P_{MF}(\mathbf{k}, E)$ can be written as (compare to Eq. (3.53))

$$P_{MF}(\mathbf{k}, E) = \sum_\alpha Z_\alpha |\phi_\alpha(\mathbf{k})|^2 f(E - B_\alpha) \ , \tag{3.56}$$

with

$$f(E) = \frac{Z_\alpha}{\pi} \frac{\Gamma_\alpha}{E^2 + \Gamma_\alpha^2} \ , \tag{3.57}$$

which amounts to assume

$$\widetilde{\phi}_\alpha(\mathbf{k}) = \sqrt{Z_\alpha} \phi_\alpha(\mathbf{k}) \, . \tag{3.58}$$

The calculation of Z_α, called spectroscopic strength (or spectroscopic factor), can be carried out within the framework of many-body theory. The starting point is the definition

$$\widetilde{\phi}_\alpha(\mathbf{k}) = \int d^3r \, \widetilde{\phi}_\alpha(\mathbf{r}) e^{-i\mathbf{k}\cdot\mathbf{r}} \ , \tag{3.59}$$

where

$$\widetilde{\phi}_\alpha(\mathbf{r}) = \sqrt{A} \int d^3r_2 \cdots d^3r_A \, \Psi_\alpha^*(\mathbf{r}_2, \ldots, \mathbf{r}_A) \Psi_0(\mathbf{r}, \mathbf{r}_2, \ldots, \mathbf{r}_A) \tag{3.60}$$

$\Psi_0(\mathbf{r}, \mathbf{r}_2, \ldots, \mathbf{r}_A)$ being the ground state of the A-particle system and $\Psi_\alpha(\mathbf{r}_2, \ldots, \mathbf{r}_A)$ the state of $(A-1)$-particle in which a state α is removed.

Although this identification is not rigorous, as correlations push a small fraction of the strength of the state α to very large energy, Z_α can be regarded as the occupation probability of the single particle state.

It is common practice to distinguish between two types of correlations: long- and short-range correlations. The long-range correlations are related to collective excitations of the system. The short-range correlations (SRC) are instead connected to the strongly repulsive core of the NN interaction. Inclusion of correlations requires

the use of a realistic phenomenological nuclear Hamiltonian of the form (3.28), obtained by fitting nuclear properties and nucleon-nucleon scattering data.

Our work has been carried out within a scheme in which non perturbative effects due to the short-range repulsion are embodied in the basis functions. This approach, called the Correlated Basis Function theory, will be briefly discuss in the next Subsection.

3.7.2 The Correlated Basis Function theory

The aim of the Correlated Basis Function (CBF) theory [36] is the solution of the many-body Schrödinger equation

$$H\Psi(1,\ldots,A) = E\Psi(1,\ldots,A)\,,\tag{3.61}$$

where $\Psi(1,\ldots,A)$ is the wave function describing the system of A particles. Eq. (3.61) is solved by using the variational principle

$$E[\Psi] = \frac{\langle\Psi|\,H\,|\Psi\rangle}{\langle\Psi|\Psi\rangle} \geq E_0\,,\tag{3.62}$$

E_0 being the true ground state energy; note that the larger the overlap $\langle\Psi_0|\Psi\rangle$ the closer $E[\Psi]$ is to E_0, Ψ_0 being the true ground state. The minimum obtained in this manner is an upper bound of the eigenvalue of the Eq. (3.61). We search solutions of the type

$$\Psi(1,\ldots,A) = F(1,\ldots,A)\Phi(1,\ldots,A)\,,\tag{3.63}$$

in which $F(1,\ldots,A)$ is a many-body correlation operator and $\Phi(1,\ldots,A)$ is a Slater determinant composed of single-particle wave functions. The operator $F(1,\ldots,A)$, embodying the correlation structure induced by the NN interaction, is written in the form

$$F(1,\ldots,A) = \mathcal{S}\left(\prod_{i<j=1}^{A} f_{ij}\right)\,,\tag{3.64}$$

where $\mathcal{S}$ is the symmetrization operator and the functions f_{ij} are expressed in terms of the two-body *correlation functions* $f^n(r_{ij})$. The structure of the f_{ij} must reflect the complexity of the NN potential; hence, we can write

$$f_{ij} = \sum_{n=1}^{6} f^n(r_{ij})O_{ij}^n\,,\tag{3.65}$$

with the O_{ij}^n defined by Eq. (3.21). The shapes of the radial functions $f^n(r)$ are determined using the variational principle in Eq. (3.62), this procedure leads to a set of Euler-Lagrange equations, whose solutions satisfy the boundary conditions

$$\lim_{r\to\infty} f^n(r) = \begin{cases} 1 & n=1 \\ 0 & n>1 \end{cases}\,.\tag{3.66}$$

The short range behavior of the two-nucleon correlation functions is such that the quantity

$$f_{ij}^\dagger H_{ij} f_{ij} = f_{ij}^\dagger\left(\frac{\mathbf{p}_i^2}{2m} + \frac{\mathbf{p}_j^2}{2m} + v_{ij}\right)f_{ij}\,,\tag{3.67}$$

which reduces to H_{ij} at large interparticle distances, is well behaved as $r \to 0$.

More generally, one can define a complete, although non orthonormal, set of correlated states. For example, in the case of uniform nuclear matter, the unperturbed Fermi gas states $|n_{FG}\rangle$ are replaced by the set of correlated states

$$|n\rangle = \frac{F |n_{FG}\rangle}{\langle n_{FG}| F^\dagger F |n_{FG}\rangle^{1/2}} \, . \tag{3.68}$$

Once the correlated basis has been defined, the nuclear Hamiltonian can be split in two pieces

$$H = H_0 + H_1 \, , \tag{3.69}$$

where H_0 and H_1 denote the diagonal and off-diagonal components of H, respectively, defined by the equations

$$\langle m| H_0 |n\rangle = \delta_{mn} \langle m| H |n\rangle \, , \tag{3.70}$$

$$\langle m| H_1 |n\rangle = (1 - \delta_{mn}) \langle m| H |n\rangle \, . \tag{3.71}$$

The above definitions imply that, if the correlated states have large overlaps with the eigenstates of H, the matrix element of H_1 are small, and the perturbative expansions in powers of H_1 is rapidly convergent.

3.7.3 Spectroscopic factors in uniform nuclear matter and lead

In this Section we outline the calculation of the spectroscopic factors using correlated wave functions. For the sake of simplicity, we will consider isospin symmetric nuclear matter. Due to transition invariance, in this system, single particle states are plane waves[4]:

$$\phi_\alpha(\mathbf{r}) = \phi_h(\mathbf{r}) = \frac{e^{i\mathbf{h}\cdot\mathbf{r}}}{\sqrt{V}} \, , \tag{3.72}$$

where V is the normalization volume. The spectroscopic factor defined in Eq. (3.54) can be written as

$$Z_h = \int d^3k \, |\widetilde{\phi}_h(\mathbf{k})|^2 \, , \tag{3.73}$$

where $\widetilde{\phi}_h(\mathbf{k})$ is the matrix element to be computed defined as (see Eq. (3.60))

$$\widetilde{\phi}_h(\mathbf{k}) = \sqrt{A} \int d^3r_1 \cdots d^3r_A \, \Psi_h^*(\mathbf{r}_2, \ldots, \mathbf{r}_A) \Psi_0(\mathbf{r}_1, \ldots, \mathbf{r}_A) e^{-i\mathbf{k}\cdot\mathbf{r}_1} \, , \tag{3.74}$$

$\Psi_0(\mathbf{r}_1, \ldots, \mathbf{r}_A)$ being the ground state of the A-particle system and $\Psi_h(\mathbf{r}_2, \ldots, \mathbf{r}_A)$ the state of $(A-1)$-particle in which a state of momentum $\mathbf{h}$ is removed within the Fermi sea. Within the correlated basis function formalism, according to Eq. (3.63), the wave functions can be written in the form:

$$\Psi_0(\mathbf{r}_1, \ldots, \mathbf{r}_A) = F_A \Phi(\mathbf{r}_1, \ldots, \mathbf{r}_A) \, , \tag{3.75}$$

$$\Psi_h(\mathbf{r}_2, \ldots, \mathbf{r}_A) = F_{A-1} \Phi_h(\mathbf{r}_2, \ldots, \mathbf{r}_A) \, , \tag{3.76}$$

---

[4]The dependence on spin and isospin degrees of freedom does not play a role in this context, and will be omitted.

where $\Phi(\mathbf{r}_1, \ldots, \mathbf{r}_A)$ and $\Phi_h(\mathbf{r}_2, \ldots, \mathbf{r}_A)$ are Slater determinants defined in Eq. (3.32). The many-body correlation operators F_A and F_{A-1} are given by (see the previous Section)

$$F_A = \prod_{j>i=1}^{A} f(r_{ij}), \tag{3.77}$$

$$F_{A-1} = \prod_{j>i=2}^{A} f(r_{ij}). \tag{3.78}$$

In the case discussed in this Section the correlation operator is real. Hence, Eq. (3.74) becomes

$$\widetilde{\phi}_h(\mathbf{k}) = \sqrt{A} \int d^3r_1 \cdots d^3r_A \, \Phi_h^*(\mathbf{r}_2, \ldots, \mathbf{r}_A) F_{A-1} F_A \Phi_0(\mathbf{r}_1, \ldots, \mathbf{r}_A) e^{-i\mathbf{k}\cdot\mathbf{r}_1}. \tag{3.79}$$

We can now expand

$$\begin{aligned}
F_{A-1}F_A &= \left[\prod_{k=2}^{A} f(r_{1k}) \right]\left[\prod_{j>i=2}^{A} f^2(r_{ij}) \right] \\
&= \left[\prod_{k=2}^{A} \Big(1 + g(r_{1k})\Big) \right]\left[\prod_{j>i=2}^{A} \Big(1 + h(r_{ij})\Big) \right] \\
&= 1 + \sum_{k=2}^{A} g(r_{1k}) + \sum_{j>i=2}^{A} h(r_{ij}) + \ldots,
\end{aligned} \tag{3.80}$$

where $g(r_{1k}) = f(r_{1k}) - 1$ and $h(r_{ij}) = f^2(r_{ij}) - 1$. We are interested to the leading order, i.e. $1 + \sum_{k=2}^{A} g(r_{1k})$, thus Eq. (3.79) becomes

$$\begin{aligned}
\widetilde{\phi}_h(\mathbf{k}) = \sqrt{A} \int d^3r_1 \cdots d^3r_A \left[1 + (A-1)g(r_{12}) \right] \\
\times \, \Phi_h^*(\mathbf{r}_2, \ldots, \mathbf{r}_A) \Phi_0(\mathbf{r}_1, \ldots, \mathbf{r}_A) e^{-i\mathbf{k}\cdot\mathbf{r}_1} + \ldots.
\end{aligned} \tag{3.81}$$

Using the relation

$$\Phi_h^*(\mathbf{r}_2, \ldots, \mathbf{r}_A)\Phi_0(\mathbf{r}_1, \ldots, \mathbf{r}_A) = \Phi_h^*(\mathbf{r}_2, \ldots, \mathbf{r}_A) \sum_\alpha \frac{e^{i\mathbf{k}_\alpha \cdot \mathbf{r}_1}}{\sqrt{V}} \frac{1}{\sqrt{A}} \Phi_\alpha(\mathbf{r}_2, \ldots, \mathbf{r}_A), \tag{3.82}$$

where the sum is over the states of the Fermi gas, the first term of the right-hand side of Eq. (3.79) is given by

$$\begin{aligned}
\frac{1}{\sqrt{V}} \int d^3r_1 \sum_\alpha e^{-i(\mathbf{k}-\mathbf{k}_\alpha)\cdot\mathbf{r}_1} \\
\times \int d^3r_2 \cdots d^3r_A \, \Phi_h^*(\mathbf{r}_2, \ldots, \mathbf{r}_A)\Phi_\alpha(\mathbf{r}_2, \ldots, \mathbf{r}_A) = \frac{(2\pi)^3}{\sqrt{V}} \delta(\mathbf{k} - \mathbf{h}),
\end{aligned} \tag{3.83}$$

where we used the orthonormal condition

$$\int d^3r_2 \cdots d^3r_A \, \Phi_h^*(\mathbf{r}_2, \ldots, \mathbf{r}_A)\Phi_\alpha(\mathbf{r}_2, \ldots, \mathbf{r}_A) = \delta_{h\alpha}. \tag{3.84}$$

Using a further expansion of the Slater determinants

$$
\Phi_h^*(\mathbf{r}_2, \ldots, \mathbf{r}_A)\Phi_0(\mathbf{r}_1, \ldots, \mathbf{r}_A) = \sum_{\gamma \neq h} \frac{e^{-i\mathbf{k}_\gamma \cdot \mathbf{r}_2}}{\sqrt{V}} \frac{1}{\sqrt{A-1}} \Phi_{h\gamma}^*(\mathbf{r}_3, \ldots, \mathbf{r}_A)
$$
$$
\times \sum_\alpha \frac{e^{i\mathbf{k}_\alpha \cdot \mathbf{r}_1}}{\sqrt{V}} \sum_{\beta \neq \alpha} \frac{e^{i\mathbf{k}_\beta \cdot \mathbf{r}_2}}{\sqrt{V}} \frac{1}{\sqrt{A(A-1)}} \Phi_{\alpha\beta}(\mathbf{r}_3, \ldots, \mathbf{r}_A), \quad (3.85)
$$

the second term of the right-hand side of Eq. (3.79) is given by

$$
\frac{1}{V^{3/2}} \int d^3r_1 d^3r_2 \, g(r_{12}) \sum_\alpha \sum_{\beta \neq \alpha} \sum_{\gamma \neq h} \left[e^{-i(\mathbf{k}-\mathbf{k}_\alpha)\cdot\mathbf{r}_1} e^{-i(\mathbf{k}_\gamma - \mathbf{k}_\beta)\cdot\mathbf{r}_2} \right]
$$
$$
\times \int d^3r_3 \cdots d^3r_A \, \Phi_{h\gamma}^*(\mathbf{r}_3, \ldots, \mathbf{r}_A)\Phi_{\alpha\beta}(\mathbf{r}_3, \ldots, \mathbf{r}_A). \quad (3.86)
$$

If we use the orthonormal condition

$$
\int d^3r_3 \cdots d^3r_A \, \Phi_{h\gamma}^*(\mathbf{r}_3, \ldots, \mathbf{r}_A)\Phi_{\alpha\beta}(\mathbf{r}_3, \ldots, \mathbf{r}_A) = \delta_{h\alpha}\delta_{\gamma\beta} - \delta_{h\beta}\delta_{\gamma\alpha}, \quad (3.87)
$$

the expression in Eq. (3.86) becomes

$$
\frac{1}{V^{3/2}} \int d^3r_1 d^3r_2 \, g(r_{12}) \sum_\alpha \left[e^{-i(\mathbf{k}-\mathbf{h})\cdot\mathbf{r}_1} - e^{-i(\mathbf{k}-\mathbf{k}_\alpha)\cdot\mathbf{r}_1} e^{-i(\mathbf{k}_\alpha-\mathbf{h})\cdot\mathbf{r}_2} \right]. \quad (3.88)
$$

The above integral can be solved using the transformation of variables

$$
\mathbf{r}_1 = \mathbf{R} + \frac{\mathbf{r}_{12}}{2}, \quad \mathbf{r}_2 = \mathbf{R} - \frac{\mathbf{r}_{12}}{2}, \quad (3.89)
$$

and passing to the continuum, i.e.

$$
\sum_\alpha \to \frac{V}{(2\pi)^3} \int d^3k. \quad (3.90)
$$

Hence, we have

$$
\frac{1}{V^{3/2}} \int d^3r_1 d^3r_2 \, g(r_{12}) \frac{V}{(2\pi)^3} \int d^3k \, e^{-i(\mathbf{k}-\mathbf{h})\cdot\mathbf{r}_1} = \frac{(2\pi)^3}{\sqrt{V}} \delta(\mathbf{k}-\mathbf{h}) \frac{\rho}{\nu} \widetilde{g}(0), \quad (3.91)
$$

in which we used

$$
\frac{V}{(2\pi)^3} \int d^3k = \frac{V}{(2\pi)^3} \frac{4}{3}\pi|\mathbf{k}_F|^3 = V\frac{\rho}{\nu}, \quad (3.92)
$$

$\mathbf{k}_F$, ρ and ν being the Fermi momentum, the nucleon density and the degeneracy, respectively, and $\widetilde{g}$ denote the Fourier transform of g. Moreover, we have

$$
\frac{1}{V^{3/2}} \int d^3r_1 d^3r_2 \, g(r_{12}) \frac{V}{(2\pi)^3} \int d^3k \, e^{-i(\mathbf{k}-\mathbf{k}_\alpha)\cdot\mathbf{r}_1} e^{-i(\mathbf{k}_\alpha-\mathbf{h})\cdot\mathbf{r}_2}
$$
$$
= \frac{1}{V^{3/2}} \int d^3R \, d^3r_{12} \, g(r_{12}) \frac{V}{(2\pi)^3} \int d^3k \, e^{-i(\mathbf{k}-\mathbf{h})\cdot\mathbf{R}} e^{-i(\mathbf{k}+\mathbf{h}-2\mathbf{k}_\alpha)\cdot\frac{\mathbf{r}_{12}}{2}}
$$
$$
= \frac{(2\pi)^3}{\sqrt{V}} \delta(\mathbf{k}-\mathbf{h}) \frac{\rho}{\nu} \int d^3r_{12} \, g(r_{12}) \, l(\mathbf{k}_F \cdot \mathbf{r}_{12}) e^{-i\mathbf{k}\cdot\mathbf{r}_{12}}, \quad (3.93)
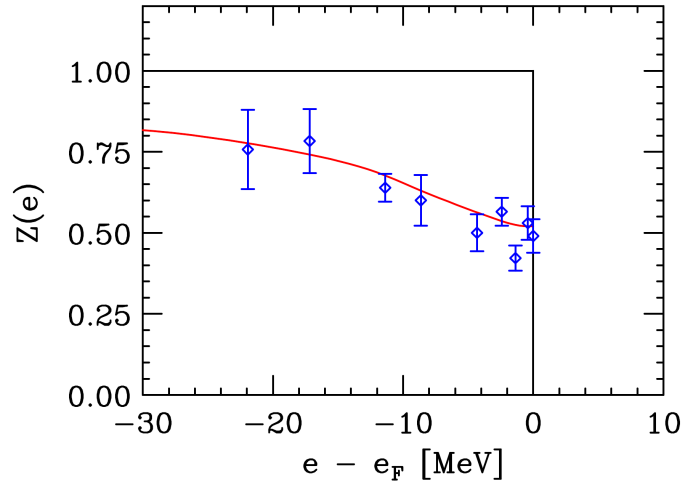$$

Figure 3.11. Spectroscopic strength in function of the energy $Z(e)$, e_F is the Fermi energy. The red line gives the estimated $Z(e)$ in ^{208}Pb. Experimental data are taken from Ref. [37]

in which we used

$$\frac{1}{(2\pi)^3} \int d^3k \, e^{i\mathbf{k}_\alpha \cdot \mathbf{r}_{12}} = \frac{\rho}{\nu} \, l(\mathbf{k}_\alpha \cdot \mathbf{r}_{12}), \tag{3.94}$$

the function $l(x)$ is defined as

$$l(x) = \frac{3}{x^3} \left(\sin x - x \cos x \right). \tag{3.95}$$

Using the results of Eqs. (3.83), (3.91) and (3.93), $\widetilde{\phi}_h(\mathbf{k})$ in Eq. (3.81) is given by

$$\widetilde{\phi}_h(\mathbf{k}) = \frac{(2\pi)^3}{\sqrt{V}} \, \delta(\mathbf{k} - \mathbf{h}) \left\{ 1 + \frac{\rho}{\nu} \left[\widetilde{g}(0) - \int d^3x \, g(x) \, l(\mathbf{k}_F \cdot \mathbf{x}) e^{-i\mathbf{k} \cdot \mathbf{x}} \right] \right\} + \ldots \, . \tag{3.96}$$

The contributions to $\widetilde{\phi}_h(\mathbf{k})$ can be represented by diagrams that can be classified according to their topological structure and summed up to all orders solving a set of coupled integral equations [38]. The results of these calculations, corrected to account for surface effects, turn out to be in fairly good agreement with the data obtained from electron scattering experiments with a ^{208}Pb target (see Fig. 3.11).

Chapter 4

Calculation of nuclear matrix elements

The Fermi (F) and Gamow-Teller (GT) transition matrix elements for $2\beta_{0\nu}$ decay obtained using the closure approximation given by Eqs. (2.46) and (2.47) can be written in the general form

$$M_{0\nu}^\alpha = \langle \Psi_f, \mathcal{J}_f^\pi | \sum_{j,k=1}^A \tau_j^+ \tau_k^+ O_{jk}^\alpha(r) |\Psi_i, \mathcal{J}_i^\pi\rangle\,. \tag{4.1}$$

where $\alpha = F$, GT, Ψ_i and Ψ_f are the ground states of the intial and final nucleus, respectively, $\mathcal{J}_i^\pi$ and $\mathcal{J}_f^\pi$ are the total angular momentum and parity of the initial and final nucleus, respectively. $O_{jk}^\alpha(r)$ is an operator defined as

$$O_{jk}^F(r) = \mathbb{1}\, H(r) = S_{jk}^F\, H(r)\,, \tag{4.2}$$

$$O_{jk}^{GT}(r) = (\boldsymbol{\sigma}_j \cdot \boldsymbol{\sigma}_k)\, H(r) = S_{jk}^{GT}\, H(r)\,, \tag{4.3}$$

where $H(r)$ si the neutrino potential given by

$$H(r) = \frac{2R_A}{\pi r} \int_0^{+\infty} \frac{\sin(qr)}{q + \langle E\rangle}\, dq\,. \tag{4.4}$$

In the above equations, $r = |\mathbf{r}_j - \mathbf{r}_k|$, R_A is the nuclear radius and $\langle E\rangle$ is the average energy of the virtual intermediate states used in the closure approximation.

The aim of this Chapter is to describe the structure of $M_{0\nu}^\alpha$ in the pure shell model picture and after with inclusion of correlation effects.

4.1 Pure shell model

We assume that two neutrons of the initial state nucleus decay while the other nucleons act as spectators. Due to the two-body nature of the transition operator, the matrix element in Eq. (4.1) can be reduced to a sum of products of the so called two-body transition densities and antisymmetrized two-body matrix elements, i.e.

$$M_{0\nu}^\alpha = \sum_{j_1,j_2,j_1',j_2',J} TBTD\,(j_1, j_2, j_1', j_2', J, \mathcal{J}_i^\pi, \mathcal{J}_f^\pi)$$

$$\times \langle j_1' j_2';\, J\,T;\, \mathcal{J}_i^\pi|\, \tau_1^+ \tau_2^+ O_{12}^\alpha(r) \,|j_1 j_2;\, J\,T;\, \mathcal{J}_f^\pi\rangle_a\,. \tag{4.5}$$

In the above equation, the indeces 1 and 2 label the quantum numbers of the two decaying neutrons, while 1 and 2 with primes refer to the final protons, j is the total angular momentum quantum number of a nucleon participating in the decay, while J is the total angular momentum quantum number of the pair of nucleons participating in the decay, T is the total isospin of the pair of nucleons which takes the value of 1 both for the intial and final state and $|\cdots\rangle_a$ denotes an antisymmetrized two-particle state. The coefficients $TBTD\,(j_1, j_2, j_1', j_2', J, \mathcal{J}_i^\pi, \mathcal{J}_f^\pi)$ are the two-body transition densities and take into account how the spectator nucleons rearrange themselves.

In order to carry out the calculation, the two-body matrix element in Eq. (4.5) must be decomposed into products of reduced matrix elements of operators acting in spin and coordinate space. In addition, the coordinate space matrix element must be decomposed in two contributions, arising from the center of mass and relative motion.

Hence, the matrix elements of O_{12}^α for non-antisymmetrized jj-coupling scheme can be written as

$$
\langle k_1' l_1' j_1', k_2' l_2' j_2'; J\,T = 1;\, \mathcal{J}_i^\pi| O_{12}^\alpha(r) |k_1 l_1 j_1,\, k_2 l_2 j_2; J\,T = 1; \mathcal{J}_f^\pi\rangle
$$
$$
= \sum_{S,\Lambda} \left\langle l_1' \frac{1}{2} j_1',\, l_2' \frac{1}{2} j_2' \,\bigg|\, \frac{1}{2}\frac{1}{2}S,\, l_1' l_2' \Lambda \right\rangle_J \left\langle l_1 \frac{1}{2} j_1,\, l_2 \frac{1}{2} j_2 \,\bigg|\, \frac{1}{2}\frac{1}{2}S,\, l_1 l_2 \Lambda \right\rangle_J
$$
$$
\times \frac{1}{\sqrt{2S+1}} \left\langle \frac{1}{2}\frac{1}{2}S \,\|\, S_{12}^\alpha \,\|\, \frac{1}{2}\frac{1}{2}S \right\rangle
$$
$$
\times \sum_{k,l,K,L}\; \sum_{k',l',K',L'} \langle kl,\, KL|k_1 l_1,\, k_2 l_2\rangle_\Lambda\, \langle k'l',\, K'L'|k_1' l_1',\, k_2' l_2'\rangle_\Lambda\, \langle k'l'|\, H(r)\, |kl\rangle,
$$
$$
\tag{4.6}
$$

where

$$
\left\langle l_1 \frac{1}{2} j_1,\, l_2 \frac{1}{2} j_2 \,\bigg|\, \frac{1}{2}\frac{1}{2}S,\, l_1 l_2 \Lambda \right\rangle_J = \sqrt{(2j_1+1)(2j_2+1)(2S+1)(2\Lambda+1)} \begin{pmatrix} l_1 & \frac{1}{2} & j_1 \\ l_1 & \frac{1}{2} & j_2 \\ \Lambda & S & J \end{pmatrix},
$$
$$
\tag{4.7}
$$

in which k and l with labels are the principal and angular momentum quantum numbers of a nucleon participating in the decay, respectively, while k and l without labels are the principal and angular momentum quantum numbers of the relative motion, respectively, K and L are the principal and angular momentum quantum numbers of the center of mass motion, Λ and S are the orbital angular momentum and the spin quantum numbers of the pair of nucleons, respectively. The last factor in Eq. (4.7) is a 9-j symbol which takes into account the coupling of angular momenta. $\langle kl,\, KL|k_1 l_1,\, k_2 l_2\rangle_\Lambda$, called *Talmi-Moshinsky brackets*, are the coefficients of the transformation from the $(\mathbf{r}_1, \mathbf{r}_2)$ representation to the $(\mathbf{r} = (\mathbf{r}_1 - \mathbf{r}_2), \mathbf{R} = (\mathbf{r}_1 + \mathbf{r}_2)/2)$:

$$
\langle \mathbf{r}_1|k_1 l_1\rangle \langle \mathbf{r}_2|k_2 l_2\rangle = \sum_{k,l,K,L} \langle kl,\, KL|k_1 l_1,\, k_2 l_2\rangle_\Lambda\, \langle \mathbf{r}|kl\rangle \langle \mathbf{R}|KL\rangle. \tag{4.8}
$$

The Talmi-Moshinsky transformation is only possible for harmonic oscillator radial wave function. This is why we choose to use this basis. The reduced matrix elements

of the relevant operators S_{ij}^α in Eq. (4.6) are given by

$$\left\langle \frac{1}{2}\frac{1}{2}S \, \| \, \mathbb{1} \, \| \, \frac{1}{2}\frac{1}{2}S \right\rangle = \sqrt{2S+1} \,, \tag{4.9}$$

$$\left\langle \frac{1}{2}\frac{1}{2}S \, \| \, (\boldsymbol{\sigma}_1 \cdot \boldsymbol{\sigma}_2) \, \| \, \frac{1}{2}\frac{1}{2}S \right\rangle = \sqrt{2S+1}[2S(S+1)-3] \,. \tag{4.10}$$

The radial relative motion matrix element is given by

$$\langle k'l' | \, H(r) \, | kl \rangle = \int_0^{+\infty} r^2 dr \, R_{k'l'}(r) H(r) R_{kl}(r) \,, \tag{4.11}$$

$R_{kl}(r)$ and $R_{k'l'}(r)$ being the radial wave functions of the harmonic oscillator potential of the initial and final state, respectively.

The antisymmetrized form of the two-body matrix elements can be obtained using

$$\langle j_1' j_2'; \, JT; \, \mathcal{J}_i^\pi | \, \tau_1^+ \tau_2^+ O_{12}^\alpha(r) \, | j_1 j_2; \, JT; \, \mathcal{J}_i^\pi \rangle_a = \frac{1}{\sqrt{(1+\delta_{j_1' j_2'})(1+\delta_{j_1 j_2})}}$$
$$\times [\langle j_1' j_2'; \, JT; \, \mathcal{J}_i^\pi | \, \tau_1^+ \tau_2^+ O_{12}^\alpha(r) \, | j_1 j_2; \, JT; \, \mathcal{J}_f^\pi \rangle$$
$$- (-1)^{j_1+j_2+J} \langle j_1' j_2'; \, JT; \, \mathcal{J}_i^\pi | \, \tau_1^+ \tau_2^+ O_{12}^\alpha(r) \, | j_2 j_1; \, JT; \, \mathcal{J}_f^\pi \rangle] \,. \tag{4.12}$$

4.2   Including correlations

In our work we will neglect the contribution of non central correlations. Hence, Eq. (3.65) reduces to

$$f_{12} = f_c(r)\mathbb{1} + f_\sigma(r)(\boldsymbol{\sigma}_1 \cdot \boldsymbol{\sigma}_2) + f_\tau(r)(\boldsymbol{\tau}_1 \cdot \boldsymbol{\tau}_2) + f_{\sigma\tau}(r)(\boldsymbol{\sigma}_1 \cdot \boldsymbol{\sigma}_2)(\boldsymbol{\tau}_1 \cdot \boldsymbol{\tau}_2) \,. \tag{4.13}$$

For neutron-neutron and proton-proton pairs, having $T = 1$, we have

$$(\boldsymbol{\tau}_1 \cdot \boldsymbol{\tau}_2) = \frac{1}{2}[4T(T+1)-6] = 1 \,, \tag{4.14}$$

leading to

$$f_{12}(r) = [f_c(r) + f_\tau(r)]\mathbb{1} + [f_\sigma(r) + f_{\sigma\tau}(r)](\boldsymbol{\sigma}_1 \cdot \boldsymbol{\sigma}_2) \,. \tag{4.15}$$

The implementation of correlation effects can be carried out replacing the wave functions

$$\phi_\alpha(\mathbf{r}_1)\phi_\beta(\mathbf{r}_2) \to f_{12}(r) \, \phi_\alpha(\mathbf{r}_1)\phi_\beta(\mathbf{r}_2) \,, \tag{4.16}$$

or, equivalently, one can replace the bare transition operators with effective transition operators

$$O_{12}^\alpha(r) \to \tilde{O}_{12}^\alpha(r) = f_{12}^\dagger(r) \, O_{12}^\alpha(r) \, f_{12}(r) = f_{12}^2(r) O_{12}^\alpha(r) \,. \tag{4.17}$$

In the following, for sake of semplicity, we will omit the dependence on r. Using the property $(\boldsymbol{\sigma}_1 \cdot \boldsymbol{\sigma}_2)^2 = 3 - (\boldsymbol{\sigma}_1 \cdot \boldsymbol{\sigma}_2)$, we obtain

$$f_{12}^2 = [(f_c+f_\tau)^2 + 3(f_\sigma+f_{\sigma\tau})^2]\mathbb{1} + 2(f_\sigma+f_{\sigma\tau})[(f_c+f_\tau)-(f_\sigma+f_{\sigma\tau})](\boldsymbol{\sigma}_1 \cdot \boldsymbol{\sigma}_2) \,. \tag{4.18}$$

In our analysis we will consider two cases:

- $(f_c + f_\tau) \neq 0$ and $(f_\sigma + f_{\sigma\tau}) = 0$, the effective Fermi and Gamow-Teller operators take the form:

$$\tilde{O}_{12}^F = (f_c + f_\tau)^2 \, O_{12}^F \,, \tag{4.19}$$

$$\tilde{O}_{12}^{GT} = (f_c + f_\tau)^2 \, O_{12}^{GT} \,; \tag{4.20}$$

- $(f_c + f_\tau) \neq 0$ and $(f_\sigma + f_{\sigma\tau}) \neq 0$, the effective Fermi and Gamow-Teller operators take the form:

$$\tilde{O}_{12}^F = [(f_c + f_\tau)^2 + 3(f_\sigma + f_{\sigma\tau})^2] \, O_{12}^F$$
$$\quad + 2(f_\sigma + f_{\sigma\tau})[(f_c + f_\tau) - (f_\sigma + f_{\sigma\tau})] \, O_{12}^{GT} \,, \tag{4.21}$$

$$\tilde{O}_{12}^{GT} = 6(f_\sigma + f_{\sigma\tau})[(f_c + f_\tau) - (f_\sigma + f_{\sigma\tau})] \, O_{12}^F$$
$$\quad + [(f_c + f_\tau)^2 + 7(f_\sigma + f_{\sigma\tau})^2 - 4(f_c + f_\tau)(f_\sigma + f_{\sigma\tau})] \, O_{12}^{GT} \,. \tag{4.22}$$

Note that due to the presence of spin dependent correlations, in the second case, the Fermi tranistions acquire a Gamow-Teller-like part and vice versa.

The implementation of correlation effects can be carried out in an alernative way replacing the wave functions

$$\phi_\alpha(\mathbf{r}_1)\phi_\beta(\mathbf{r}_2) \to \widetilde{\phi}_\alpha(\mathbf{r}_1)\widetilde{\phi}_\beta(\mathbf{r}_2) \,, \tag{4.23}$$

where $\widetilde{\phi}_\alpha(\mathbf{r}_1)$ and $\widetilde{\phi}_\beta(\mathbf{r}_2)$ are the depleted shell model states defined in Eq. (3.60) and written as

$$\widetilde{\phi}_\alpha(\mathbf{r}_1) = \sqrt{Z_\alpha}\phi_\alpha(\mathbf{r}_1) \,, \tag{4.24}$$

$$\widetilde{\phi}_\beta(\mathbf{r}_2) = \sqrt{Z_\beta}\phi_\beta(\mathbf{r}_2) \,, \tag{4.25}$$

where Z_α and Z_β are the spectroscopic factors.

In the next Chapter we will discuss the implementation of correlation effects in the two ways explained above in Eqs. (4.17) and (4.23) for the calculation of the neutrinoless double beta decay matrix element.

Chapter 5

Numerical calculations

As our analysisis is aimed at studying the effects of nucleon-nucleon correlations, we will keep the complications associated with the shell model description to a minimum.

In our work we analyzed the reaction

$$^{48}_{20}\text{Ca} \rightarrow {}^{48}_{22}\text{Ti} + e^- + e^- \; . \tag{5.1}$$

The transition above is from the ground state of ^{48}Ca with $\mathcal{J}^{\pi}_{^{48}\text{Ca}} = 0^+$ to the ground state of ^{48}Ti with $\mathcal{J}^{\pi}_{^{48}\text{Ti}} = 0^+$; the energy level scheme is shown in Fig. 5.1. We choose to study the reaction (5.1) for many reasons [39]. First of all, ^{48}Ca is the lightest element that can undergo double beta decay and its shell structure is quite simple, as the number of protons (20) and neutrons (28) are both magic numbers corresponding to closed shells. As shown in Table 3.1 the neutrons fill all the levels of the shells $1s_{\frac{1}{2}}$, $1p_{\frac{3}{2}}$, $1p_{\frac{1}{2}}$, $1d_{\frac{5}{2}}$, $2s_{\frac{1}{2}}$, $1d_{\frac{3}{2}}$ and $1f_{\frac{7}{2}}$; while the protons fill up the levels $1s_{\frac{1}{2}}$, $1p_{\frac{3}{2}}$, $1p_{\frac{1}{2}}$, $1d_{\frac{5}{2}}$, $2s_{\frac{1}{2}}$ and $1d_{\frac{3}{2}}$. Moreover, ^{48}Ca has $Q_{2\beta} = 4.271\,\text{MeV}$, the highest $Q_{2\beta}$-value in nature which could contribute to an increased decay probability. In addition, the high-energy γ and β radiation emitted in this process could help eliminate most of the background noise. Another important reason to choose ^{48}Ca for the study of $2\beta_{0\nu}$ decay is that shell model calculations have provided the correct prediction of $2\beta_{2\nu}$ decay halflife for this element [9, 40]. On the other hand, the small natural abundance of this isotope, 0.187%, increases the difficulty of an experimental investigation. In addition, the results of previous calculations [41, 42] suggest that the nuclear matrix element of ^{48}Ca is smaller, by a factor of 4-5, than those of other 2β emitters, such as ^{76}Ge and ^{82}Se [43]. However, experiments on double beta decay of ^{48}Ca, suce as CANDLES [44] and CARVEL [45], may reach the sensitivity required for measuring such transitions, and the availability of theoretical predictions may be useful.

In this Chapter we will describe the calculation of the neutrinoless double beta decay matrix element in the two different ways described in Section 4.2. In Section 5.1 the calculation is carried out replacing the Fermi and Gamow-Teller operators with effective operators using correlation functions consistently determined by a realistic phenomenological Hamiltonian within the framework of the correlated basis function theory [46]. In Section 5.2 we will replace the shell model wave functions with the
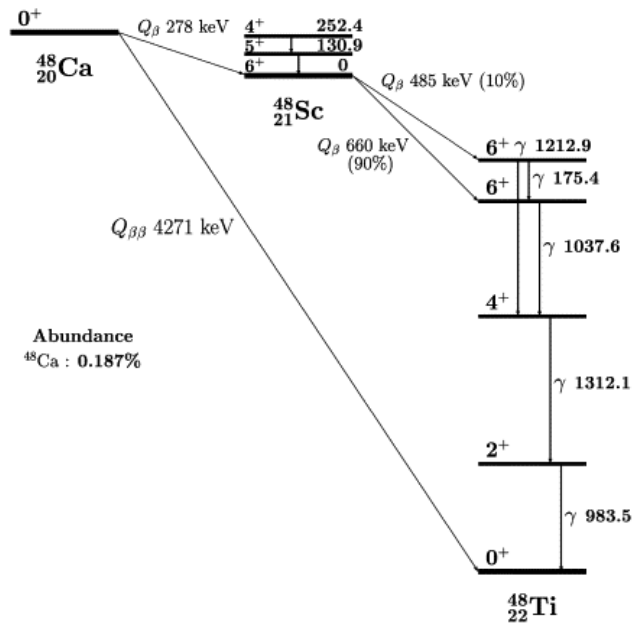
Figure 5.1. Energy level scheme of double beta decay $^{48}_{20}\text{Ca} \to {}^{48}_{22}\text{Ti}$

depleted shell model wave functions using spectroscopic factors also computed within the correlated basis function theory in [36].

5.1 Using correlated two-nucleon states

5.1.1 Hilbert space

In our work, in order to carry out the calculation of the Fermi and Gamow-Teller transition matrix elements $M^{\alpha}_{0\nu}$ of Eq. (4.5), we will consider the case in which the neutrons and protons involved in the decay processes only occupy the $1f_{\frac{7}{2}}$ shell. As a consequence, in the non-antisymmetrized matrix element of Eq. (4.6), we set

$$k_1 = k_2 = k'_1 = k'_2 = 0\,, \tag{5.2}$$

$$l_1 = l_2 = l'_1 = l'_2 = 3\,, \tag{5.3}$$

$$j_1 = j_2 = j'_1 = j'_2 = \frac{7}{2}\,. \tag{5.4}$$

Because the transition operators act only on the relative wave functions, we have that the quantum numbers relative to the center of mass motion are conserved, i.e.

$$K = K'\,, \quad L = L'\,. \tag{5.5}$$

In addition, as we do not include the effects of non-central correlations, we have

$$l = l'\,. \tag{5.6}$$

In conclusion, the matrix element of Eq. (4.6) becomes

$$\langle k_1' l_1' j_1', k_2' l_2' j_2'; J\,T=1; 0^+ |\, O_{12}^\alpha(r)\, |k_1 l_1 j_1,\, k_2 l_2 j_2; J\,T=1; 0^+ \rangle$$

$$= \sum_{S,\Lambda} \left| \left\langle l_1 \frac{1}{2} j_1,\, l_2 \frac{1}{2} j_2 \left| \frac{1}{2}\frac{1}{2} S,\, l_1 l_2 \Lambda \right. \right\rangle_J \right|^2 \frac{1}{\sqrt{2S+1}} \left\langle \frac{1}{2}\frac{1}{2} S \,\|\, S_{12}^\alpha \,\|\, \frac{1}{2}\frac{1}{2} S \right\rangle$$

$$\times \sum_{k,k',l,K,L} \langle kl,\, KL|k_1 l_1,\, k_2 l_2 \rangle_\Lambda \,\langle k'l,\, KL|k_1 l_1,\, k_2 l_2 \rangle_\Lambda \,\langle k'l|\, H(r)\, |kl \rangle\,. \quad (5.7)$$

Moreover, conservation of energy requires that

$$2k_1 + l_1 + 2k_2 + l_2 = 2k_1' + l_1' + 2k_2' + l_2' = 6\,, \quad (5.8)$$

which implies in turn

$$2k + l + 2K + L = 2k' + l' + 2K' + L' = 6\,, \quad (5.9)$$

and, using Eqs. (5.5) and (5.6), we obtain

$$k = k'\,. \quad (5.10)$$

Using the above constraints, the analytic form of the nuclear matrix element in Eq. (5.7) further simplifies in the following way:

$$\langle k_1' l_1' j_1', k_2' l_2' j_2'; J\,T=1; 0^+ |\, O_{12}^\alpha(r)\, |k_1 l_1 j_1,\, k_2 l_2 j_2; J\,T=1; 0^+ \rangle$$

$$= \sum_{S,\Lambda} \left| \left\langle l_1 \frac{1}{2} j_1,\, l_2 \frac{1}{2} j_2 \left| \frac{1}{2}\frac{1}{2} S,\, l_1 l_2 \Lambda \right. \right\rangle_J \right|^2 \frac{1}{\sqrt{2S+1}} \left\langle \frac{1}{2}\frac{1}{2} S \,\|\, S_{12}^\alpha \,\|\, \frac{1}{2}\frac{1}{2} S \right\rangle$$

$$\times \sum_{k,l,K,L} |\langle kl,\, KL|k_1 l_1,\, k_2 l_2 \rangle_\Lambda|^2 \,\langle kl|\, H(r)\, |kl \rangle\,. \quad (5.11)$$

If we substitute the values of the quantum numbers in the equation above, we obtain:

$$\left\langle 0\,3\,\frac{7}{2},\, 0\,3\,\frac{7}{2};\, J\,1;\, 0^+ \left|\, O_{12}^\alpha(r)\, \right|\, 0\,3\,\frac{7}{2},\, 0\,3\,\frac{7}{2};\, J\,1;\, 0^+ \right\rangle$$

$$= \sum_{S,\Lambda} \left| \left\langle 3\,\frac{1}{2}\,\frac{7}{2},\, 3\,\frac{1}{2}\,\frac{7}{2} \left| \frac{1}{2}\frac{1}{2} S,\, 3\,3\,\Lambda \right. \right\rangle_J \right|^2 \frac{1}{\sqrt{2S+1}} \left\langle \frac{1}{2}\frac{1}{2} S \,\|\, S_{12}^\alpha \,\|\, \frac{1}{2}\frac{1}{2} S \right\rangle$$

$$\times \sum_{k,l,K,L} |\langle kl,\, KL|0\,3,\, 0\,3 \rangle_\Lambda|^2 \,\langle kl|\, H(r)\, |kl \rangle\,. \quad (5.12)$$

We still have to fix the bounds on the sums over the quantum numbers. From energy conservation in Eq. (5.9) we get

$$\sum_{k,l,K,L} \to \sum_{L=0}^{6} \sum_{l=0}^{6-L} \sum_{K=0}^{\frac{1}{2}(6-L-l)}\,, \quad (5.13)$$

where, as a consequence, the value of k is fixed. Being the total spin of a couple of two fermions, S can only take the values 0 and 1. The sum over Λ, having $l_1 = l_2 = 3$, runs from 0 to 6 but, to conserve parity it only includes even values: 0, 2,

J	$TBTD\left(J,0^{+}\right)$
0	1.214
2	-0.572
4	0.021
6	0.000

Table 5.1. Numerical values of the two-body transition densities $TBTD\left(J,0^{+}\right)$

4, 6.. Finally, the total angular momentum of a pair of nucleons with $j_1 = j_2 = 7/2$, J, runs from 0 to 7, but we only have to keep even values, as required by the antisymmetrization of the two-body matrix element in Eq. (4.12).

Using the definition of 9-j symbols of Eq. (4.7), the final expression for the nuclear matrix element of Eq. (4.5) is given by

$$M_{0\nu}^{\alpha} = \sum_{J=0,2,4,6} TBTD\left(J,0^{+}\right) \sum_{S=0,1} \sum_{\Lambda=0,2,4,6} 64(2\Lambda+1)(2S+1) \begin{pmatrix} 3 & \frac{1}{2} & \frac{7}{2} \\ 3 & \frac{1}{2} & \frac{7}{2} \\ \Lambda & S & J \end{pmatrix}^{2}$$

$$\times \frac{1}{\sqrt{2S+1}} \left\langle \frac{1}{2}\frac{1}{2}S \parallel S_{12}^{\alpha} \parallel \frac{1}{2}\frac{1}{2}S \right\rangle$$

$$\times \sum_{L=0}^{6} \sum_{l=0}^{6-L} \sum_{K=0}^{\frac{1}{2}(6-L-l)} |\langle kl,\, KL|0\,3,\, 0\,3\rangle_{\Lambda}|^{2} \langle kl|\, H(r)\,|kl\rangle. \tag{5.14}$$

The numerical values of the two-body transition densities, $TBTD\left(J,0^{+}\right)$, computed in [47], are listed in Table 5.1.

5.1.2 Correlation functions

To extend our calculation using the correlated wave function formalism, we need the analytic form of the correlation functions of Eq. (3.65). We have used $f_1(r) \equiv f_c(r) + f_\tau(r)$ and $f_2(r) \equiv f_\sigma(r) + f_{\sigma\tau}(r)$, where $f_c(r)$, $f_\tau(r)$, $f_\sigma(r)$ and $f_{\sigma\tau}(r)$ are the correlation functions introduced in Section 4.2, and obtained in [46] using a realistic nuclear Hamiltonian. The numerical results for these functions have been fitted with the following analytic expressions:

$$f_1(r) = a - be^{-cr^2} + de^{-e(r-f)^2}, \tag{5.15}$$

$$f_2(r) = ae^{-br^2}(1 + cr + dr^2). \tag{5.16}$$

The parameter values are given in Table 5.2, while the shapes of the correlation functions are plotted in Figs. 5.2 and 5.3.

5.1.3 Numerical results

Using the analytic form for the correlation functions of Eqs. (5.15) and (5.16), we can write down the expressions of the Fermi and Gamow-Teller nuclear transition matrix elements of Eq. (5.14) considering two interesting cases.
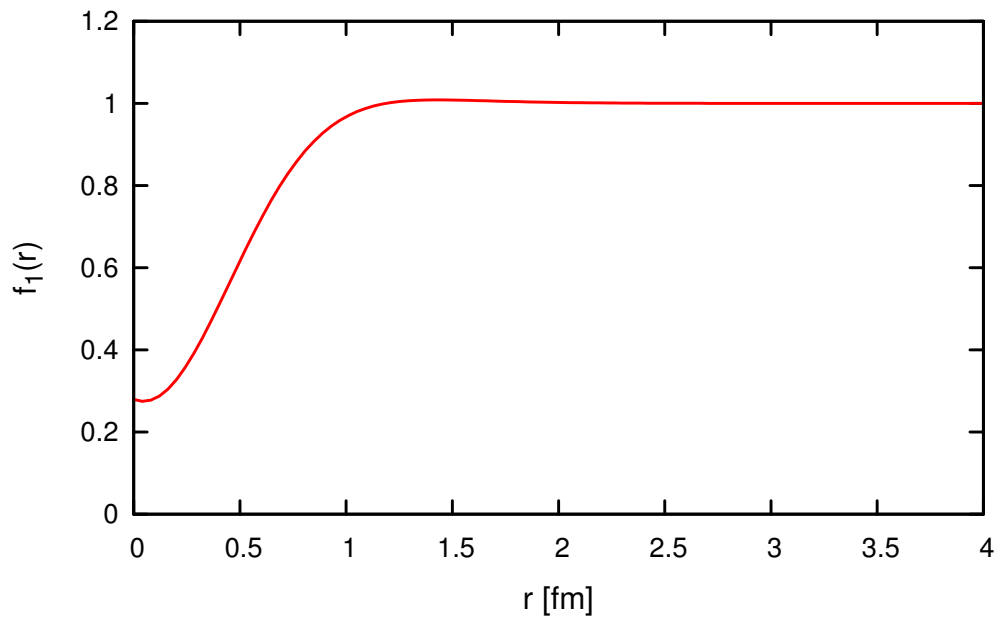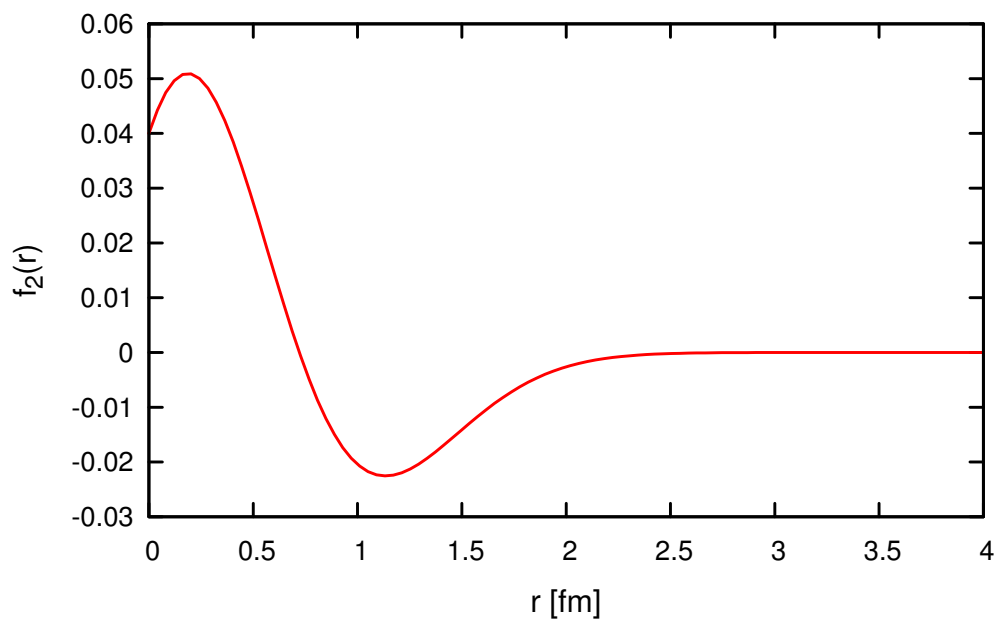
Figure 5.2. Fit function $f_1(r)$.

Figure 5.3. Fit function $f_2(r)$

$f_1(r)$	Value	$f_2(r)$	Value
a	1.00	a	0.04
b	0.92	b	1.39
c	2.56	c	2.92
d	0.33	d	-5.97
e	0.57		
f	-0.94		

Table 5.2. Fit parameters for the correlation functions.

- $f_1(r) \neq 0$ and $f_2(r) = 0$. Using the effective Fermi and Gamow-Teller operators of Eqs. (4.19) and (4.20), we get

$$
M_{0\nu}^F = \sum_{J=0,2,4,6} TBTD\,(J,0^+) \sum_{S=0,1} \sum_{\Lambda=0,2,4,6} 64(2\Lambda+1)(2S+1) \begin{pmatrix} 3 & \frac{1}{2} & \frac{7}{2} \\ 3 & \frac{1}{2} & \frac{7}{2} \\ \Lambda & S & J \end{pmatrix}^2
$$

$$
\times \sum_{L=0}^{6} \sum_{l=0}^{6-L} \sum_{K=0}^{\frac{1}{2}(6-L-l)} |\langle kl,\, KL|0\,3,\, 0\,3\rangle_\Lambda|^2 \, \langle kl| \, f_1^2(r)H(r) \, |kl\rangle , \quad (5.17)
$$

$$
M_{0\nu}^{GT} = \sum_{J=0,2,4,6} TBTD\,(J,0^+) \sum_{S=0,1} \sum_{\Lambda=0,2,4,6} 64(2\Lambda+1)(2S+1) \begin{pmatrix} 3 & \frac{1}{2} & \frac{7}{2} \\ 3 & \frac{1}{2} & \frac{7}{2} \\ \Lambda & S & J \end{pmatrix}^2
$$

$$
\times [2S(S+1)-3] \sum_{L=0}^{6} \sum_{l=0}^{6-L} \sum_{K=0}^{\frac{1}{2}(6-L-l)} |\langle kl,\, KL|0\,3,\, 0\,3\rangle_\Lambda|^2 \, \langle kl| \, f_1^2(r)H(r) \, |kl\rangle .
$$

$$
(5.18)
$$

- $f_1(r) \neq 0$ and $f_2(r) \neq 0$. Using the effective Fermi and Gamow-Teller operators of Eqs. (4.21) and (4.22), we get

$$
M_{0\nu}^F = \sum_{J=0,2,4,6} TBTD\,(J,0^+) \sum_{S=0,1} \sum_{\Lambda=0,2,4,6} 64(2\Lambda+1)(2S+1) \begin{pmatrix} 3 & \frac{1}{2} & \frac{7}{2} \\ 3 & \frac{1}{2} & \frac{7}{2} \\ \Lambda & S & J \end{pmatrix}^2
$$

$$
\times \sum_{L=0}^{6} \sum_{l=0}^{6-L} \sum_{K=0}^{\frac{1}{2}(6-L-l)} |\langle kl,\, KL|0\,3,\, 0\,3\rangle_\Lambda|^2 \left\{ \langle kl| \left[f_1^2(r) + 3f_2^2(r) \right] H(r) \, |kl\rangle \right.
$$

$$
\left. + [2S(S+1)-3] \, \langle kl| \, 2f_2(r) \left[f_1(r) - f_2(r) \right] H(r) \, |kl\rangle \right\} , \quad (5.19)
$$

$$M_{0\nu}^{GT} = \sum_{J=0,2,4,6} TBTD\,(J,0^+) \sum_{S=0,1} \sum_{\Lambda=0,2,4,6} 64(2\Lambda+1)(2S+1) \begin{pmatrix} 3 & \frac{1}{2} & \frac{7}{2} \\ 3 & \frac{1}{2} & \frac{7}{2} \\ \Lambda & S & J \end{pmatrix}^2$$

$$\times \sum_{L=0}^{6} \sum_{l=0}^{6-L} \sum_{K=0}^{\frac{1}{2}(6-L-l)} |\langle kl,\,KL|0\,3,\,0\,3\rangle_\Lambda|^2 \left\{ \langle kl|\,6f_2(r)\Big[f_1(r)-f_2(r)\Big]H(r)\,|kl\rangle \right.$$

$$\left. + \big[2S(S+1)-3\big]\,\langle kl|\Big[f_1^2(r)+7f_2^2(r)-4f_1(r)f_2(r)\Big]H(r)\,|kl\rangle \right\}. \quad (5.20)$$

Numerical calculations have been carried out setting the harmonic oscillator constant to the value $\nu = 0.126\,\mathrm{fm}^{-2}$ and the average energy of the intermediate states $\langle E\rangle{=}7.72\,\mathrm{Mev}$ [39].

The Fermi and Gamow-Teller matrix elements can be written as

$$M_{0\nu}^\alpha = \int_0^{+\infty} dr\, g^\alpha(r) \ . \quad (5.21)$$

We have developed a FORTRAN code to compute integrals of the form of Eq. (5.21), where the integration region extends up to $R_{\mathrm{max}} = 20\,\mathrm{fm}$. The values of the Talmi-Moshinsky brackets have been obtained from the FORTRAN subroutine TMB [48] while for the 9-j symbols we have used the FORTRAN subroutine W9J described in [49]. Altogether, the calculations of $\mathcal{M}_{0\nu}$ requires few seconds of CPU time in a personal computer of intermediate level.

The inclusion of correlations results in a modification of the integrand, $g^\alpha(x)$, in the matrix elements. In Figs. 5.4 and 5.5 we comapre $g^\alpha(x)$ for the Fermi and Gamow-Teller matrix elements, considering three cases: pure shell model, adding spin-independent correlation and, finally, adding both spin-independent and spin-dependent correlations. It clearly appears that the main effect associated with the spin-independent correlation function $f_1(r)$ is a suppression at $r \lesssim 1\,\mathrm{fm}$, arising from the short range repulsive core of the NN interaction. Moreover, in Table 5.3 we have reported the computed numerical values for the neutrinoless double beta decay $\mathcal{M}_{0\nu}$ in the three cases.

Fig. 5.6 shows the dependence of $\mathcal{M}_{0\nu}$ on the average energy of the intermediate states $\langle E\rangle$; values from 0 to 15 MeV have been considered. Fig. 5.6 suggests that the closure approximation does not critically depend on the value of $\langle E\rangle$.

The results of our numerical calculations indicate that the inclusion of spin independent correlations leads to a suppression of the shell model matrix element of $\sim 20\%$, while spin-dependent correlations produce an increase of $\sim 3\%$.

The results of previous studies, carried out neglecting spin-dependent effects, have shown a strong dependence on the choice of $f_1(r)$. For example, the authors of reference [39] found that, while using the Miller-Spencer correlation function leads to a suppression of the Fermi and Gamow-Teller matrix elements of $\sim 35\%$ and $\sim 15\%$, respectively. Using the so called AV18 model leads to a smaller suppression of $M_{0\nu}^F$ and an enhancement of $M_{0\nu}^{GT}$. In this context, is very important to point

Figure 5.4. Integrand of the Fermi matrix element in three cases: pure nuclear shell model (red line), nuclear shell model with central correlations (green line) and nuclear shell model with central and spin-dependent correlations.
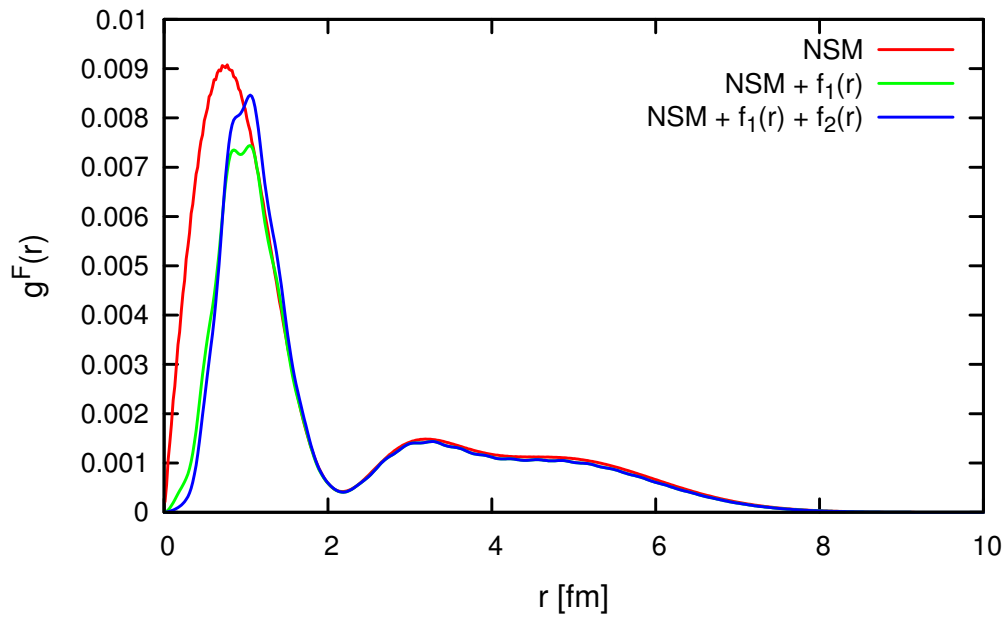

Figure 5.5. Integrand of the Gamow-Teller matrix element in three cases: pure nuclear shell model (red line), nuclear shell model with central correlations (green line) and nuclear shell model with central and spin-dependent correlations.
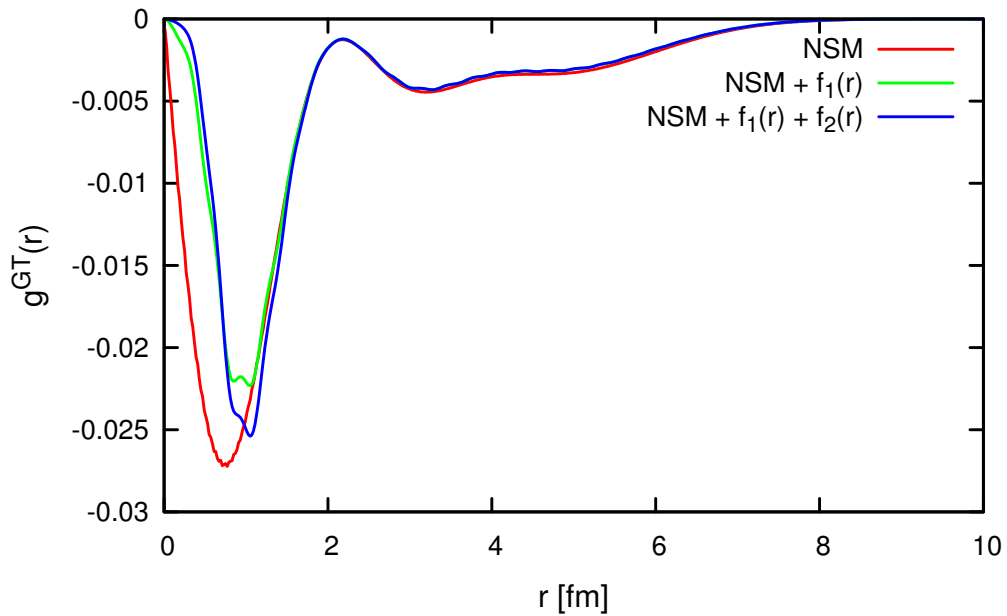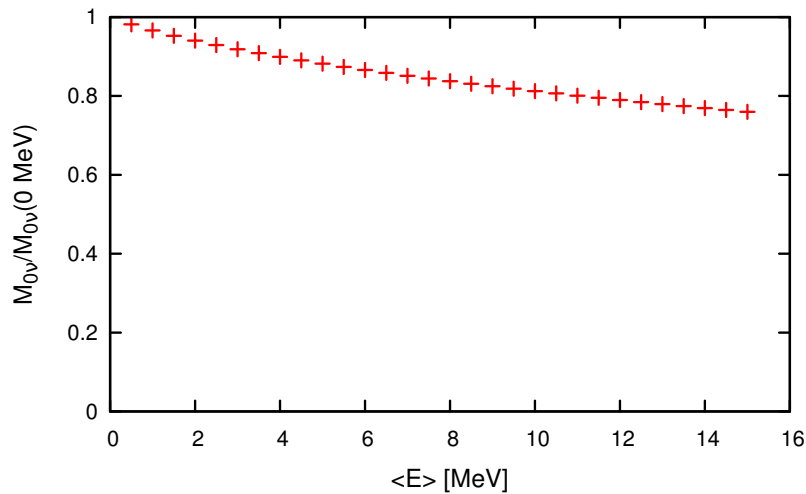
Figure 5.6. Dependence of $\mathcal{M}_{0\nu}$ divided by $\mathcal{M}_{0\nu}$ calculated at $\langle E \rangle = 0 \, \mathrm{MeV}$ on the average energy of the intermediate states $\langle E \rangle$.

out that in our calculation the correlation function are consistently determined by a realistic phenomenological Hamiltonian, through a many-body calculation.

	$M_{0\nu}^{F}$	$M_{0\nu}^{GT}$	$\mathcal{M}_{0\nu}$
NSM	0.756	-2.269	-2.753
NSM $+ f_1(r)$	0.584	-1.752	-2.126
NSM $+ f_1(r) + f_2(r)$	0.598	-1.793	-2.175

Table 5.3. Matrix element values obtained numerically.

5.2 Using spectroscopic factors

As pointed out above, the implementation of correlation effects can be alternatively carried out using spectroscopic factors. As discussed in Sections 3.7 and 4.2, the shell model wave function of each neutron of $^{48}\mathrm{Ca}$ in the initial state is rescaled by a factor $\sqrt{Z_{1f_{7/2}}^{n}(^{48}\mathrm{Ca})}$, and that of each proton in the final state of $^{48}\mathrm{Ti}$ by a factor $\sqrt{Z_{1f_{7/2}}^{p}(^{48}\mathrm{Ti})}$. As a consequence, the neutrinoless double beta decay transition matrix element, $\mathcal{M}_{0\nu}$, is rescaled by a total factor

$$\mathcal{M}_{0\nu} \to \widetilde{\mathcal{M}}_{0\nu} = \left[1 - Z_{1f_{7/2}}^{p}(^{48}\mathrm{Ti}) \right] Z_{1f_{7/2}}^{n}(^{48}\mathrm{Ca}) \, \mathcal{M}_{0\nu} \,. \tag{5.22}$$

In our discussion we assume $1 - Z_{1f_{7/2}}^{p}(^{48}\mathrm{Ti}) \simeq Z_{1f_{7/2}}^{n}(^{48}\mathrm{Ca})$, i.e.

$$\mathcal{M}_{0\nu} \to \widetilde{\mathcal{M}}_{0\nu} = \left[Z_{1f_{7/2}}^{n}(^{48}\mathrm{Ca}) \right]^{2} \mathcal{M}_{0\nu} \,. \tag{5.23}$$

Although the validity of this assumption should be carefully investigated, nuclear matter results suggest that it is quite accurate. The calculation of the spectroscopic factors of doubly closed shell nuclei has been carried out in Ref. [36] using correlated basis function theory with more refined correlations. The computed values are $Z^n_{1f_{7/2}}(^{48}\mathrm{Ca}) = 0.91 \div 0.95$, leading to a suppression of the shell modell matrix element of $\sim 10 \div 20\,\%$. Therefore the results obtained in this manner are consistent with those of Subsection 5.1.3.

Conclusions

We have performed a numerical study of the effects of nucleon-nucleon correlations on the nuclear matrix element of neutrinoless double beta decay of ^{48}Ca. Our work is motivated by the fact that correlation effects have been shown to play a critical role in electron-nucleus scattering, and are expected to be relevant in any processes involving a nucleon pair.

We have considered two different strategies, both based on the formalism of correlated basis functions. Compared to previous studies, this approach allows for a consistent treatment of spin-dependent correlations. The correlation functions have been obtained from highly realistic models of the nuclear Hamiltonian, providing an excellent description of the properties of the two-nucleon system and light nuclei. The same correlation functions have also been extensively and successfully used in the analysis of electron-nucleus scattering data [50].

Our numerical results suggest that including correlations leads to a suppression of the nuclear matrix element of $\sim 20\,\%$. This estimate is quite robust, as it turns out to be largely independent of the procedure employed to carry out the calculations.

Including spin-dependent correlations through a modification of the two-nucleon states leads to a mixing of the Fermi and Gamow-Teller contributions to the transition matrix elements. The Gamow-Teller transition acquires in fact a Fermi-like like contribution, and *vice versa*. However, the results of our calculations show that this effect is quite small, thus suggesting that correlation effects can also be described by modifying the normalization of the shell model states through the inclusion of spectroscopic factors $Z_\alpha < 1$. This change of normalization accounts for the depletion of the Fermi sea arising from scattring processes involving strongly correlated nucleons. The results obtained from the two different implementations of correlations appear to be consistent, and suggest that their effects are sizable.

Our study should be regarded as exploratory, as it involves a number of simplifying assumptions. We have considered ^{48}Ca, which is the lightest element that can undergo double β-decay and has the highest $Q_{2\beta}$-value in nature, because its shell structure is quite simple. Moreover we have only studied transitions between nucleons in the $1f_{\frac{7}{2}}$ shell. However, it has to be emphasized that, in principle, the formalism we have employed allows one to carry out a more realistic calculation of the neutrinoless double β-decay in a fully consistent fashion. For example, the effective Hamiltonian constructed within the correlated basis function approach, could be used in the shell model determination of the two-body transition densities.

Appendix A

Properties of the operators O_{ij}^n

In this Appendix, we discuss the properties of the six operators defined in Eq. (3.21), as well as some useful properties of the Pauli matrices.

A.1 Pauli matrices

In the standard representation, in which σ^3 is chosen to be diagonal, the threee Pauli matrices are given by (we specialize here to the spin matrices σ^i: analog properties obviously hold for the isospin matrices τ^i)

$$\sigma^1 = \begin{pmatrix} 0 & 1 \\ 1 & 0 \end{pmatrix} \ , \quad \sigma^2 = \begin{pmatrix} 0 & -i \\ i & 0 \end{pmatrix} \ , \quad \sigma^3 = \begin{pmatrix} 1 & 0 \\ 0 & -1 \end{pmatrix} \ . \tag{A.1}$$

The Pauli matrices satisfy

$$\sigma^i \sigma^j = \delta_{ij} + i\epsilon_{ijk}\sigma^k \ , \tag{A.2}$$

$$\epsilon_{ijk}\sigma^j \sigma^k = 2i\sigma^i \ , \tag{A.3}$$

that can be put in the form

$$[\sigma^i, \sigma^j] = 2i\epsilon_{ijk}\sigma^k \ , \tag{A.4}$$

$$\{\sigma^i, \sigma^j\} = 2\delta_{ij} \ , \tag{A.5}$$

where ϵ_{ijk} is the totally antisymmetric tensor and $i, j, k = 1, 2, 3$. The first properties shows that the Pauli matrices are the generators of an $SU(2)$ algebra.

A.2 Projection operators

Let now $\boldsymbol{\sigma}_1$ and $\boldsymbol{\sigma}_2$ be the vectors of Pauli matrices for particle 1 and 2, respectively (i.e. $\boldsymbol{\sigma}_1 \equiv \{\sigma_1^1, \sigma_1^2, \sigma_1^3\}$). From the properties (A.2)-(A.3), it follows that

$$(\boldsymbol{\sigma}_1 \cdot \boldsymbol{\sigma}_2)^2 = 3 - 2(\boldsymbol{\sigma}_1 \cdot \boldsymbol{\sigma}_2) \ . \tag{A.6}$$

As $(\boldsymbol{\sigma}_1 \cdot \boldsymbol{\sigma}_2)$ is a scalar quantity, we can interpret the above equation as an algebraic one, with solutions $(\boldsymbol{\sigma}_1 \cdot \boldsymbol{\sigma}_2) = -3$ and $(\boldsymbol{\sigma}_1 \cdot \boldsymbol{\sigma}_2) = 1$. They correspond to the states of

total spin $S = 0$ (spin singlet channel) and $S = 1$ (spin triplet channel), respectively. It is thus useful introducing the operators P_{2S+1} (and the analog Π_{2T+1} for the isospin states), defined as

$$P_{(S=0)} \equiv P_1 \quad = \quad \frac{1 - (\boldsymbol{\sigma}_1 \cdot \boldsymbol{\sigma}_2)}{4} \ , \tag{A.7}$$

$$P_{(S=1)} \equiv P_3 \quad = \quad \frac{3 + (\boldsymbol{\sigma}_1 \cdot \boldsymbol{\sigma}_2)}{4} \ , \tag{A.8}$$

which project onto states of definte total spin 0 or 1, respectively:

$$P_{2S+1}|S'\rangle = \delta_{SS'}|S'\rangle \ , \tag{A.9}$$

The projection operators satisfy to

$$P_{2S+1}^2 \quad = \quad P_{2S+1} \ , \tag{A.10}$$
$$P_1 + P_3 \quad = \quad \mathbb{1} \ , \tag{A.11}$$
$$P_1 P_3 = P_3 P_1 \quad = \quad 0 \ , \tag{A.12}$$

where $\mathbb{1}$ is the two-dimensional identity matrix.

A.3 Spin and isospin exchange operators

Consider the two-nucleon spin states (or the analog isospin states)

$$
\begin{aligned}
|0\,0\rangle \quad &= \quad \frac{1}{\sqrt{2}} \left(|\uparrow\downarrow\rangle - |\downarrow\uparrow\rangle \right) \ , \\
|1-1\rangle \quad &= \quad |\downarrow\downarrow\rangle \ , \\
|1\,0\rangle \quad &= \quad \frac{1}{\sqrt{2}} \left(|\uparrow\downarrow\rangle + |\downarrow\uparrow\rangle \right) \ , \\
|1\,1\rangle \quad &= \quad |\uparrow\uparrow\rangle \ ,
\end{aligned}
$$

where $|0\,0\rangle \equiv |S = 0\, M_S = 0\rangle$ etc., and the inverse relations

$$
\begin{aligned}
|\uparrow\uparrow\rangle \quad &= \quad |1\,1\rangle \ , \\
|\uparrow\downarrow\rangle \quad &= \quad \frac{1}{\sqrt{2}} \left(|1\,0\rangle + |0\,0\rangle \right) \ , \\
|\downarrow\uparrow\rangle \quad &= \quad \frac{1}{\sqrt{2}} \left(|1\,0\rangle - |0\,0\rangle \right) \ , \\
|\downarrow\downarrow\rangle \quad &= \quad |1-1\rangle \ .
\end{aligned}
$$

From properties (A.9), and from

$$
\begin{aligned}
(P_3 - P_1) |\uparrow\uparrow\rangle = |\uparrow\uparrow\rangle \quad &, \quad (P_3 - P_1) |\downarrow\downarrow\rangle = |\downarrow\downarrow\rangle \ , \\
(P_3 - P_1) |\uparrow\downarrow\rangle = |\downarrow\uparrow\rangle \quad &, \quad (P_3 - P_1) |\downarrow\uparrow\rangle = |\uparrow\downarrow\rangle \ ,
\end{aligned}
$$

it follows that $P_\sigma \equiv P_3 - P_1$ is the spin-exchange operator, satisfying

$$P_\sigma |S\,M_S\rangle = (-)^{S+1}|S\,M_S\rangle \ . \tag{A.13}$$

A similar exchange operator can be defined for isospin, $P_\tau \equiv \Pi_3 - \Pi_1$, with

$$P_\tau |T\, M_T\rangle = (-)^{T+1} |T\, M_T\rangle . \tag{A.14}$$

Combining the above results we find

$$P_{\sigma\tau} \equiv P_\sigma P_\tau = \frac{1}{4} \Big(1 + (\boldsymbol{\sigma}_1 \cdot \boldsymbol{\sigma}_2) \Big) \Big(1 + (\boldsymbol{\tau}_1 \cdot \boldsymbol{\tau}_2) \Big) , \tag{A.15}$$

with

$$P_{\sigma\tau} |S\, M_S,\, T\, M_T\rangle = (-)^{S+T} |S\, M_S,\, T\, M_T\rangle . \tag{A.16}$$

A.4 The tensor operator S_{12}

The tensor operator S_{12} is defined as

$$S_{12} \equiv \frac{3}{r^2}\, (\boldsymbol{\sigma}_1 \cdot \mathbf{r})\, (\boldsymbol{\sigma}_2 \cdot \mathbf{r}) - (\boldsymbol{\sigma}_1 \cdot \boldsymbol{\sigma}_2) , \tag{A.17}$$

where $\mathbf{r}$ is the relative coordinate of particels 1 and 2 while $r = |\mathbf{r}|$.

Making use of Eq.(A.2), it can be shown that

$$S_{12}(\boldsymbol{\sigma}_1 \cdot \boldsymbol{\sigma}_2) = (\boldsymbol{\sigma}_1 \cdot \boldsymbol{\sigma}_2) S_{12} = S_{12} . \tag{A.18}$$

As we saw, $(\boldsymbol{\sigma}_1 \cdot \boldsymbol{\sigma}_2) = 1$ on triplet states, while $(\boldsymbol{\sigma}_1 \cdot \boldsymbol{\sigma}_2) = -3$ on singlet states. The above equation thus implies that the tensor operator only acts on triplet states and

$$[S_{12},\, P_3] = 0 . \tag{A.19}$$

Moreover,

$$S_{12}^2 = 6 - 2 S_{12} + 2(\boldsymbol{\sigma}_1 \cdot \boldsymbol{\sigma}_2) . \tag{A.20}$$

The tensor operator is a function of $\mathbf{r}$ satisfying

$$\boldsymbol{\nabla} S_{12} = \frac{3}{r^2}\left[\boldsymbol{\sigma}_1\, (\boldsymbol{\sigma}_2 \cdot \mathbf{r}) + \boldsymbol{\sigma}_2\, (\boldsymbol{\sigma}_1 \cdot \mathbf{r}) - 2\frac{\mathbf{r}}{r^2}\, (\boldsymbol{\sigma}_1 \cdot \mathbf{r})\, (\boldsymbol{\sigma}_2 \cdot \mathbf{r}) \right] , \tag{A.21}$$

$$\nabla^2 S_{12} = -\frac{6}{r^2} S_{12} . \tag{A.22}$$

For any function $u(r)$, Eq.(A.21) implies

$$(\boldsymbol{\nabla} u) \cdot (\boldsymbol{\nabla} S_{12}) = \frac{du}{dr}\frac{\mathbf{r}}{r} \cdot (\boldsymbol{\nabla} S_{12}) = 0 . \tag{A.23}$$

Moreover

$$(\boldsymbol{\nabla} S_{12})^2 = \frac{6}{r^2}\, (8 - S_{12}) , \tag{A.24}$$

$$[S_{12},\, (\boldsymbol{\nabla} S_{12})] = \frac{36}{r^2}\, i\, (\mathbf{S} \times \mathbf{r}) , \tag{A.25}$$

$$[S_{12},\, (\boldsymbol{\nabla} S_{12})]\, \boldsymbol{\nabla} = \frac{36}{r^2}\, (\mathbf{L} \cdot \mathbf{S}) , \tag{A.26}$$

where $\mathbf{S} = (\boldsymbol{\sigma}_1 + \boldsymbol{\sigma}_2)/2$ and $\mathbf{L} = \mathbf{r} \times \mathbf{p} = -i\,(\mathbf{r} \times \boldsymbol{\nabla})$ is the orbital angular momentum operator of the relative motion.

From Equation (A.22), we can calculate

$$\left[S_{12},\ \nabla^2 S_{12} \right] = 0 \ , \tag{A.27}$$

and

$$(\boldsymbol{\nabla} S_{12})\ [S_{12},\ \boldsymbol{\nabla}] = -\,(\boldsymbol{\nabla} S_{12})^2 \ . \tag{A.28}$$

A.5   Algebra of the six operators (??)

Equations (A.6), (A.18) and (A.20) show that the six operators

$$O^{1,\dots,6} = 1,\ (\boldsymbol{\tau}_1 \cdot \boldsymbol{\tau}_2),\ (\boldsymbol{\sigma}_1 \cdot \boldsymbol{\sigma}_2),\ (\boldsymbol{\sigma}_1 \cdot \boldsymbol{\sigma}_2)(\boldsymbol{\tau}_1 \cdot \boldsymbol{\tau}_2),\ S_{12},\ S_{12}(\boldsymbol{\tau}_1 \cdot \boldsymbol{\tau}_2) \ , \tag{A.29}$$

close an algebra, i.e. they satisfy

$$O^i O^j = \sum_k K_{ij}^k O^k \ . \tag{A.30}$$

The coefficients K_{ij}^k are easily obtained by calculating

$$O^1 O^i = O^i O^1 = O^i \implies K_{1i}^k = K_{i1}^k = \delta_i^k$$

$$O^2 O^2 = 3O^2 - 2O^2 \implies K_{22}^k = 3\delta_1^k - 2\delta_2^k \ ,$$

$$O^2 O^3 = O^3 O^2 = O^4 \implies K_{23}^k = K_{32}^k = \delta_4^k \ ,$$

$$O^2 O^4 = 3O^3 - 2O^4 \implies K_{24}^k = K_{42}^k = \delta_3^k - 1\delta_4^k \ ,$$

$$O^2 O^5 = O^5 O^2 = O^6 \implies K_{25}^k = K_{52}^k = \delta_6^k \ ,$$

$$O^2 O^6 = O^6 O^2 = 3O^5 - 2O^6 \implies K_{26}^k = K_{62}^k = 3\delta_5^k - 2\delta_6^k \ ,$$

$$O^3 O^3 = 3O^1 - 2O^3 \implies K_{33}^k = 3\delta_1^k - 2\delta_3^k \ ,$$

$$O^3 O^4 = O^4 O^3 = 3O^2 - 2O^4 \implies K_{34}^k = K_{43}^k = 3\delta_2^k - 2\delta_4^k \ ,$$

$$O^3 O^5 = O^5 O^3 = O^5 \implies K_{35}^k = K_{53}^k = \delta_5^k \ ,$$

$$O^3 O^6 = O^6 O^3 = O^6 \implies K_{36}^k = K_{63}^k = \delta_6^k \ ,$$

$$O^4 O^4 = 9O^1 - 6O^2 - 6O^3 + 4O^4 \implies K_{44}^k = 9\delta_1^k - 6\delta_2^k - 6\delta_3^k + 4\delta_4^k \ ,$$

$$O^4 O^5 = O^5 O^4 = O^6 \implies K_{45}^k = K_{54}^k = \delta_6^k \ ,$$

$$O^4 O^6 = O^6 O^4 = 3O^5 - 2O^6 \implies K_{46}^k = K_{64}^k = 3\delta_5^k - 2\delta_6^k \ ,$$

$$O^5 O^5 = 6O^1 + 2O^3 - 2O^5 \implies K_{55}^k = 6\delta_1^k + 2\delta_3^k - 2\delta_5^k \ ,$$

$$O^5 O^6 = O^6 O^5 = 6O^2 + 2O^4 - 2O^6 \implies K_{56}^k = K_{65}^k = 6\delta_2^k + 2\delta_4^k - 2\delta_6^k \ ,$$

$$O^6 O^6 \ = \ 18O^1 - 12O^2 + 6O^3 - 4O^4 - 6O^6 + 4O^6$$
$$\implies K_{66}^k = 18\delta_1^k - 12\delta_2^k + 6\delta_3^k - 4\delta_4^k - 6\delta_4^k + 4\delta_6^k \ .$$

A.6   Matrix elements

Finally, we report a number of expectation values of operators involving Pauli matrices, in two-nucleon states of definite total spin and isospion, $|S\ M_S,\ T\ M_T\rangle$.

$$\langle P_{2S'+1}\Pi_{2T'+1}\rangle = \delta_{SS'}\delta_{TT'}\ , \tag{A.31}$$

$$\langle P_{2S'+1}\Pi_{2T'+1}P_{\sigma\tau}\rangle = (-)^{S+T}\delta_{SS'}\delta_{TT'}\ , \tag{A.32}$$

$$\sum_{SM_S}\delta_{S'1}\langle S_{12}P_{2S'+1}\Pi_{2T'+1}\rangle = \delta_{S'1}\delta_{TT'}\sum_{M_S}\langle 1\ M_S|S_{12}|1\ M_S\rangle = 0\ , \tag{A.33}$$

$$\sum_{SM_S}\delta_{S'1}\langle S_{12}P_{2S'+1}\Pi_{2T'+1}P_{\sigma\tau}\rangle = 0\ . \tag{A.34}$$

A.7   Matrix elements . . .

The explicit expressions for the matrices entering Eq.(**??**), defined by

$$A^i_{\lambda\mu} = \langle\lambda\mu|O^i_{12}|\lambda\mu\rangle\ ,\quad B^i_{\lambda\mu} = \langle\lambda\mu|O^i_{12}|\mu\lambda\rangle\ , \tag{A.35}$$

where $|\lambda\mu\rangle$ denotes the two-nucleon spin-isospin state, can be easily obtained from the above properties of the six operators $O^{n\leq 6}$.

We find

$$
A^1 \;=\; \begin{pmatrix} 1 & 1 & 1 & 1 \\ 1 & 1 & 1 & 1 \\ 1 & 1 & 1 & 1 \\ 1 & 1 & 1 & 1 \end{pmatrix} , \tag{A.36}
$$

$$
A^2 \;=\; \begin{pmatrix} 1 & 1 & -1 & -1 \\ 1 & 1 & -1 & -1 \\ -1 & -1 & 1 & 1 \\ -1 & -1 & 1 & 1 \end{pmatrix} , \tag{A.37}
$$

$$
A^3 \;=\; \begin{pmatrix} 1 & -1 & 1 & -1 \\ -1 & 1 & -1 & 1 \\ 1 & -1 & 1 & -1 \\ -1 & 1 & -1 & 1 \end{pmatrix} , \tag{A.38}
$$

$$
A^4 \;=\; \begin{pmatrix} 1 & -1 & -1 & 1 \\ -1 & 1 & 1 & -1 \\ -1 & 1 & 1 & -1 \\ 1 & -1 & -1 & 1 \end{pmatrix} , \tag{A.39}
$$

$$
A^5 \;=\; \begin{pmatrix} 1 & 1 & -1 & -1 \\ 1 & 1 & -1 & -1 \\ -1 & -1 & 1 & 1 \\ -1 & -1 & 1 & 1 \end{pmatrix} \left(3\cos^2\theta - 1\right) = A^2 \left(3\cos^2\theta - 1\right) , \tag{A.40}
$$

$$
A^6 \;=\; \begin{pmatrix} 1 & -1 & -1 & 1 \\ -1 & 1 & 1 & -1 \\ -1 & 1 & 1 & -1 \\ 1 & -1 & -1 & 1 \end{pmatrix} \left(3\cos^2\theta - 1\right) = A^4 \left(3\cos^2\theta - 1\right) , \tag{A.41}
$$

$$
B^1 \;=\; \begin{pmatrix} 1 & 0 & 0 & 0 \\ 0 & 1 & 0 & 0 \\ 0 & 0 & 1 & 0 \\ 0 & 0 & 0 & 1 \end{pmatrix} , \tag{A.42}
$$

$$
B^2 \;=\; \begin{pmatrix} 1 & 0 & 2 & 0 \\ 0 & 1 & 0 & 2 \\ 2 & 0 & 1 & 0 \\ 0 & 2 & 0 & 1 \end{pmatrix} , \tag{A.43}
$$

$$
B^3 \;=\; \begin{pmatrix} 1 & 2 & 0 & 0 \\ 2 & 1 & 0 & 0 \\ 0 & 0 & 1 & 2 \\ 0 & 0 & 2 & 1 \end{pmatrix} , \tag{A.44}
$$

$$
B^4 \;=\; \begin{pmatrix} 1 & 2 & 2 & 4 \\ 2 & 1 & 4 & 2 \\ 2 & 4 & 1 & 2 \\ 4 & 2 & 2 & 1 \end{pmatrix} , \tag{A.45}
$$

$$
B^5 \;=\; \begin{pmatrix} 1 & -1 & 0 & 0 \\ -1 & 1 & 0 & 0 \\ 0 & 0 & 1 & -1 \\ 0 & 0 & -1 & 1 \end{pmatrix} \left(3\cos^2\theta - 1\right) , \tag{A.46}
$$

$$
B^6 \;=\; \begin{pmatrix} 1 & -1 & 2 & -2 \\ -1 & 1 & -2 & 2 \\ 2 & -2 & 1 & -1 \\ -2 & 2 & -1 & 1 \end{pmatrix} \left(3\cos^2\theta - 1\right) , \tag{A.47}
$$

where θ is the angle between $\mathbf{r}$ and the z axis.

A.8   Change of representation

In this Section we discuss the different representation for the operators of the "v_6" algebra. A generic operator x can be written as

$$x = \sum_{p=1}^{6} x_{ij}^p O^p = x_c + x_\tau(\boldsymbol{\tau}_1 \cdot \boldsymbol{\tau}_2) + x_\sigma(\boldsymbol{\sigma}_1 \cdot \boldsymbol{\sigma}_2) + x_{\sigma\tau}(\boldsymbol{\sigma}_1 \cdot \boldsymbol{\sigma}_2)(\boldsymbol{\tau}_1 \cdot \boldsymbol{\tau}_2) + x_t S_{12} + x_{t\tau} S_{12}(\boldsymbol{\tau}_1 \cdot \boldsymbol{\tau}_2) ,$$

(A.48)

in the basis of operators (A.29), or as

$$x = \sum_{TS} \left[x_{T0} + \delta_{S1} x_{tT} S_{12} \right] P_{2S+1} \Pi_{2T+1} ,$$

(A.49)

in the "TS-representation".

The transformation matrix is given by

$$\begin{pmatrix} 1 & -3 & -3 & 9 \\ 1 & 1 & -3 & -3 \\ 1 & -3 & 1 & -3 \\ 1 & 1 & 1 & 1 \end{pmatrix} \begin{pmatrix} x_c \\ x_\tau \\ x_\sigma \\ x_{\sigma\tau} \end{pmatrix} = \begin{pmatrix} x_{00} \\ x_{10} \\ x_{01} \\ x_{11} \end{pmatrix} ,$$

(A.50)

$$\begin{pmatrix} 1 & -3 \\ 1 & 1 \end{pmatrix} \begin{pmatrix} x_t \\ x_{t\tau} \end{pmatrix} = \begin{pmatrix} x_{t0} \\ x_{t1} \end{pmatrix} ,$$

(A.51)

or

$$\begin{cases} x_{TS} = x_c + (4T - 3)x_\tau + (4S - 3)x_\sigma + (4S - 3)(4T - 3)x_{\sigma\tau} , \\[2mm] x_{tT} = x_t + (4T - 3)x_{tT} . \end{cases}$$

(A.52)

The inverse transformation is given by

$$\frac{1}{16} \begin{pmatrix} 1 & 3 & 3 & 9 \\ -1 & 1 & -3 & 3 \\ -1 & -3 & 1 & 3 \\ 1 & -1 & -1 & 1 \end{pmatrix} \begin{pmatrix} x_{00} \\ x_{10} \\ x_{01} \\ x_{11} \end{pmatrix} = \begin{pmatrix} x_c \\ x_\tau \\ x_\sigma \\ x_{\sigma\tau} \end{pmatrix} ,$$

(A.53)

$$\frac{1}{4} \begin{pmatrix} 1 & 3 \\ -1 & 1 \end{pmatrix} \begin{pmatrix} x_{t0} \\ x_{t1} \end{pmatrix} = \begin{pmatrix} x_t \\ x_{t\tau} \end{pmatrix} ,$$

(A.54)

Appendix B

Correlated two particles states

At lowest order of CBF, the effective interaction V_{eff} is defined by the equation

$$\langle H \rangle = \langle 0_{FG}|T_0 + V_{\text{eff}}|0_{FG}\rangle \ . \tag{B.1}$$

As the above equation suggests, the approach based on the effective interaction allows one to obtain any nuclear matter observables using perturbation theory in the FG basis. The effective interaction is given by XXX

$$V_{\text{eff}} = \sum_{i<j} v_{\text{eff}}(ij) \ , \tag{B.2}$$

where

$$v_{\text{eff}}(ij) = f_{ij}\left(-\frac{1}{m}\nabla^2 + v(ij)\right)f_{ij} = \sum_{p=1}^{6} v_{\text{eff}}^p(r_{ij})O_{ij}^p \ , \tag{B.3}$$

O_{ij}^p being the operators listed in Eq. (3.21). The energy per nucleon in the Hartree-Fock approximation is then given by

$$\frac{E}{N} = \frac{3}{5}\frac{p_F^2}{2m} + \frac{1}{N}\sum_{i<j}\langle ij|\,v_{\text{eff}}(ij)\,|ij\rangle_a \ , \tag{B.4}$$

where p_F is the Fermi momentum. Assuming that the correlation operator be hermitian, the second term in the right hand side of the above equation can be written as

$$\sum_{i<j}\langle ij|\,v_{\text{eff}}(ij)\,|ij\rangle_a = \sum_{i<j}\langle ij|\,\frac{1}{2}\Big[f_{12},[\,t_1+t_2,\,f_{12}]\Big] + f_{12}v_{12}f_{12}\,|ij-ji\rangle \ , \quad \text{(B.5)}$$

with

$$t_i = -\frac{1}{2m}\nabla_i^2 \ , \quad t_1 + t_2 = -\frac{1}{m}\nabla^2 - \frac{1}{4m}\nabla_R^2 \ , \tag{B.6}$$

where $\boldsymbol{\nabla}$ acts on the relative coordinate $\mathbf{r}$, while $\boldsymbol{\nabla}_R$ acts on the center of mass coordinate $\mathbf{R}$, defined as

$$\mathbf{r} = \mathbf{r}_1 - \mathbf{r}_2 \ , \quad \mathbf{R} = \frac{1}{2}(\mathbf{r}_1 + \mathbf{r}_2) \ , \tag{B.7}$$

respectively.

Including only the static part of the interaction, both the correlation function f_{12} and the two-nucleon potential v_{12} are written as

$$f_{12} = \sum_{p=1}^{6} f^p(r_{12}) O_{12}^p \quad , \quad v_{12} = \sum_{p=1}^{6} v^p(r_{12}) O_{12}^p \ . \tag{B.8}$$

The FG two-nucleon state is given by

$$
\begin{aligned}
|ij\rangle &= \frac{1}{V} \, e^{i(\mathbf{k}_i \cdot \mathbf{r}_1 + \mathbf{k}_j \cdot \mathbf{r}_2)} \, |S\,M_S, \, T\,M_T\rangle \\
&= \frac{1}{V} \, e^{i(\mathbf{k} \cdot \mathbf{r} + \mathbf{K} \cdot \mathbf{R})} \, |S\,M_S, \, T\,M_T\rangle \ ,
\end{aligned} \tag{B.9}
$$

with

$$
\begin{aligned}
|\mathbf{k}_i|, \ |\mathbf{k}_j| &\leq p_F \\
\mathbf{k} = \frac{1}{2}(\mathbf{k}_i - \mathbf{k}_j) \quad &, \quad \mathbf{K} = \mathbf{k}_i + \mathbf{k}_j \ .
\end{aligned} \tag{B.10}
$$

We will discuss the potential and kinetic energy term separately.

B.1 Potential energy

Consider the operator
$$w_{12} = f_{12} v_{12} f_{12} \ , \tag{B.11}$$
and the decomposition of f_{12} in the TS-representation

$$f_{12} = \sum_{ST} \left[f_{ST} + \delta_{S1} f_{tT} S_{12} \right] P_{2S+1} \Pi_{2T+1} \ . \tag{B.12}$$

In the above equation, P_{2S+1} and Π_{2T+1} are spin and isospin projection operators. By writing the corresponding decomposition for w_{12} and v_{12} and calculating

$$
\begin{aligned}
w_{12} = \sum_{TS} &\left\{ \delta_{S0} f_{T0}^2 v_{T0} + \delta_{S1} \left\{ v_{T1} \left[f_{T1}^2 + 8 f_{tT}^2 + 2 \left(f_{T1} f_{tT} - f_{tT}^2 \right) S_{12} \right] + \right. \right. \\
&+ \left. \left. v_{tT} \left[16 \left(f_{T1} f_{tT} - f_{tT}^2 \right) + \left(f_{T1}^2 - 4 f_{T1} f_{tT} + 12 f_{t1}^2 \right) S_{12} \right] \right\} \right\} P_{2S+1} \Pi_{2T+1} \ ,
\end{aligned}
$$

we can identify

$$
\begin{aligned}
w_{T0} &= v_{T0} \ f_{T0}^2 \\
w_{T1} &= v_{T1}\left(f_{T1}^2 + 8 f_{tT}^2 \right) + 16 v_{tT}\left(f_{T1} f_{tT} - f_{tT}^2 \right) \\
w_{tT} &= 2 v_{T1}\left(f_{T1} f_{tT} - f_{tT}^2 \right) + v_{tT}\left(f_{T1}^2 - 4 f_{T1} f_{tT} + 12 f_{t1}^2 \right) \ .
\end{aligned} \tag{B.13}
$$

After replacing

$$\sum_{i<j} \rightarrow \frac{1}{2} \sum_{ij} \ , \tag{B.14}$$

the potential energy contribution reads

$$
\begin{aligned}
\langle w \rangle \;=\; & \frac{1}{2}\frac{1}{V^2}\sum_{SM_S}\sum_{TM_T}\sum_{\mathbf{k}_i\mathbf{k}_j}\sum_{S'T'}\bigg\{\int d^3r_1 d^3r_2 \Big[w_{S'T'}(r)\langle P_{2S'+1}\Pi_{2T'+1}\rangle + \\
& \delta_{S'1}w_{tT'}(r)\langle S_{12}P_{2S'+1}\Pi_{2T'+1}\rangle\Big] - \int d^3r_1 d^3r_2\, e^{i(\mathbf{k}_i\cdot\mathbf{r}-\mathbf{k}_j\cdot\mathbf{r})} \qquad (\text{B.15}) \\
& \Big[w_{S'T'}(r)\langle P_{2S'+1}\Pi_{2T'+1}P_{\sigma\tau}\rangle + \delta_{S'1}w_{tT'}(r)\langle S_{12}P_{2S'+1}\Pi_{2T'+1}P_{\sigma\tau}\rangle\Big]\bigg\}\,,
\end{aligned}
$$

where $P_{\sigma\tau}$ is the spin-isospin exchange operator[1]. The expectation values $\langle O\rangle$ are taken over two-nucleon states of definite total spin and isospin $|S\,M_S,\,T\,M_T\rangle$. Using

$$
\int d^3r_1 d^3r_2 = \int d^3r\, d^3R = V\int d^3r \qquad (\text{B.20})
$$

and the definition of the Slater function,

$$
\sum_{|\mathbf{k}|\leq p_F} e^{i\mathbf{k}\cdot\mathbf{r}} = \frac{V}{(2\pi)^3}\int_{|\mathbf{k}|\leq p_F} d^3k\, e^{i\mathbf{k}\cdot\mathbf{r}} = \frac{N}{\nu}\ell(p_F r)\,, \qquad (\text{B.21})
$$

we finally obtain

$$
\langle w\rangle = \frac{1}{2}\frac{1}{V^2}\frac{N^2}{\nu^2}V\sum_{ST}(2S+1)(2T+1)\int d^3r\, w_{ST}(r)\left[1-(-1)^{S+T}\ell^2(p_F r)\right]\,, \qquad (\text{B.22})
$$

i.e., in the case of symmetric nuclear matter ($\nu = 4$),

$$
\begin{aligned}
\frac{1}{N}\langle w\rangle \;=\; & \frac{\rho}{32}\int d^3r\Big\{[w_{00}(r)+9w_{11}(r)]a_-(p_F r) + \\
& + [3w_{01}(r)+3w_{10}(r)]a_+(p_F r)\Big\}\,, \qquad (\text{B.23})
\end{aligned}
$$

where $\rho = N/V$ is the density and

$$
a_\pm(x) = 1\pm\ell^2(x)\,. \qquad (\text{B.24})
$$

---

[1] $P_\sigma \equiv P_3 - P_1$ is the spin-exchange operator, satisfying

$$
P_\sigma|S\,M_S\rangle = (-)^{S+1}|S\,M_S\rangle\,. \qquad (\text{B.16})
$$

A similar exchange operator can be defined for isospin, $P_\tau \equiv \Pi_3 - \Pi_1$, with

$$
P_\tau|T\,M_T\rangle = (-)^{T+1}|T\,M_T\rangle\,. \qquad (\text{B.17})
$$

Combining the above results we find

$$
P_{\sigma\tau}\equiv P_\sigma P_\tau = \frac{1}{4}\Big(1+(\boldsymbol{\sigma}_1\cdot\boldsymbol{\sigma}_2)\Big)\Big(1+(\boldsymbol{\tau}_1\cdot\boldsymbol{\tau}_2)\Big)\,, \qquad (\text{B.18})
$$

with

$$
P_{\sigma\tau}|S\,M_S,\,T\,M_T\rangle = (-)^{S+T}|S\,M_S,\,T\,M_T\rangle\,. \qquad (\text{B.19})
$$

B.2 Kinetic energy

Let us now discuss the kinetic contribution to the energy, given by

$$\frac{1}{2}\left[f_{12},\left[\,t_1+t_2,\;f_{12}\right]\right]=-\frac{1}{2m}\left[f_{12},\left[\,\nabla^2,\;f_{12}\right]\right]\,. \tag{B.25}$$

We consider spin-zero and spin-one channels separately.

Spin-zero channels In these channels, the relevant part of the correlation function is given by

$$f_{12}=\sum_T f_{T0}(r)\,P_1\Pi_{2T+1}\,. \tag{B.26}$$

Making use of the results of Appendix **??**, as well as of

$$\left[f_{T0},\,\nabla^2 f_{T0}\right]=0\;\;,\;\;\left[f_{T0},\,(\boldsymbol{\nabla}f_{T0})\boldsymbol{\nabla}\right]=-(\boldsymbol{\nabla}f_{T0})^2\,, \tag{B.27}$$

we find

$$
\begin{aligned}
\left[f_{12},\left[\,\nabla^2,\;f_{12}\right]\right] &= \sum_{TT'}\left[f_{T0}\,P_1\,\Pi_{2T+1},\left[\nabla^2,\;f_{T0}\right]P_1\,\Pi_{2T'+1}\right]\\
&= \sum_{TT'}\left[f_{T0},\left[\nabla^2,\;f_{T0}\right]\right]P_1^2\Pi_{2T+1}\Pi_{2T'+1}\\
&= \sum_{T}\left[f_{T0},\,(\nabla^2 f_{T0})+2(\boldsymbol{\nabla}f_{T0})\boldsymbol{\nabla}\right]P_1\,\Pi_{2T+1}\\
&= 2\sum_{T}\left[f_{T0},\,(\boldsymbol{\nabla}f_{T0})\boldsymbol{\nabla}\right]P_1\,\Pi_{2T+1}\\
&= -2\sum_{T}(\boldsymbol{\nabla}f_{T0})^2\,P_1\,\Pi_{2T+1}\,.
\end{aligned} \tag{B.28}
$$

Finally,

$$-\frac{1}{2m}\left[f_{12},\left[\,\nabla^2,\;f_{12}\right]\right]=\frac{1}{m}\sum_T(\boldsymbol{\nabla}f_{T0})^2\,P_1\,\Pi_{2T+1}\,. \tag{B.29}$$

Spin-one channels In these channels, the correlation function is given by

$$f_{12}=\sum_T\left[f_{T1}(r)+f_{tT}(r)S_{12}\right]P_3\,\Pi_{2T+1}\,. \tag{B.30}$$

Relying once more on Appendix **??**, we calculate

$$\sum_{T'}\left[\nabla^2,\,(f_{T'1}+f_{tT'}S_{12})P_3\,\Pi_{2T'+1}\right]=\sum_{T'}\left\{[\nabla^2,\,f_{T'1}]+[\nabla^2,\,f_{tT'}S_{12}]\right\}P_3\,\Pi_{2T'+1}$$

$$=\sum_{T'}\left\{(\nabla^2 f_{T'1})+2(\boldsymbol{\nabla}f_{tT'})\boldsymbol{\nabla}+(\nabla^2 f_{tT'}S_{12})+2(\boldsymbol{\nabla}f_{tT'}S_{12})\boldsymbol{\nabla}\right\}P_3\,\Pi_{2T'+1}$$

$$=\sum_{T'}\left\{(\nabla^2 f_{T'1})+2(\boldsymbol{\nabla}f_{tT'})\boldsymbol{\nabla}+(\nabla^2 f_{tT'})S_{12}+(\nabla^2 S_{12})f_{tT'}\right.$$

$$+ 2(\boldsymbol{\nabla} f_{tT'})(\boldsymbol{\nabla} S_{12}) + 2S_{12}(\boldsymbol{\nabla} f_{tT'})\boldsymbol{\nabla} + 2f_{tT'}(\boldsymbol{\nabla} S_{12})\boldsymbol{\nabla}\Big\} P_3\,\Pi_{2T'+1} \ . \tag{B.31}$$

Hence, the commutator in Eq.(B.25) can be rewritten as

$$\begin{aligned}
\Big[f_{12}, \big[\, \nabla^2,\, f_{12}\,\big]\Big] &= \sum_{TT'} \Big[(f_{T1} + f_{tT}S_{12})\,P_3\,\Pi_{2T+1}, \{\dots\}\,P_3\,\Pi_{2T'+1}\Big] \\
&= \sum_T \Big[f_{T1} + f_{tT}S_{12}, \{\dots\}\Big] P_3\,\Pi_{2T+1} \\
&= \sum_T \Big(F_T^{(1)} + F_T^{(2)}\Big) P_3\,\Pi_{2T+1} \ , \tag{B.32}
\end{aligned}$$

with

$$F_T^{(1)} = \Big[f_{T1}, \{\dots\}\Big] \quad , \quad F_T^{(2)} = \Big[f_{tT}S_{12}, \{\dots\}\Big] \ , \tag{B.33}$$

and

$$\begin{aligned}
\{\dots\} &= \Big\{(\nabla^2 f_{T'1}) + 2(\boldsymbol{\nabla} f_{tT'})\boldsymbol{\nabla} + (\nabla^2 f_{tT'})S_{12} + (\nabla^2 S_{12})f_{tT'} \\
&\quad + 2(\boldsymbol{\nabla} f_{tT'})(\boldsymbol{\nabla} S_{12}) + 2S_{12}(\boldsymbol{\nabla} f_{tT'})\boldsymbol{\nabla} + 2f_{tT'}(\boldsymbol{\nabla} S_{12})\boldsymbol{\nabla}\Big\} \ . \tag{B.34}
\end{aligned}$$

We find

$$F_T^{(1)} = -2(\boldsymbol{\nabla} f_{T1})^2 - 2(\boldsymbol{\nabla} f_{T1})(\boldsymbol{\nabla} f_{tT})S_{12} \ , \tag{B.35}$$

and

$$\begin{aligned}
F_T^{(2)} &= \Big[f_{tT}S_{12},\, 2(\boldsymbol{\nabla} f_{T1})\boldsymbol{\nabla}\Big] + \Big[f_{tT}S_{12},\, 2S_{12}(\boldsymbol{\nabla} f_{T1})\boldsymbol{\nabla}\Big] + \\
&\quad + \Big[f_{tT}S_{12},\, 2f_{T1}(\boldsymbol{\nabla} S_{12})\boldsymbol{\nabla}\Big] = \\
&= -2(\boldsymbol{\nabla} f_{T1})(\boldsymbol{\nabla} f_{tT})S_{12} - 2(\boldsymbol{\nabla} f_{tT})^2 S_{12}^2 + \\
&\quad + 2f_{tT}^2\Big[S_{12},\, (\boldsymbol{\nabla} S_{12})\boldsymbol{\nabla}\Big] \\
&= -2\ (\boldsymbol{\nabla} f_{T1})(\boldsymbol{\nabla} f_{tT})S_{12} - 2(\boldsymbol{\nabla} f_{tT})^2(8 - 2S_{12})\ + \\
&\quad - 2f_{tT}^2\left[\frac{36}{r^2}\ (\mathbf{L}\cdot\mathbf{S}) + \frac{6}{r^2}\ (8 - S_{12})\right] \ . \tag{B.36}
\end{aligned}$$

Collecting all pieces togheter, we find for the spin-one channels

$$\begin{aligned}
-\frac{1}{2m}\Big[f_{12}, \big[\, \nabla^2,\, f_{12}\,\big]\Big] &= \frac{1}{m}\sum_T \Big\{(\boldsymbol{\nabla} f_{T1})^2 + (\boldsymbol{\nabla} f_{T1})(\boldsymbol{\nabla} f_{tT}S_{12}) + \\
&\quad + (\boldsymbol{\nabla} f_{tT})^2(8 - 2S_{12})\ + f_{tT}^2\left[\frac{36}{r^2}\ (\mathbf{L}\cdot\mathbf{S}) + \frac{6}{r^2}\ (8 - S_{12})\right]\Big\} P_3\,\Pi_{2T+1} \\
&= \frac{1}{m}\sum_{TS} \Big\{(\boldsymbol{\nabla} f_{TS})^2 + \delta_{S1}\Big[2(\boldsymbol{\nabla} f_{TS})(\boldsymbol{\nabla} f_{tT})S_{12} + \\
&\quad + (\boldsymbol{\nabla} f_{tT})^2 S_{12}^2 + f_{tT}\frac{36}{r^2}\ (\mathbf{L}\cdot\mathbf{S}) + \frac{6}{r^2}\ (8 - S_{12})\Big]\Big\} P_{2S+1}\Pi_{2T+1} \\
&= \sum_{TS} \Big\{t_{TS}(r) + \delta_{S1}\Big[t_{tT}(r)S_{12} + t_{bT}(r)(\mathbf{L}\cdot\mathbf{S})\Big]\Big\} P_{2S+1}\Pi_{2T+1} \ , \tag{B.37}
\end{aligned}$$

with

$$
\begin{aligned}
t_{T0} &= \frac{1}{m}(\boldsymbol{\nabla} f_{T0})^2 \\
t_{T1} &= \frac{1}{m}\Big[(\boldsymbol{\nabla} f_{T1})^2 + 8(\boldsymbol{\nabla} f_{tT})^2 + \frac{48}{r^2}\, f_{tT}^2\Big] \\
t_{tT} &= \frac{1}{m}\Big[2(\boldsymbol{\nabla} f_{T1})(\boldsymbol{\nabla} f_{tT}) - 2(\boldsymbol{\nabla} f_{tT})^2 - \frac{6}{r^2}\, f_{tT}^2\Big] \\
t_{bT} &= \frac{1}{m}\frac{36}{r^2}\, f_{tT}^2 \;.
\end{aligned}
$$

B.3   Final expression for $(\Delta E)_2$

We can rewrite

$$
(\Delta E)_2 = \sum_{i<j}\langle ij|W_{12}|ij - ji\rangle \;, \tag{B.38}
$$

with

$$
W_{12} = -\frac{1}{m}\Big[f_{12},\, \big[\,\nabla^2,\, f_{12}\big]\Big] + f_{12} v_{12} f_{12}
$$

$$
= \sum_{TS}\Big\{W_{TS}(r) + \delta_{S1}\Big[W_{tT}(r)S_{12} + W_{bT}(r)(\mathbf{L}\cdot\mathbf{S})\Big]\Big\}P_{2S+1}\Pi_{2T+1}\;,
$$

where

$$
\begin{aligned}
W_{T0} &= \frac{1}{m}(\boldsymbol{\nabla} f_{T0})^2 + v_{T0}f_{T0}^2 \\
W_{T1} &= \frac{1}{m}\Big[(\boldsymbol{\nabla} f_{T1})^2 + 8(\boldsymbol{\nabla} f_{tT})^2 + \frac{48}{r^2}\, f_{tT}^2\Big] + \\
&\quad + v_{T1}\Big(f_{T1}^2 + 8f_{tT}^2\Big) + 16v_{tT}\Big(f_{T1}f_{tT} - f_{tT}^2\Big) \\
W_{tT} &= \frac{1}{m}\Big[2(\boldsymbol{\nabla} f_{T1})(\boldsymbol{\nabla} f_{tT}) - 2(\boldsymbol{\nabla} f_{tT})^2 - \frac{6}{r^2}\, f_{tT}^2\Big] + \\
&\quad + 2v_{T1}\Big(f_{T1}f_{tT} - f_{tT}^2\Big) + v_{tT}\Big(f_{T1}^2 - 4f_{T1}f_{tT} + 12f_{t1}^2\Big) \\
W_{bT} &= \frac{1}{m}\,\frac{36}{r^2}\, f_{tT}^2 \;.
\end{aligned}
$$

Making use of the expression for the expectation values given in Appendix **??**, we finally obtain (compare to Eq.(B.23))

$$
\begin{aligned}
\frac{(\Delta E)_2}{N} &= \frac{\rho}{32}\int d^3 r\Big\{\Big[W_{00}(r) + 9W_{11}(r)\Big]a_-(p_F r) + \\
&\quad + \Big[3W_{01}(r) + 3W_{10}(r)\Big]a_+(p_F r)\Big\}\;. \tag{B.39}
\end{aligned}
$$

Bibliography

[1] J. Gómez-Cadenas, J. Martín-Albo, M. Mezzetto, F. Monrabal, and M. Sorel, Il Nuovo Cimento **35**, 29 (2012)

[2] E. Majorana, Il Nuovo Cimento (1924-1942) **14**, 171 (1937)

[3] C. Giunti and C. Kim, *Fundamentals of Neutrino Physics and Astrophysics* (Oxford University Press, 2007)

[4] G. L. Fogli, E. Lisi, A. Marrone, A. Palazzo, and A. M. Rotunno, Phys. Rev. D **84**, 053007 (2011)

[5] M. Goeppert-Mayer, Phys. Rev. **48**, 512 (1935)

[6] W. H. Furry, Phys. Rev. **56**, 1184 (1939)

[7] S. Cowell, Phys. Rev. C **73**, 028501 (2006)

[8] A. S. Barabash, Phys. Rev. C **81**, 035501 (2010)

[9] A. Balysh *et al.*, Phys. Rev. Lett. **77**, 5186 (1996)

[10] V. Brudanin, N. Rukhadze, C. Briancon, V. Egorov, V. Kovalenko, *et al.*, Phys. Lett. **B495**, 63 (2000)

[11] R. L. Flack *et al.* (NEMO-3 Collaboration), J. Phys. Conf. Ser. **136**, 022032 (2008)

[12] F. Avignone, Prog. Part. Nucl. Phys. **32**, 223 (1994)

[13] A. Morales, Nucl. Phys. B (Proc. Suppl.) **77**, 335 (1999)

[14] C. Dorr and H. Klapdor-Kleingrothaus, Nucl. Instrum. Methods A **513**, 596 (2003)

[15] R. Arnold *et al.*, Phys. Rev. Lett. **95**, 182302 (2005)

[16] S. R. Elliott, A. A. Hahn, M. K. Moe, M. A. Nelson, and M. A. Vient, Phys. Rev. C **46**, 1535 (1992)

[17] R. Arnold *et al.*, Nucl. Phys. A **636**, 209 (1998)

[18] R. Arnold *et al.*, Nucl. Phys. A **658**, 299 (1999)

[19] J. Argyriades *et al.*, Nucl. Phys. A **847**, 168 (2010)

[20] D. Dassié *et al.*, Phys. Rev. D **51**, 2090 (1995)

[21] A. De Silva, M. K. Moe, M. A. Nelson, and M. A. Vient, Phys. Rev. C **56**, 2451 (1997)

[22] H. Ejiri *et al.*, J. Phys. Soc. Jpn. **64**, 339 (1995)

[23] F. A. Danevich *et al.*, Phys. Rev. C **68**, 035501 (2003)

[24] R. Arnold *et al.*, Z. Phys. C **72**, 239 (1996)

[25] C. Arnaboldi, C. Brofferio, C. Bucci, S. Capelli, O. Cremonesi, *et al.*, Phys. Lett. **B557**, 167 (2003)

[26] V. Tretyak *et al.*, AIP Conf. Proc. **1180**, 135 (2009)

[27] N. Ackerman *et al.*, Phys. Rev. Lett. **107**, 212501 (2011)

[28] J. Argyriades *et al.* (NEMO Collaboration), Phys. Rev. C **80**, 032501 (2009)

[29] S. Umehara *et al.*, Phys. Rev. C **78**, 058501 (2008)

[30] H. Klapdor-Kleingrothaus *et al.*, Eur. Phys. J. A. **12**, 147 (2001)

[31] A. Barabash and V. Brudanin (NEMO Collaboration), Phys. Atom. Nucl. **74**, 312 (2011)

[32] E. Andreotti, C. Arnaboldi, F. Avignone, M. Balata, I. Bandac, *et al.*, Astropart. Phys. **34**, 822 (2011)

[33] R. Bernabei *et al.*, Phys. Lett. B **546**, 23 (2002)

[34] O. Benhar, Nucl. Phys. A (Proc. Suppl.) **139**, 15 (2005)

[35] G. Kramer, H. Block, and L. Lapikas, Nucl. Phys. **A679**, 267 (2001)

[36] C. Bisconti, F. A. d. Saavedra, and G. Co', Phys. Rev. C **75**, 054302 (2007)

[37] E. Quint, Ph.D. Thesis. University of Amsterdam (unpublished)(1988)

[38] O. Benhar, A. Fabrocini, and S. Fantoni, Phys. Rev. C **41**, R24 (1990)

[39] M. Horoi and S. Stoica, Phys. Rev. C **81**, 024321 (2010)

[40] E. Caurier, A. Zuker, and A. Poves, Phys. Lett. **B252**, 13 (1990)

[41] J. Retamosa, E. Caurier, and F. Nowacki, Phys. Rev. C **51**, 371 (1995)

[42] E. Caurier, F. Nowacki, and A. Poves, Eur. Phys. J. **A36**, 195 (2008)

[43] E. Caurier, J. Menéndez, F. Nowacki, and A. Poves, Phys. Rev. Lett. **100**, 052503 (2008)

[44] I. Ogawa *et al.* (CANDLES Collaboration), J. Phys. Conf. Ser. **375**, 042018 (2012)

[45] Y. Zdesenko, F. Avignone, V. Brudanin, F. Danevich, V. Kobychev, *et al.*, Astropart. Phys. **23**, 249 (2005)

[46] M. Valli, Ph.D. Thesis. 'Sapienza' Università di Roma(2007)

[47] B. Brown, (World Scientific), 42(1985)

[48] G. Kamuntavi, R. Kalinauskas, B. Barrett, S. Mickevicius, and D. Germanas, Nucl. Phys. A **191**, 695 (2001)

[49] Y.-N. C. Shan-Tao Lai, Computer physics and communications **544**, 70 (1992)

[50] O. Benhar, D. Day, and I. Sick, Rev. Mod. Phys. **80**, 189 (2008)